Mercury dynamics in the anadromous Arctic char (*Salvelinus alpinus*) and food webs of inner Frobisher Bay, Nunavut

by

Isabel R. Hilgendag

A thesis

presented to the University of Waterloo

in fulfillment of the

thesis requirement for the degree of

Master of Science

in

Biology

Waterloo, Ontario, Canada, 2022

Author's Declaration

This thesis consists of material all of which I authored or co-authored: see Statement of Contributions included in the thesis. This is a true copy of the thesis, including any required final revisions, as accepted by my examiners.

I understand that my thesis may be made electronically available to the public.

Statement of Contributions

Isabel R. Hilgendag was the sole author of Chapters 1, 2, and 4 which were written under the supervision of Dr. Heidi Swanson and Dr. Michael Power. Chapter 3 was written for publication and is an exception to sole authorship; contributions to the work are outlined below.

Chapter 3: Mercury biomagnification in benthic, pelagic, and benthopelagic food webs in an Arctic marine ecosystem. I.R. Hilgendag, H.K. Swanson, C.W. Lewis, A.D. Ehrman, M. Power.

While the research was my own, all authors provided valuable contributions to the research. IRH and CWL conducted the field work. IRH and ADE conducted the laboratory work. IRH conducted the data analysis and writing of the paper. HKS and MP provided guidance for the conceptualization of the study. CWL, ADE, HKS, and MP provided financial support. All authors provided editorial comments to the written work. This chapter was published as:

Hilgendag, I.R., Swanson, H.K., Lewis, C.W., Ehrman, A.D., & Power M. (2022). Mercury biomagnification in benthic, pelagic, and benthopelagic food webs in an Arctic marine ecosystem. *Science of the Total Environment, 841*. https://doi.org/10.1016/j.scitotenv.2022.156424

Abstract

Mercury (Hg) is a ubiquitous toxic metal that bioaccumulates in organisms and biomagnifies in food webs. Evaluating Hg bioaccumulation and biomagnification in Arctic marine ecosystems is critical for understanding Hg dynamics and estimating exposure to fish and wildlife consumed by humans. In this thesis, I investigated inter-individual variability in biological factors affecting Hg accumulation in anadromous Arctic char (*Salvelinus alpinus*), as well as food web structure and Hg biomagnification in the benthic, pelagic, and benthopelagic marine food webs of inner Frobisher Bay, in Nunavut, Canada. Stable isotope ratios of carbon ($\delta^{13}C$) and nitrogen ($\delta^{15}N$), as well as concentrations of Hg were measured in 119 anadromous Arctic char and 62 taxa of fish, invertebrates, and zooplankton that had been sampled in inner Frobisher Bay in 2018 and 2019. Mean concentrations of total mercury (THg) and relationships between THg and biological variables known to influence Hg concentrations in fish (e.g., fork length, weight, age, growth rate, trophic position, carbon source, Fulton's condition factor, gonadosomatic index, and hepatosomatic index) were compared between immature and mature Arctic char. The immature Arctic char exhibited greater inter-individual variability in factors affecting THg accumulation compared to the mature Arctic char, and $\delta^{15}N$ (i.e., marine prey reliance) was a strong predictor of THg concentrations for all individuals. Biomagnification of methyl mercury (MeHg) in each food web was quantified with Trophic Magnification Slopes (TMS; calculated as the slope of the linear regression of $\log_{10}$ MeHg concentrations and $\delta^{15}N$ values) and Trophic Magnification Factors (TMF; calculated as the antilog of the regression slope). Rates of MeHg biomagnification were highest in the benthopelagic food web (TMS = 0.201; TMF = 1.59), followed by the pelagic food web (TMS = 0.183; TMF = 1.52), and lastly the benthic food web (TMS = 0.079; TMF = 1.20), and $\delta^{15}N$ explained 88%, 79%, and 9% of variation in MeHg concentrations in each food web, respectively. Results from food web structure analyses indicated that the benthic food web had the greatest trophic diversity, trophic redundancy, and largest isotopic niche area of all food webs studied. The results indicated that greater food web complexity reduces rates of MeHg biomagnification. The research presented in this thesis demonstrated that there are a variety of biological and ecological factors that influence Hg bioaccumulation and biomagnification in Arctic marine organisms and food webs. The acquisition of comprehensive Hg and food web structure data, in association with Canada's Coastal Environmental Baseline Program, broadened the scope of understanding of Hg dynamics in an Arctic marine

ecosystem, and provides important baseline information pertinent for future spatial and temporal comparisons and evaluations of effects of resource development and climate change.

Acknowledgements

First and foremost, I would like to thank my supervisors, Dr. Heidi Swanson and Dr. Michael Power. Thank you for entrusting me with this research, I am exceptionally grateful for your endless guidance, mentorship, and support. Thank you for answering my plethora of questions, for many wonderful opportunities, for dousing anxiety with comic relief, and for sharing an abundance of sage advice. Secondly, I would like to thank my committee members, Dr. Ashley Ehrman and Dr. Roland Hall; thank you for sharing your wealth of knowledge, providing me with guidance, and for your positive encouragement.

A great big thank you to individuals from Fisheries and Oceans Canada, University of Manitoba, the Iqaluit Amaruq Hunters and Trappers Association, Nunavut Arctic College Environmental Technology Program staff and students, and Iqaluit community members for their immense help in sample collection and various other aspect related to field work. Namely, thanks to Jennifer Amagoalik, Usaaraq (Jari) Aariak, Veronica Dueck, Christina Schaefer, Jordan Kroeker, Tony Saraino, Kailtin Lagerwerf, Aimee Finley, Emmeline Dean, Jonathan Lewis, Syola Ikkidluak, Jeremiah Young, Jennifer Kilabuk, Anika Bychok, Ross Tallman, Jenny Mosesie, Shauna Seeteenak, and Joy Emiktowt. Special thanks to Christopher Lewis for all his hard work and dedication in planning and coordinating field work logistics, and for making the 2019 field season an unforgettable experience! Thank you also to Zoya Martin and Adam O'Dell for coordinating the Sylvia Grinnell Arctic char samples, for responding to my many emails, for digging-up data, and Zoya – thank you for letting me help-out at the DIDSON camp, it was a wonderful experience! Thank you to Mathew Alainga for taking us out on his boat to make field work possible, and for making field work days all the more entertaining with daily Inuktitut lessons and the occasional dance to The Jerry Cans. I am grateful to Scott Grant and Philip Walsh (Fisheries and Marine Institute of Memorial University of Newfoundland) for allowing me to join them on a sampling trip to Faris Island. A big thank you, also, to so many others who made this research possible!

Thank you to Reem El Mugammar and Bill Mark at the University of Waterloo Environmental Isotopes Laboratory for timely analysis of my stable isotope samples and for providing guidance. Big thanks also to Phil Peterson from ATS Scientific Inc. for teaching me how to use the DMA-80, for answering my many emails, and for helping me solve the catalyst tube crisis. Thank you also to Matilda Henriksson; you made time spent in the lab with the DMA-80 all the more fun!

Thank you to all my fellow lab members for helping me navigate graduate studies. Thank you for teaching me various lab techniques, taking the time to edit my work, helping me with R, reviewing my presentations, answering my many questions, and for your cherished friendship. Namely, thanks to Jacob Burbank, Britney Firth, Keith McAllister, Adam Kuhrt, Bronte McPhedran, Mehdi Moslemi Aqdam, Tara Boag, Spencer Weinstein, Madeleine Prater, Rosie Smith, Jared Ellenor, Chris Therrien, Ari Yamaguchi, Samantha Burke, Heather Dixon, Kristen Bill, Noel Soogrim, Jess Kidd, Taylor Luu, and Amy Nguyen. A big thank you also to Drew Thompson and Katelyn Gao for all their help with my lab work.

I am very grateful for the following sources of financial support: Natural Sciences and Engineering Research Council of Canada (NSERC) Discovery Grants to Dr. Heidi Swanson and Dr. Michael Power, Fisheries and Oceans Canada Coastal Environmental Baseline Program, NSERC Alexander Graham Bell Canada Graduate Scholarship, Weston Family Award in Northern Research, Brian M. Jessop Graduate Scholarship in Fisheries Science, Ram & Lekha Tumkur Memorial Graduate Scholarship, and the University of Waterloo.

Last, but not least, a great big thank you to my family and friends for their immense encouragement and continued support! Thank you to my Mom and Dad (Petra and Wilhelm Hilgendag), my siblings (Conrad, Lukas, and Julia Hilgendag), and my extended siblings (Björn Gather and Susi Lenz). Thank you also to the Klunder's (Elke, Gerry, Willem, and Simon), and thank you to Oma (Rosemarie Hilgendag) for providing me with lots of coffee and cake whenever I felt tired or discouraged. A special thank you to Fiona Flynn for her continued friendship and a big thank you to her family (Emmett, Phyllis, and Pearse Flynn) for their generosity and kindness, and for providing me with many delicious meals and entertaining conversations.

Dedication

This thesis is dedicated to my parents, Petra and Wilhelm Hilgendag. Thank you for your unwavering support and encouragement in all my academic endeavours and wild adventures, and for challenging me to work hard in the pursuit of my dreams. Vielen vielen Dank Mama und Papa, ich habe euch sehr Lieb!

Table of Contents

List of Figures

List of Tables

List of Abbreviations

AHTA	Amaruq Hunters and Trappers Association
AIC_C	Akaike's Information Criterion corrected for small sample size
AMAP	Arctic Monitoring and Assessment Program
ANCOVA	Analysis of Covariance
ANOVA	Analysis of Variance
ASGM	Artisanal and Small-Scale Gold Mining
B	Benthic
BP	Benthopelagic
BRI	Benthic Reliance Index
C	Carbon
CD	Mean distance to centroid
CEBP	Coastal Environmental Baseline Program
CI	Confidence Interval
cm	centimetre
CO_2	carbon dioxide
CR	delta thirteen carbon ($\delta^{13}C$) range
CRM	Certified Reference Material
df	degrees of freedom
DFO	Fisheries and Oceans Canada
DMA	Direct Mercury Analyzer
dw	dry weight
Fig.	Figure
FL	fork length
g	gram
GEM	Gaseous Elemental Mercury
GN	Government of Nunavut
GSI	Gonadosomatic Index
Hg (II)	Inorganic divalent mercury
Hg	Mercury
hr	hour
hrs	hours
HSD	Honestly Significant Difference
HSI	Hepatosomatic Index
IM-hi	Immature high mercury
IM-lo	Immature low mercury
IQR	Interquartile Range
K	Fulton's condition factor
kg	kilogram
km	kilometre
L	Litre
LGR	Log_{10} growth rate
Log	Logarithm
Log_{10}	Logarithm base ten
LWT	Log_{10} weight
m	metre

MAT	Mature
MeHg	Methyl mercury
mL	millilitre
mm	millimetre
N	Nitrogen
n	number of samples
NA	not analyzed or not available
NCP	Northern Contaminants Program
ng	nanogram
ng/g	nanograms per gram
n_M	total number of samples analyzed for methyl mercury
NND	mean nearest neighbour distance
NR	delta fifteen nitrogen ($\delta^{15}N$) range
NRCC	National Research Council of Canada
n_T	total number of samples analyzed for total mercury
OPP	Oceans Protection Plan
P	Pelagic
p	p-value
PAM	Partitioning Around Medoids
POM	Particulate Organic Matter
ppm	parts per million
R^2	R squared
R^2_{adj}	adjusted R squared
RPD	Relative Percent Difference
RSS	Residual Sum of Squares
SD	Standard Deviation
SDNND	Standard Deviation of Nearest Neighbour Distance
SE	Standard Error
SEA_B	Bayesian Standard Ellipse Area
SEA_C	Standard Ellipse Area corrected for small sample size
TA	Total Area
TEF	Trophic Enrichment Factor
THg	Total mercury
TL	Trophic Level
TMF	Trophic Magnification Factor
TMS	Trophic Magnification Slope
vs	versus
w_i	Akaike weight
ww	wet weight

List of Symbols

%	Percent
% MeHg	Percent methyl mercury
[MeHg]	Methyl mercury concentration
[THg]	Total mercury concentration
<	Less than
=	Equals
>	Greater than
±	plus/minus
‰	Permil
^{o}C	Degrees Celsius
×	Times
α	alpha
δ	Delta
Δ	Difference
$\delta^{13}C$	delta thirteen carbon
$\delta^{15}N$	delta fifteen nitrogen
$\delta^{15}N_{adj}$	adjusted delta fifteen nitrogen
µg	microgram
µm	micrometre

Chapter 1
General Introduction

1.1 Mercury

Mercury (Hg) is a heavy metal that is a neurotoxin and endocrine disruptor that can cause adverse health effects in both humans and wildlife (Crump & Trudeau, 2009; Scheuhammer et al., 2007). Negative health effects associated with Hg exposure in humans and other vertebrates include visual impairment, ataxia, lethargy, and developmental impairment (Scheuhammer et al., 2007; Wolfe et al., 1998). One of the biggest sources of Hg exposure to humans is through the consumption of fish (UNEP, 2019b; WHO, 1990), and thus risks and benefits of fish consumption must be carefully assessed, particularly in regions where wild-harvested fish are a critical subsistence food source (Priest & Usher, 2004). Mercury in tissues can also affect general health and fitness of organisms in Arctic ecosystems (Chételat et al., 2020), with muscle tissue toxicity thresholds in fish ranging from 0.33 – 0.50 ppm wet weight (Barst et al., 2019; Beckvar et al., 2005). Examination of Hg concentrations in fish, and the aquatic food webs that support them, lends insight into rates of Hg accumulation and helps inform policies and predictions about future risks posed by fishery-based food sources (CACAR, 2012).

Mercury is emitted from a variety of natural and anthropogenic processes (e.g., Gworek et al., 2017). Weathering of Hg-containing minerals, volcanic activity, and other geothermal activities are examples of natural sources of Hg emissions (AMAP, 2011). Examples of present-day anthropogenic Hg emissions are artisanal and small-scale gold mining (ASGM), fossil fuel combustion, and industrial metal working processes (UNEP, 2019b). Approximately 1.54 million tonnes of Hg have been released into the environment from anthropogenic sources, 73% of which was released after the start of the Industrial Era in 1850 (Streets et al., 2017). While atmospheric Hg emissions have increased approximately 3-fold since 1850 (Lindberg et al., 2007; Streets et al., 2017), emissions have decreased in recent years due to tighter global restrictions initiated by the 2013 Minamata Convention (Minamata, 2021; UNEP, 2019a) and due to technological advances in metallurgical industries (Mukherjee, 1999), such as the implementation of air pollution control devices called scrubbers (e.g., Diaz-Somoano et al., 2007).

Mercury is primarily released as gaseous elemental mercury (GEM; Hg (0)), a volatile and stable form of Hg that is transported atmospherically and has a relatively long residence time in the atmosphere (i.e., months), which can lead to its deposition in high altitude and/or latitude regions (e.g., CACAR, 2012). GEM is oxidized to soluble inorganic divalent mercury, Hg (II); both GEM and Hg (II) are deposited to terrestrial and aquatic ecosystems via wet and/or dry deposition, and are relatively non-toxic forms of Hg (Bargagli et al., 2007; Kirk et al., 2012; Obrist et al., 2017). Through the process of methylation, Hg (II)

may be further transformed into organic monomethyl mercury (MeHg; CH_3Hg), the bioavailable toxic form of Hg, or dimethyl mercury [$(CH_3)_2Hg$], which is often transformed back to mono MeHg (Gworek et al., 2016; King et al., 2000; Kirk et al., 2012). In aquatic environments, methylation is driven by sulfate- and iron- reducing bacteria and methanogens in benthic and pelagic habitats, and by a variety of microorganisms associated with biofilms and periphyton (Branfireun et al., 2020; Lehnherr, 2014; Paranjape & Hall, 2017). In marine waters, methylation is also driven by heterotrophic bacteria and macroalgae in oxygen-deficient zones of the water column (Regnell & Watras, 2019). While there are many biotic and abiotic processes that regulate rates of Hg methylation and demethylation in the Arctic marine environment, a surplus of Hg methylation relative to demethylation leads to uptake into lower trophic level biota, and Hg bioaccumulation through food webs (Lehnherr et al., 2011).

Methyl mercury (MeHg) bioaccumulates and biomagnifies in organisms and food webs (Chouvelon et al., 2018; Gray, 2002; Lavoie et al., 2013). The most prominent route of MeHg exposure to higher trophic level organisms, such as fish, is through diet (Chételat et al., 2020; Hall et al., 1997). Once ingested and absorbed through the digestive tract, MeHg binds to the sulfur-containing thiol group in amino acids, cysteine and methionine, and thus accumulates in protein-rich tissues in organisms (Hughes, 1957; Lemes & Wang, 2009). MeHg accumulates in biota when the rate of intake is greater than the rate of elimination (Trudel & Rasmussen, 2001). In food webs, MeHg concentration increases with each successive increase in trophic level; this process is termed biomagnification (Borgå et al., 2011; Gray, 2002; Kidd et al., 1995). The rate at which MeHg biomagnifies in food webs is quantified as the Trophic Magnification Slope or Trophic Magnification Factor (Borgå et al., 2011), and has been studied for many marine and freshwater food webs (see Lavoie et al., 2013). Estimating the rate of MeHg biomagnification in food webs is important for understanding spatial and temporal variability in organismal Hg concentrations, and for developing an understanding of the pathways of MeHg exposure to organisms within food webs (e.g., Borgå et al., 2011; Lavoie et al., 2013).

Documented links between rates of Hg methylation and temperature (e.g., Monperrus et al., 2007; Ramlal et al., 1993; Yang et al., 2016) suggest that global cycling of Hg is susceptible to climate-induced environmental change. Several environmental variables, including temperature, reduced sea-ice, and permafrost thaw influence Hg transport and fate as well as the rate and extent of Hg accumulation and biomagnification in organisms and food webs (e.g., CCCR, 2019; Krabbenhoft & Sunderland, 2013; Stern et al., 2012). Climate-induced changes to ecosystems may lead to increasing MeHg accumulation in top predators as potential changes to energy pathways within and among food webs could alter either the rate of MeHg biomagnification or the amount of MeHg at the base of food webs (Chen et al., 2014; Griffiths et al., 2017; Post, 2002a; Stern et al., 2012). The Canadian Arctic is warming at three times the global rate

(CCCR, 2019) and climate-induced environmental changes may lead to greater Hg bioavailability as historical Hg deposits become bioavailable (CACAR, 2012; Dietz et al., 2019; Sunderland & Selin, 2013; UNEP 2019b). It is currently difficult to predict effects of change on Hg accumulation, magnification, and concentrations in Arctic biota, which is due in part to a paucity of data. Thus, the acquisition of improved baseline information on coastal marine ecosystems being currently affected by climate-driven environmental change, such as in northern Canada, is important, and will facilitate improved understanding of the impacts of changing Hg bioavailability on Arctic marine ecosystems.

1.2 Arctic char

Arctic char (*Salvelinus alpinus*) is an iteroparous salmonid species with a circumpolar distribution in the northern hemisphere (Johnson, 1980; Klemetsen et al., 2003; Power & Reist, 2018). Euryphagy and a plastic life history have contributed to their adaptation to rigorous Arctic environments (e.g., Amundsen, 1995; Power et al., 2008), where they are a highly valued food source. In Nunavut, Arctic char are considered one of the most important subsistence fish species (Priest & Usher, 2004; Roux et al., 2011).

Arctic char are habitat generalists and have several life-history types, including resident, landlocked, and anadromous. While resident and landlocked Arctic char remain in freshwater for the duration of their life, anadromous Arctic char migrate to the marine environment (Johnson, 1980). Anadromous Arctic char spawn in freshwater lakes and rivers and begin annual migrations to marine waters during summer between 2 and 11 years of age (Johnson 1980; Power & Reist, 2018). Duration of time spent at sea is variable and ranges between 30 to 70 days (Jørgensen et al., 1997; Klemetsen et al., 2003; Power & Reist, 2018).

Anadromy in fish is thought to confer a fitness advantage because of higher productivity in the marine environment which provides greater food availability relative to freshwater environments at higher latitudes (Gross et al., 1988; McDowall, 2008). As a result, a high percentage (> 90%) of muscle biomass in anadromous Arctic char is derived from marine prey (Swanson et al., 2011a; Davidsen et al., 2020). Arctic char are opportunistic feeders that forage on a variety of benthic and pelagic biota, and often exhibit an ontogenetic diet shift, switching from small invertebrates to fish as they grow in size and age (Kahilainen et al., 2017; Keva et al., 2017; Riget et al., 2000). In the marine environment, Arctic char are thought to remain in the upper 3 m of the water column and do deep repetitive foraging dives to depths of over 30 m (Mulder et al., 2020; Spares et al., 2012). The importance of different marine prey items for Arctic char is spatially dependent and depends on availability (Dempson et al., 2002). In general, marine crustaceans and pelagic fishes are the most important prey items (Davidsen et al., 2020). At various sampling locations in northern Labrador, 85-92% of the total weight of Arctic char stomach contents were composed of mysids,

amphipods, sculpins (*Cottidae* spp.), capelin (*Mallotus villosus*), and sand lance (*Ammodytes* spp.) (Dempson et al., 2002). In Cumberland Sound, Nunavut, amphipods, copepods, and fish, specifically Arctic cod (*Boreogadus saida*) and sculpin were the most abundant prey identified in Arctic char stomachs (Klemetsen et al., 2003; Moore & Moore, 1974). In Frobisher Bay, Nunavut, Grainger (1953) recorded over 30 different prey species in Arctic char stomachs, with the most abundant taxa being amphipods, mysids, and sculpins. Spares et al. (2012) also examined stomach contents of Frobisher Bay Arctic char, and found major taxa to be crustaceans (mysids, amphipods, decapods), polychaetes, insects, and fish (Atlantic spiny lumpsucker (*Eumicrotremus spinosus*), pricklebacks (*Lumpenus* spp.), capelin, sculpins, Arctic cod).

As a result of predominantly feeding in the marine environment where THg concentrations in prey are relatively low and where fish grow relatively quickly, anadromous Arctic char muscle tissue tends to have THg concentrations that are below the 0.5 ppm Health Canada guideline for commercial sale (Health Canada, 2007; Lockhart et al. 2005; Riget et al. 2000; Swanson et al. 2011b). In fish, exposure to Hg mainly occurs via consumption of Hg-contaminated prey (Hall et al., 1997). Ingested Hg may be excreted after detoxification in the liver (Eagles-Smith et al., 2009; Farris et al., 1993), or eliminated via transfer to offspring during oogenesis (Alvarez et al., 2006; Hammerschmidt et al., 1999; Sackett et al., 2013). Hg accumulates in fish and other biota when the rate of intake is greater than the rate of elimination (Trudel & Rasmussen, 2001). Intraspecific variation in Hg concentrations often occurs even when individuals are in sympatry. Mercury concentrations in fish often increase with fish age and size, as a result of ontogenetic diet shifts to the consumption of higher trophic level prey, and/or reductions in capacity to eliminate Hg with increasing senescence (Cabana & Rasmussen, 1994; Grieb et al., 1990; Harris & Bodaly, 1998; Power et al., 2002). Somatic growth dilution (where a high growth rate results in greater biomass gain relative to MeHg intake) and Hg depuration via transfer to offspring are mechanisms that reduce the THg concentrations in fish (Alvarez et al., 2006; Karimi et al., 2007; Sackett et al., 2013). Habitat use, prey choice, and food web structure also influence Hg concentrations in fish; consumption of more benthic prey relative to pelagic prey, as well as the consumption of lower trophic level organisms often results in lower Hg concentrations (Kidd et al., 1995; Power et al., 2002; Rikardsen et al., 2000).

1.3 Stable Isotopes

Stable isotopes are non-radioactive chemical elements that have the same number of protons but a differing number of neutrons, a characteristic that has made them useful for a variety of applications, including examining trophic relationships in aquatic ecosystems (Fry, 2006). Carbon and nitrogen stable isotope ratios ($\delta^{13}C$ and $\delta^{15}N$ when estimated relative to international standards, respectively) are most commonly used for studying aquatic trophic interactions because they integrate an organism's dietary information over time. Stable isotope ratios can provide a better long-term estimate of diet sources

compared to the traditional method of stomach content analysis, which only provides dietary information prior to an organism's capture (e.g., Hesslein et al., 1993; Knudsen et al., 2011). Stable isotope fractionation, the separation of lighter (fewer neutrons) and heavier (more neutrons) isotopes, occurs due to a series of biochemical reactions associated with food digestion and nutrient assimilation that results in the differential incorporation of isotopes in biological tissues (Fry, 2006).

Ratios of stable carbon isotopes, $\delta^{13}C$, are typically used to differentiate among habitats and basal food web carbon sources (DeNiro & Epstein, 1978). In marine ecosystems, phytoplankton are more depleted in ^{13}C relative to more enriched benthic algae, periphyton, and macrophytes (Fry & Sherr, 1984); this results in organisms associated with pelagic food webs to have generally lower $\delta^{13}C$ values compared to organisms associated with benthic food webs (e.g., France, 1995; Tamelander et al., 2006). Using different pathways of CO_2 incorporation, taxa such as phytoplankton and kelp have relatively lower and higher $\delta^{13}C$ values, respectively (Fry & Sherr, 1984; Rounick & Winterbourn, 1986), thereby facilitating distinction between pelagic- and benthic-based food webs. As fractionation of $\delta^{13}C$ with successive trophic transfer is minimal, i.e., average change approximates 0.4 ‰ per trophic transfer (Kahilainen et al., 2016; Post, 2002b; Vander Zanden et al., 2011), the relative reliance of higher level consumers on pelagic and benthic carbon sources may be estimated (Fry, 2006).

Stable nitrogen isotope ratios, $\delta^{15}N$, can be used to indicate an organism's trophic level (DeNiro & Epstein, 1981) because $\delta^{15}N$ ratios increase with each trophic transfer. Enrichment occurs as organisms excrete nitrogenous waste, such as ammonia or urea, which is depleted in ^{15}N (Montoya, 2007). Although the average increase in $\delta^{15}N$ is thought to approximate 3.4 ‰ for each trophic level (Post, 2002b; Søreide et al., 2006), increases in $\delta^{15}N$ from prey to predator can range between 1.4 ‰ and 3.8 ‰, depending on the organisms being studied and the study system (Hobson & Welch, 1992; McCutchan et al., 2003).

Together, $\delta^{13}C$ and $\delta^{15}N$ values are useful for describing food web relationships among species, within and among communities, and can facilitate examination of contaminant transfer pathways in food webs (e.g., Borgå et al., 2011; Lavoie et al., 2010; 2013). Stable isotope bivariate plots (e.g., $\delta^{13}C$ on the x-axis, $\delta^{15}N$ on the y-axis) provide a general overview of trophic levels and patterns of resource use, and there are a variety of metrics based on bivariate stable isotope data that can be used to further quantify differences in structure within and among food web compartments and food webs (Layman et al., 2007). For example, species or food web isotopic niche space can be quantified and compared in terms of the range of resource use, trophic diversity, estimates of isotopic niche space and niche space overlap, and probable reliance on diverse prey items using a variety of analytical tools as described in Jackson et al., 2011, Layman et al. 2007, Layman et al., 2012, Newsome et al., 2012, Schmidt et al., 2007, Stock et al., 2018.

Layman et al. (2007) proposed several metrics that could be used to characterize structure of food webs. These metrics include: $\delta^{15}N$ range (vertical range), $\delta^{13}C$ range (horizontal range), mean distance to centroid (average degree of species spacing and trophic diversity), mean nearest neighbour distance (redundancy of trophic ecologies), standard deviation of nearest neighbour distance (evenness of species packing), and total area (total resource use). The original calculation of these metrics relied on geometric methods – namely Euclidean distances and area of convex hull (Layman et al., 2007) – which have some drawbacks (see Jackson et al., 2011). Thus, additional metrics are used to quantity food web area; standard ellipse area corrected for small sample size (SEA_C) is a measure of total food web area that is less affected by outliers than area of a convex hull, and Bayesian standard ellipse area (SEA_B) is an estimate of total food web area within a Bayesian framework that provides error margins (Jackson et al., 2011).

Overall, stable isotopes are potentially useful as tools for examining trophic relationships among organisms in aquatic food webs, and when used in conjunction with contaminant concentrations, such as Hg, can provide an invaluable resource for tracing contaminant pathways in food webs.

1.4 Frobisher Bay

Frobisher Bay is a 265 km semi-enclosed embayment located in southeastern Baffin Island, Nunavut, Canada, lying between the Meta Incognita Peninsula to the West, and the Hall Peninsula to the East (Deering et al., 2018). Inner Frobisher Bay is a low-relief, glacially carved inlet (< 350 m deep) and is defined as the furthest inland area of the bay, approximately 25 km × 70 km (63ºN; 68ºW; Deering et al., 2018; Spares et al., 2015). Inner Frobisher Bay has a large tidal range, with tidal amplitudes in the inner bay ranging from approximately 7 to 11 m (McCann & Dale, 1986; Spares et al., 2015) which thoroughly mix surface waters (Deering et al., 2018; McCann et al., 1981). The boulder-strewn tidal flats are largely comprised of gravel and sand, which overlay a silt and clay substrate (McCann et al., 1981; McCann & Dale, 1986). The seabed geomorphology of inner Frobisher Bay is quite variable, with shallow and deep sections (Deering et al 2018). Early research expeditions to Frobisher Bay on the *Calanus* characterized the flora and fauna (Dunbar, 1956).

The Sylvia Grinnell River and the Bay of Two Rivers (located on the West side of the inner bay) provide freshwater input to the bay and are known to be important migratory rivers for anadromous Arctic char (Spares et al., 2015). The anadromous Arctic char that feed in Frobisher Bay near Iqaluit, Nunavut, are smaller (length-wise) and younger relative to many Arctic char populations in the Canadian Arctic (Evans et al., 2015; Gallagher & Dick, 2010; Kristofferson & Sopuck, 1983; Roux et al., 2011), which is believed to have resulted in part because of historical fishing pressure (Gallagher & Dick, 2010; VanGerwen-Toyne et al., 2013).

A commercial fishery for Arctic char in the Sylvia Grinnell River operated from 1947 to 1951, and from 1959 to 1966 (Grainger, 1953; Hunter, 1976), but was closed in 1966 due to reduced catch-per-unit effort (Gallagher & Dick, 2010; VanGerwen-Toyne et al., 2013). The CPUE declined from 97.1 kg in 1959 to 21.8 kg in 1966 (Gallagher & Dick, 2010). Subsistence and recreational fisheries have continued since the fishery closure (VanGerwen-Toyne et al., 2013). Grainger (1953) observed that Arctic char from this population matured at age 11 and at a fork length of 450 mm, whereas recent observations show that Arctic char mature at ages 8 – 9 and at a fork length of 410 mm (Gallagher & Dick, 2010). The Sylvia Grinnell Arctic char continue to have smaller sizes and earlier female maturation compared to pre-commercial fishing which ended over 30 years ago (Roux et al 2011). Recently, Gallagher & Dick (2010) demonstrated that the proportion of older fish (age > 14) has increased; however, fish age and size structures have not returned to pre-commercial fishing levels.

1.5 Research Objectives

Mercury is a heavy metal that threatens the health of Arctic ecosystems and those who rely on them for food sources (e.g., Chételat et al., 2020; Dietz et al., 2009, 2019; Douglas et al., 2012). Although effort has been made to reduce global anthropogenic Hg emissions since the establishment of the Minamata convention (UNEP, 2021), present-day anthropogenic emissions paired with the re-emission of legacy Hg deposits, result in Hg levels that are orders of magnitude higher than natural emissions (e.g., Outridge et al., 2018). Furthermore, climate change is rapidly altering the Arctic environment (CCCR, 2019; IPCC, 2013), adding a level of uncertainty as to whether Hg levels will increase or decrease in organisms (AMAP, 2011). Baseline information for Hg in Arctic ecosystems is therefore critical for defining existing levels, against which future measures can be compared to understand how Hg is changing over time. Baseline data will also help inform future global and national management and regulation of Hg, as well as decisions about whether northern foods continue to remain safe for consumption.

Iqaluit, the capital city of Nunavut, lies at the head of Frobisher Bay and is one of six coastal communities chosen for Canada's Coastal Environmental Baseline Program (CEBP; DFO, 2020a). The CEBP is part of the national Oceans Protection Plan (OPP) and is being facilitated by Fisheries and Oceans Canada (DFO; DFO, 2020c). The purpose of the program is to acquire baseline information on the current health of Canadian marine ecosystems and to gain a better understanding of the key marine processes thought likely to be affected by urbanization and/or climate change (DFO, 2020c). Iqaluit, in particular, is expected to become a major port for shipments along the Northwest Passage and will experience a greater frequency of ship traffic as a result (DFO, 2020c; Ding & Li, 2022). Since 2017, baseline data in and around Frobisher Bay have been collected for the Iqaluit CEBP by DFO, the Amaruq Hunters and Trappers Association (AHTA), the Government of Nunavut (GN), universities, nongovernmental organizations, and

community field assistants (DFO, 2020b). Although the Hg concentrations in Arctic environments and biota are of significant concern, there have been no comprehensive Hg baseline data collected for the organisms of inner Frobisher Bay since 2010 (van der Velden et al., 2013b), despite the importance of the marine ecosystem as a source of wild-caught fish for the local Inuit in Iqaluit. Accordingly, the research presented herein seeks to update the available data on Hg in the Frobisher Bay ecosystem by investigating inter-individual variability of Hg concentrations in anadromous Arctic char, coupled with an examination of the Hg concentrations in the marine organisms making up the benthic, pelagic, and benthopelagic food webs in which Arctic char potentially feed.

In Chapter 2, the research objectives were to: (1) determine whether THg concentrations varied between mature and immature anadromous Arctic char of Frobisher Bay, and 2) assess how relationships between THg and common biological covariates of THg (e.g., fork length, weight, age, growth rate, trophic position, carbon source, Fulton's condition factor, gonadosomatic index, hepatosomatic index) differed between mature and immature anadromous Arctic char. To address these objectives, 119 Arctic char were captured in several locations in inner Frobisher Bay during 2018 and 2019 using 50 m long multi-mesh gillnets. Muscle tissue samples were analyzed for stable isotope ratios ($\delta^{15}N$ and $\delta^{13}C$), total mercury concentrations (THg), and a subset of samples were analyzed for methyl mercury concentrations (MeHg). It was hypothesized that (H1) relationships between THg concentration and biological covariates (e.g., fork length, age) differ as a function of maturity status (i.e., immature, mature), tending to be stronger in mature than in immature individuals, and (H2) the inter-individual variability in THg in immature and mature Arctic char would be best explained by differences in age, trophic position (i.e., $\delta^{15}N$), and relative reliance on benthic versus pelagic prey resources, with differences in the importance of each factor varying as a function of maturity status.

In Chapter 3, the research objectives were to: (1) compare the structure of the benthic, benthopelagic, and pelagic food webs of inner Frobisher Bay; (2) determine and compare % MeHg, THg concentrations, and MeHg concentrations in food web taxa; and (3) determine and compare rates of MeHg biomagnification in the benthic, benthopelagic, and pelagic food webs of inner Frobisher Bay, and compare those rates to literature values for other Arctic marine food webs. To address these objectives, a variety of zooplankton, invertebrates, and fish species were collected from intertidal and nearshore sites of inner Frobisher Bay. The samples were subsequently analyzed for stable isotope ratios ($\delta^{15}N$ and $\delta^{13}C$), total mercury concentrations (THg), and methyl mercury concentrations (MeHg). The obtained data were then used to test the hypotheses that rates of biomagnification of MeHg would differ significantly among the three food webs and that THg would be highest in the pelagic food web and lowest in the benthic food web.

Overall, results from my research were used to lend insight into the trophic ecology of a large diversity of understudied organisms, allow greater understanding of how benthic, benthopelagic, and pelagic food webs differ from each other and affect rates of Hg biomagnification, and facilitate greater mechanistic knowledge regarding causes of inter-individual variation in Hg concentrations in anadromous Arctic char. The research presented herein provides valuable baseline information for the CEBP and can be used to elucidate potential changes to Hg concentrations in organisms over time.

Chapter 2
Drivers of variability in mercury accumulation in anadromous Arctic char (*Salvelinus alpinus*) of inner Frobisher Bay, Nunavut

2.1 Introduction

Mercury (Hg) is a toxic heavy metal that is largely present in the Arctic as a result of global long-range atmospheric transport processes (Bargagli et al., 2007; Chaulk et al., 2011). Because it is a neurotoxin and endocrine disruptor, exposure to Hg can cause numerous adverse health effects in humans and other organisms (Scheuhammer et al., 2007; Wolfe et al., 1998). The prevalence of Hg in the Arctic is of particular concern because of the consumption of traditional subsistence foods, including fish (Chételat et al., 2020; Douglas et al., 2012). In Nunavut, Arctic char (*Salvelinus alpinus*) is the most important subsistence fish for Indigenous peoples (Priest & Usher, 2004; Thompson, 2005; Wesche & Chan, 2010) and consumption of wild-caught fish can be a significant source of Hg exposure. Methyl mercury is the toxic, organic form of mercury. In fish muscle tissue, approximately 90% of total Hg (THg) occurs as methylmercury (MeHg) and THg is often used as a proxy for MeHg (Bloom, 1992; Grieb et al., 1990; Lescord et al., 2018).

Arctic char is an iteroparous salmonid with multiple life-history types (Klemetsen et al., 2003). Anadromous Arctic char first migrate to sea between the ages of 2 and 11 (Johnson 1980; Power & Reist, 2018) and spend 30-70 days each summer feeding in the marine environment before returning to freshwater to spawn and overwinter (Jørgensen et al., 1997; Klemetsen et al., 2003; Power & Reist, 2018). Rapid growth at sea significantly increases both size and energetic reserves prior to the onset of maturation (Johnson 1980; Loewen et al., 2010). Although anadromous Arctic char accumulate Hg as a result of marine feeding, previous researchers have reported that they generally have total mercury (THg) concentrations that are below guidelines for commercial sale (Riget et al., 2000; Swanson et al., 2011b; van der Velden et al., 2013a). Nevertheless, there is variation among individuals in reported concentration levels, and factors that may be contributing to variation among individuals are not fully understood in many systems.

Maturity (i.e., immature vs mature) may affect THg concentrations in anadromous Arctic char as they are noted for their reproductive plasticity (Power et al., 2008). Spawning readiness and periodicity differ widely within and among populations (Murdoch et al., 2015). Thus, individuals can exhibit high individual-level variation in reproductive energy investment (Jobling et al., 1998), which can affect THg concentrations. Immature Arctic char appear to be more likely to consume freshwater organisms to supplement their diet while overwintering in freshwater (Rikardsen et al., 2003) than mature Arctic char, and freshwater prey generally have higher THg concentrations than marine prey (e.g., Farmer et al., 2010;

Fry & Chumchal, 2012; Smylie et al., 2016;). Winter feeding on freshwater zooplankton, which are typically relatively high in THg (Kahilainen et al., 2016; Keva et al., 2017; Power et al., 2002), has been noted in both Norway (Rikardsen et al., 2002, 2003) and Canada (Mulder et al., 2018). Differences between immature and mature Arctic char in the relative contributions of marine-derived vs freshwater-derived prey, as well as energy investment, may influence both exposure to, and accumulation of, Hg and contribute to among-individual variation in Hg concentrations.

Variables such as fork length (e.g., Tran et al., 2015), weight (e.g., Martyniuk et al., 2020), age (e.g., van der Velden et al., 2013a), and growth rate (e.g., van der Velden et al., 2012; Ward et al., 2010) are also known to influence THg concentrations in fish, and often differ between immature and mature fish (e.g., Kahilainen et al., 2017; Keva et al., 2017; Ulrich & Tallman, 2021). The increased consumption of prey associated with marine migration causes rapid growth in anadromous Arctic char, particularly in immature individuals (Tveiten et al., 1996). A high somatic growth rate can act to dilute Hg and result in lower THg concentrations (Trudel & Rasmussen, 2006; Ward et al., 2010). At maturation, growth rate plateaus as energy is invested increasingly in reproduction rather than somatic growth (Jonsson & Jonsson, 1993). As a result of the relationships between levels of THg and the growth and nutritional status of affected fish, indices such as Fulton's condition factor (K), gonadosomatic index (GSI), and hepatosomatic index (HSI), have been shown to co-vary with THg concentrations in fish (e.g., Erasmus et al., 2019; Evans et al., 2015; Ramos-Osuna et al., 2020).

Trophic level and carbon source, often measured using stable isotope ratios of nitrogen (i.e., $\delta^{15}N$) and carbon (i.e., $\delta^{13}C$), respectively, can affect THg concentrations in fish (Kidd et al., 1995; Power et al., 2002), and may also differ with maturity status. As Arctic char increase in size and age, they generally undergo ontogenetic shifts in diet, switching from lower trophic level prey to higher trophic level piscivory, which is often associated with higher concentrations of THg (Lescord et al., 2018; Riget et al., 2000). For example, long-term dietary studies of anadromous Arctic char in Nain, Labrador, Canada have shown size-related differences in prey use, with fish < 150 mm favouring mysids and amphipods and predation on fish (sandlance - *Ammodytes* spp. and sculpins - *Cottidae* spp.) becoming more prevalent with increasing size (Dempson et al., 2002). In terms of carbon sources, Arctic char diets may be derived from benthic or pelagic prey sources (Rikardsen et al., 2000), with pelagic prey sources often having relatively higher THg concentrations (Power et al., 2002; Thomas et al., 2016). Reliance on marine vs freshwater prey also affects THg concentrations in anadromous Arctic char. In anadromous Arctic char, approximately 90% of body mass may be derived from marine prey sources (Davidsen et al., 2020; Swanson et al., 2011a), which leads to overall lower THg concentrations as compared to non-anadromous conspecifics (Lockhart et al., 2005; Swanson et al., 2011b; van der Velden et al., 2013a). Among anadromous Arctic char in West Greenland,

there was a notable size-dependent increase in the overall reliance on marine prey, particularly in the 20 – 30 cm size range (Davidsen et al. 2020). A greater reliance on freshwater prey sources among smaller immature smolts and post-smolts may result in higher THg concentrations compared to mature conspecifics that are more reliant on marine prey sources.

Previous studies of anadromous Arctic char have not often explicitly considered potential differences in THg concentrations between immature and mature individuals. Additionally, relationships among variables known to influence THg, such as age, size, growth rate, K, GSI, HSI, trophic level, and carbon source, have not been studied in the context of immature and mature anadromous Arctic char. Given the mean and range of differences in many of these covariates between immature and mature anadromous Arctic char, it is likely that the nature of the THg-covariate relationships and the best predictors of inter-individual variability will also vary with maturity status (e.g., Doyon et al., 1998; Smylie et al., 2016). This is an especially important knowledge gap to investigate because of the importance of size-related growth and elimination rates for determining THg concentrations in fish (e.g., Dang & Wang, 2012; Ward et al., 2010), and because relationships between relative body size and growth rate predict decreasing variation in growth rates with fish size (Peacor et al., 2007).

Given the plausible basis for differences in THg concentrations related to maturity status, the objectives here were to: 1) determine whether THg concentrations varied between mature and immature Arctic char of Frobisher Bay, and 2) assess how relationships between THg and common covariates of THg (e.g., fork length, age, condition, growth rate, indicators of diet) differed between mature and immature anadromous Arctic char. Specifically, I used measurements of THg concentrations in Arctic char dorsal muscle tissue to test the hypotheses that: [H1] relationships between THg concentration and biological covariates (e.g., fork length, age) differed as a function of maturity status (i.e., immature, mature), tending to be stronger in mature than in immature individuals; and, [H2] the inter-individual variability in THg in immature and mature Arctic char would be best explained by age, trophic position (i.e., $\delta^{15}N$), and relative reliance on benthic vs pelagic prey resources, with differences in the importance of each factor varying as a function of maturity status.

2.2 Methods

2.2.1 Study Site

Frobisher Bay is a 265 km embayment located in southeastern Baffin Island, Nunavut (Deering et al., 2018). Inner Frobisher Bay is located at the head of the bay and is a low-relief, glacially carved inlet (< 350m deep) with a large tidal range (up to 11 m) which thoroughly mixes surface waters (Deering et al., 2018; McCann et al., 1981). The Sylvia Grinnell River and the Bay of Two Rivers (Fig. 2.1) provide

freshwater input to the inner bay and are known to be important migratory passages for anadromous Arctic char that typically spend between 46 – 78 days feeding in the bay in the June to September period (Spares et al., 2015).

2.2.2 Sample Collection

Arctic char were captured from the bay between July 17th and August 17th in 2018 and July 15th and August 22nd in 2019 (Fig. 2.1, triangles) using 50 m long multi-filament gillnets (38 – 140 mm mesh sizes) set for 3 hrs before high tide and collected 1 hr after high tide. A selection of fish from across the size-range was retained (2018, n = 62; 2019, n = 57) for THg and stable isotope analyses. Fish mass (g) and fork-length (mm) were measured and used for computing Fulton's condition factor (K) after statistical verification of isometric growth (Le Cren, 1951; Fig. S2.1, Appendix A). A 30 g portion of skinless dorsal muscle tissue was excised, placed in a Whirl-Pak, and frozen at -20ºC for later laboratory analysis. Otoliths were removed for aging following methods described in Barber and McFarlane (1987). Age data were used to compute the average annual growth rate as length (mm) divided by age. Sex and maturation status (immature and mature) were determined following protocols as described in Snyder (1983), with resting, running ripe and spent individuals considered as mature. The gonadosomatic index (GSI) was calculated as the gonad weight (g) divided by total fish weight (g) and multiplied by 100 (e.g., Htun-Han, 1978). The hepatosomatic index (HSI) was calculated as the liver weight (g) divided by the total fish weight (g) and multiplied by 100 (e.g., Htun-Han, 1978).

Contemporaneous sampling of zooplankton and gastropods was completed in the bay. Zooplankton were collected with a 500 µm mesh net via 10-minute horizontal tows, conducted several times at various locations in Koojesse and Peterhead Inlets (Fig. 2.1 circles and diamonds) throughout the ice-free summer season of 2019. Zooplankton were sorted to the lowest taxonomic resolution possible and subsequently frozen to -20ºC. Gastropods were sampled from exposed substrates at low tide at multiple locations within the inner bay (Fig. 2.1 squares). Gastropods were rinsed with ultra-pure milli-q water, and the foot muscle was dissected out and frozen at -20ºC. Tissue samples from all organisms were freeze-dried (Freezone Plus 2.5 Litre Cascade Benchtop Freeze Dry Systems, Labconco, Kansas City, USA) for 48 hrs or until sufficiently dry. Samples were then homogenized with a glass mortar and pestle or stainless-steel scissors and transferred to acid-washed 20 mL borosilicate glass scintillation vials for subsequent stable isotope ($\delta^{15}N$, $\delta^{13}C$), THg and MeHg analyses (see below).

2.2.3 Stable Isotope Analysis

Prior to stable isotope analyses, inorganic carbon was removed from zooplankton with 10 % hydrochloric acid (Jacob et al., 2005). Samples were then dried in a fumehood for 24 hrs, followed by 24

hrs in a 50ºC drying oven, and were subsequently re-homogenized. Once dried, if hygroscopic salts were present, the sample was rinsed with ultra pure milli-q water, and then placed in a drying oven at 50ºC for 48 hrs, and re-homogenized.

Dried Arctic char tissue and other taxa samples were weighed into tin capsules (Tin Capsules Pressed Standard Weight 5 × 3.5mm, Elemental Microanalysis Ltd., Okehampton, UK) using an analytical balance (XP205 DeltaRange, Mettler-Toledo GmbH, Greifensee, Switzerland), with every eleventh sample weighed in duplicate. Samples were then analyzed for $\delta^{15}N$ and $\delta^{13}C$ using a 4010 Elemental Analyzer (CNSO 4010, Costech Analytical Technologies Inc., Valencia, USA) coupled to a Delta Plus Continuous Flow Isotope Ratio Mass Spectrometer (Thermo Finnigan, Bremen, Germany) at the University of Waterloo Environmental Isotope Laboratory. Machine analytical precision of ± 0.2 ‰ for $\delta^{13}C$ and ± 0.3 ‰ for $\delta^{15}N$ was verified by measurement of internal laboratory standards cross-calibrated against international standards of Vienna Pee Dee Belemnite for $\delta^{13}C$ (Craig, 1957) and atmospheric nitrogen for $\delta^{15}N$ (Mariotti, 1983). Standards included International Atomic Energy Agency standards CH6 for carbon and N1 and N2 for nitrogen. The mean relative percent difference (RPD) of analyzed sample duplicates (n = 28) was 2.6 %. As C:N ratios in general did not exceed 4, and there was no statistical relationship between C:N ratios and %C, $\delta^{13}C$ ratios were not lipid-corrected (Jardine et al., 2013).

Generated stable isotope data were used to compute a Benthic Reliance Index (BRI) using a two end-member mixing model (Hobson et al., 1994) as follows:

$$BRI = \frac{(\delta_{Sample} - \delta_{Source2})}{(\delta_{Source1} - \delta_{Source2})}$$

where δ_{Sample} is the measured $\delta^{13}C$ of the Arctic char muscle tissue, $\delta_{Source1}$ is the $\delta^{13}C$ signature (plus the standard deviation) of the benthic end-member, and $\delta_{Source2}$ is the $\delta^{13}C$ signature (minus the standard deviation) of the pelagic end-member. Arctic char tissue samples were corrected for the effect of fractionation associated with assimilation (McCutchan et al., 2003) prior to computing the BRI using the value 0.4 ‰, which has been widely used in previous studies (e.g., Kahilainen et al., 2016; Post, 2002b; Vander Zanden et al., 2011). Pooled samples of gastropod foot muscle from *Littorina* sp. (n = 6) were chosen to represent the benthic end-member ($\delta^{13}C$ mean ± S.D. = -18.07 ± 0.16 ‰). Pooled samples of the zooplankton, *Calanus* sp. (n = 18), were chosen to represent the pelagic end-member ($\delta^{13}C$ ± S.D. = -23.54 ± 0.60 ‰).

2.2.4 Mercury Analysis

Homogenized, freeze-dried Arctic char tissue samples were weighed into nickel boats to approximately 25-50 mg. Weighed samples were analyzed for total mercury (THg) following U.S. EPA

method 7473 (2007) using thermal decomposition and atomic absorption spectrophotometry with a dual-cell Milestone DMA-80 Direct Mercury Analyzer (DMA80, Milestone Inc., Shelton USA, Milestone S.r.l. Sorisole, Italy) at the University of Waterloo. Precision was assessed with the analysis of duplicates every tenth sample. Sample measurements were accepted when sample duplicates had a mean relative percent difference (RPD) < 10 %; the mean RPD of all duplicates analyzed was 4.8 %. Machine accuracy was assessed with the analysis of National Research Council of Canada (NRCC) certified reference materials (CRM), analyzed at the beginning, middle, and end of each batch of samples analyzed. CRMs (mean THg certified value ± S.D.) were fish protein (DORM-4; 0.412 ± 0.036 mg/kg) and lobster hepatopancreas (TORT-3; 0.292 ± 0.022 mg/kg). Sample measurements were accepted when analyzed CRM values were within 10 % of their certified value (U.S. EPA, 2007). The mean method detection limit, calculated as 3× the standard deviation of blanks, was 0.25 ng.

Eight samples of Arctic char muscle tissue from across a range of sizes and ages were analyzed for methyl mercury (MeHg) following U.S. EPA method 1630 (1998) using cold vapour atomic fluorescence spectroscopy (CVAFS) with a Tekran Model 2700 automated methylmercury analysis system at the Biotron Analytical Services Laboratory at Western University, London, Ontario. The mean RPD of analyzed duplicates was 9 % and the method detection limit was 0.051 ng/g. The average percent MeHg (% MeHg) was calculated for all samples by dividing the MeHg concentration ([MeHg]) by the concentration of total mercury ([THg]) and multiplying by 100 (e.g., Burke et al., 2020).

2.2.5 Data Analysis

Percent MeHg (% MeHg) was first calculated for the subsamples of Arctic char (n = 8) to determine whether the majority (> 90 %) of THg was composed of MeHg. The immature Arctic char were bimodally distributed with respect to $\delta^{15}N$ (Fig. S2.2, Appendix A) and age (Fig. S2.3, Appendix A), indicating two distinct groups among the immature Arctic char that were not a result of differences in sex, collection year, collection date, or sampling location (Table S2.1, Appendix A). A Partitioning Around Medoids (PAM) cluster analysis (Kaufman & Rousseeuw, 1990) with $\delta^{15}N$ and age was conducted to statistically separate the immature individuals into two groups (Fig. S2.4, Appendix A). Goodness of clustering was assessed with the silhouette coefficient (Rousseeuw, 1987), which ranges from -1 to 1 and a value closer to 1 indicates good clustering. The silhouette coefficients of the two clusters were 0.65 for IM-lo and 0.47 for IM-hi (Fig. S2.5, Appendix A), indicating that the two immature groups were adequately separated, and therefore subsequent analyses were conducted for two immature groups (IM-hi, IM-lo) and one mature group (MAT) of Arctic char.

An analysis of variance (ANOVA) was conducted to examine whether mean THg concentrations differed among the three groups (IM-hi, IM-lo, MAT). An ANOVA was subsequently conducted for each

biological variable (e.g., fork length, weight, growth rate, age, $\delta^{15}N$, BRI, K, GSI, HSI), to examine for possible differences among the maturity groups. ANOVAs were followed by Tukey's Honestly Significant Difference (HSD) post-hoc test (Tukey, 1953). To assess how relationships of THg concentrations and biological covariates known to influence THg (e.g., fork length, weight, growth rate, age, $\delta^{15}N$, BRI, K, GSI, HSI) differed between mature and immature fish, an analysis of covariance (ANCOVA) was performed for each covariate, with maturity group (IM-hi, IM-lo, MAT) used as the categorical independent variable and $\log_{10}$ [THg] as the dependent variable. Individuals were plotted on a bivariate plot of $\delta^{15}N$ and BRI to display potential diet differences among maturity groups. To determine whether diet differences changed with size among maturity groups, ANCOVAs were conducted for $\delta^{15}N$ as a function of fork length and BRI as a function of fork length with maturity group (IM-hi, IM-lo, MAT) as the independent categorical variable.

To further examine which biological variables best predicted [THg] in the immature and mature Arctic char, separate *a priori* general linear model sets were constructed and tested for each maturity group (IM-hi, IM-lo, MAT). THg was the dependent variable, and considered independent variables included all possible combinations of biological variables of age, growth rate, size (fork length and weight), K, GSI, HSI, and diet ($\delta^{15}N$ and BRI) starting from single variable models and ending with n = 3 variables to ensure there was enough sample size per variable. Highly collinear variables (i.e., $r > 0.90$; e.g., fork length and weight) were not included together in models (see Tables S2.3 – S2.5 in Appendix A for Pearson correlation coefficient results). A total of 34 models were considered for each group. Akaike's Information Criterion corrected for small sample size, AIC_C (Burnham & Anderson, 2002), was used to rank estimated models. Multicollinearity was assessed with tolerance and variance inflation factors (e.g., Glantz & Slinker, 2001; Hair et al., 2006) and diagnostic plots, using the olsrr package in R (Hebbali, 2020). Candidate models with ΔAIC_C values < 2 were considered equally plausible, and models with $\Delta AIC_C < 6$ were not discounted (Burnham & Anderson, 2002; Symonds & Moussalli, 2011). Models considered to be within the 95% confidence interval set had cumulative Akaike weights (i.e., w_i) that summed to 0.95 starting in order from the highest ranked model (Burnham & Anderson, 2002; Symonds & Moussalli, 2011). Factors influencing THg concentrations were considered to differ by maturity group when the top model(s) for each maturity group differed in explanatory variables.

All statistical analyses were performed with R, version 4.0.5 (R Core Team, 2020) with Type I error set to $\alpha = 0.05$. All general linear models were assessed for violations of the assumptions of normality and homoscedasticity of variance using the Shapiro-Wilk W test (Shapiro & Wilk, 1965) and by plotting residual vs predictor plots (Zar, 2018). If assumptions were not met, variables were $\log_{10}$-transformed, and the general linear model was re-estimated. If a residual was above or below the 1st quartile/3rd quartile +/-

1.5 × IQR, the associated observation was considered an outlier and was removed from the estimation data set and the general linear model was re-estimated (Zar, 2018).

2.3 Results

Results from the eight samples analyzed for both THg and MeHg indicated that the majority of THg in Arctic char muscle occurred in the form of MeHg (mean ± standard deviation (SD) of % MeHg: 94.9 ± 14.9 %, n = 8). Thus, [THg] was considered an effective proxy for [MeHg] in all subsequent analyses. Concentrations of MeHg measured from the subsamples of Arctic char dorsal muscle tissue (n = 8) yielded values ranging from 68.2 to 506.6 ng/g dry weight (dw).

Mean THg concentration ([THg]) was highest for IM-hi (379.22 ± 102.18 ng/g dw) fish compared to IM-lo and MAT fish (one-way ANOVA, $F_{2, 106} = 108.9$, $p < 0.01$; Table 2.1; Fig. 2.2; Table S2.2, Appendix A). Mean [THg] in the IM-hi fish was 4.01× and 1.98× greater than for the IM-lo and MAT fish, respectively. The frequency distribution of [THg] in MAT fish spanned a broad gradient without a clear peak value, whereas IM-lo and IM-hi fish had narrow distributions and well-defined peaks (Fig. 2.2). Differences in biological variables among maturity groups were also observed (mean ± standard deviation); IM-lo were the smallest in size (fork length = 308.47 ± 49.95 mm; weight = 369.62 ± 292.85 g), youngest in age (6 ± 1 years), had the highest growth rate (50.27 ± 7.77 mm/year), and had the highest mean BRI value (0.74 ± 0.09), compared to IM-hi and MAT (one-way ANOVA, $p < 0.05$; Table 2.1; Table S2.2, Appendix A). IM-hi had the lowest mean values for $\delta^{15}N$ (10.19 ± 1.11 ‰), K (0.96 ± 0.20) and HSI (1.49 ± 0.49; one-way ANOVA, $p < 0.05$; Table 2.1; Table S2.2, Appendix A). In general, the differences in biological variables among the groups were consistent with the observed differences in THg concentrations.

Slopes of relationships between $\log_{10}$ [THg] and considered covariates differed significantly among maturity groups (i.e., the interaction term was significant) for 8 of the 9 biological covariates measured; age, size (fork length and weight), growth rate, $\delta^{15}N$, BRI, K, and HSI (ANCOVA, $p < 0.05$; Table 2.2; Fig. 2.3). There was no significant interaction between GSI and maturity group; that is, slopes between $\log_{10}$[THg] and GSI did not vary significantly among maturity groups (ANCOVA, $p > 0.05$; Table 2.2; Fig. 2.3). The direction and magnitude of effects of most biological covariates on $\log_{10}$ [THg] appeared to change after sexual maturity was reached, with relationships tending to be stronger (i.e., more variation in the data explained and higher slope values) for the mature fish than for the immature fish for 6 of the 9 covariates (Table 2.2; Fig. 2.3).

Relationships between $\log_{10}$ [THg] and age, size, and growth rate differed significantly among maturity groups. For both groups of the immature Arctic char (i.e., IM-hi, IM-lo), relationships between $\log_{10}$ [THg] and age were not significant ($p > 0.05$; Table 2.2; Fig. 2.3), but for the mature Arctic char

(MAT), $\log_{10}$ [THg] increased with age ($p < 0.001$; Table 2.2; Fig. 2.3) and explained 23.9 % of the variability in THg. Both fork length and weight were significantly and negatively related to [THg] for both the IM-hi and MAT groups ($p < 0.01$; Table 2.2; Fig. 2.3), which was somewhat unexpected. The slope estimate for [THg] vs fork length was 2× greater for MAT fish than for IM-hi fish, and 1.83× greater for MAT fish than for IM-hi for $\log_{10}$ weight. Relationships between $\log_{10}$ [THg] and both fork length and weight were not significant for the IM-lo fish ($p > 0.05$; Table 2.2; Fig. 2.3). For the mature Arctic char, $\log_{10}$ [THg] decreased with increasing $\log_{10}$ growth rate, and growth rate explained 57.3 % of the variability in [THg] ($p < 0.001$; Table 2.2; Fig. 2.3). There was no significant relationship between [THg] and growth rate for either of the groups of immature Arctic char ($p > 0.05$; Table 2.2; Fig. 2.3).

Relationships between $\log_{10}$ [THg] and $\delta^{15}N$ and BRI differed significantly among maturity groups. Log_{10} [THg] significantly decreased as $\delta^{15}N$ increased for the immature and mature Arctic char ($p < 0.001$; Table 2.2; Fig. 2.3), with the rate of decrease being highest for IM-lo (slope = -0.162) and lowest for IM-hi (slope = -0.091). The nitrogen isotope explained 67.4 % and 69.0 % of the variability in [THg] for IM-lo and IM-hi, respectively (Table 2.2; Fig. 2.3). For IM-hi, $\log_{10}$ [THg] significantly decreased with increasing BRI ($p < 0.001$; Table 2.2; Fig. 2.3) and explained 57.1 % of the variability. There was no statistically significant relationship between $\log_{10}$ [THg] and BRI for IM-lo and MAT. The bivariate plot of $\delta^{15}N$ and BRI showed individuals of IM-lo and MAT to be similarly clustered at higher values of $\delta^{15}N$ relative to IM-hi (Fig. 2.4), whereas IM-hi had a trend of increasing BRI with increasing $\delta^{15}N$ (Pearson Correlation, $r = 0.51$, $df = 35$, $p < 0.01$; Fig. 2.4). Maturity groups exhibited significantly different trends with $\delta^{15}N$ and fork length (ANCOVA, $F_{2, 104} = 18.875$, $p < 0.001$) and BRI and fork length (ANCOVA, $F_{2, 104} = 6.776$, $p < 0.01$). For IM-lo, $\delta^{15}N$ and BRI values did not significantly change with increasing fork length ($p > 0.05$; Fig. 2.5), but IM-hi and MAT had increasing $\delta^{15}N$ values with fork length ($p < 0.001$; Fig. 2.5). IM-hi also had increasing BRI with fork length ($p < 0.001$; Fig. 2.5) but BRI did not significantly change with fork length for MAT ($p > 0.05$; Fig. 2.5).

Relationships between $\log_{10}$ [THg] and K and HSI differed among maturity groups, but relationships between $\log_{10}$ [THg] and GSI did not differ among maturity groups. The relationship between $\log_{10}$ [THg] and K was significantly negative for both IM-hi and MAT ($p < 0.01$; Table 2.2; Fig. 2.3), and explained 18.8 % and 32.4 % of variability, respectively. The relationship between $\log_{10}$ [THg] and K was not significant for IM-lo ($p > 0.05$; Table 2.2; Fig. 2.3). For both MAT and IM-hi, $\log_{10}$ [THg] significantly decreased with increasing HSI ($p < 0.001$; Table 2.2; Fig. 2.3), with the slope for MAT fish being 2.14× greater than for IM-hi fish. There was no significant relationship between $\log_{10}$ [THg] and HSI for IM-lo (> 0.05; Table 2.2; Fig. 2.3). The relationship between $\log_{10}$ [THg] and GSI was not significant for any of the three groups of fish ($p > 0.05$; Table 2.2; Fig. 2.3).

Among the candidate THg explanatory models examined and evaluated with AIC_C, the variables influencing $\log_{10}$ [THg] in models with $\Delta AIC_C < 2$ for IM-hi and MAT were essentially the same, and with the exception of $\delta^{15}N$ and age, differed from those influencing $\log_{10}$ [THg] for IM-lo (Table 2.3). For all three groups of fish, $\delta^{15}N$ was included in the top-ranked models (Table 2.3; Table 2.4). Other highly ranked models included in the 95% confidence interval sets included various subsets and combination of variables, and indicated that feeding (i.e., BRI), age and growth rate (IM-hi, IM-lo, and MAT), and size (IM-hi and IM-lo; Table 2.3; Table 2.4; Table S2.6, Appendix A) affected [THg].

2.4 Discussion

Maturity status (i.e., immature vs mature) contributed to among-individual variation in THg concentrations in anadromous Arctic char. The immature IM-hi group had the highest mean THg concentration, the immature IM-lo group had the lowest mean THg concentration, and the mature MAT group had an intermediate mean THg concentration. Results from this study indicate that mean THg concentrations and relationships between THg and biological covariates known to influence THg concentrations in fish, such as age, fork length, weight, growth rate, $\delta^{15}N$, benthic reliance index (BRI), condition (K), and hepatosomatic index (HSI) differ between immature and mature anadromous Arctic char. For 8 of the 9 biological covariates measured (the exception was gonadosomatic index, GSI), relationships with THg differed among maturity categories (i.e., heterogeneity of slopes), and for 6 of the 9 covariates, relationships were stronger (i.e., explained more of the variation in the data) for the mature Arctic char group compared to the immature groups. Several findings were consistent with our hypotheses. As hypothesized, $\delta^{15}N$, BRI, and age, with the addition of growth rate, best predicted THg for individuals of the mature and IM-hi immature groups. For the IM-lo group, $\delta^{15}N$ was the most important predictor of THg, with fork length and weight also influencing THg in IM-hi and IM-lo groups. While the key factor affecting THg accumulation was broadly similar irrespective of maturation status (e.g., $\delta^{15}N$), other factors considered important for explaining observed THg concentrations in immature Arctic char had more varied effects.

In this study, mean THg concentrations differed among the immature and mature groups of anadromous Arctic char, but not necessarily in the way that was expected; variability between the two immature groups was not predicted, and while IM-lo fish had lower concentrations of THg than MAT fish, IM-hi fish had higher concentrations of THg than MAT fish. Differences in THg concentrations between mature and immature fish have previously been associated with processes such as oogenesis (Alvarez et al., 2006; Sackett et al., 2013) or testosterone production (Madenjian et al., 2011, 2014), which can act to reduce THg concentrations and lead to lower overall THg concentrations in mature fish compared to immature conspecifics. Indirect impacts, for example, may also be associated with changes in biological

factors affecting THg accumulation as fish transition from immature juveniles to mature adults (Rowan & Rasmussen, 1996; Trudel & Rasmussen, 2001). For example, IM-lo fish had higher growth rates and lower THg concentrations than MAT fish, which may reflect faster growth related to earlier marine migrations, but requires further study.

Strength of relationships between THg concentrations and common biological covariates also differed among maturity groups, further indicating that maturity status may be an important consideration when evaluating THg concentrations in anadromous Arctic char. Although previous studies have considered including maturity as a biological factor that might affect THg concentrations (e.g., Keva et al., 2017; Smylie et al., 2016), to our knowledge, no other studies have compared relationships between THg and biological covariates when stratified by maturity categories. For most variables assessed, relationships between THg and covariates were weak or not significant for immature Arctic char whereas relationships between THg and covariates were stronger for mature conspecifics. Maturity status can affect energy allocation, proximate composition, size, and growth (Rowan & Rasmussen, 1996; Trudel & Rasmussen, 2006), which in turn can affect THg concentrations. In immature Arctic char, energy is dedicated to somatic growth rather than reproduction (Jørgensen et al., 1997; Loewen et al., 2010). Smaller, immature Arctic char that migrate to sea experience rapid growth which significantly increases both size and energetic reserves prior to the onset of maturation (Johnson, 1980; Loewen et al., 2010). Once mature, Arctic char exhibit reproductive plasticity (Power et al., 2008), and can exhibit high individual-level variation in reproductive energy investment (Jobling et al., 1998). Variation in growth rate decreases with fish size (Peacor et al., 2007), resulting in less individual variation among larger, mature fish, and stronger correlative trends with factors affecting THg accumulation in fish. Migration-related growth may differ between the two immature groups in a way that reflects recent migration history, but would require further study.

In general, THg concentrations in fish increase with fish size (e.g., Martyniuk et al., 2020; Tran et al., 2015). The generally negative relationships observed between THg and fish size in this study likely reflect greater marine prey dependence with increasing size (Davidsen et al., 2020; Smylie et al., 2016). Negative relationships between THg concentrations and indicators of somatic growth or energy storage are commonly observed (e.g., Swanson et al., 2011b; Ward et al., 2010), and in this study negative relationships between THg and K and between THg and HSI likely also reflect foraging on marine prey. High HSI values can indicate potential for Hg detoxification via metallothionein biosynthesis (Hogstrand & Haux, 1991; Scheuhammer et al., 2015) but are also indicative of greater energy reserves in association with feeding activity (Chellapa et al., 1995; Htun-Han, 1978) on abundant nutrient-rich marine prey (Boivin & Power, 1990; Dutil, 1986).

In fish, THg typically increases with age and is inversely related to growth rate (e.g., Lescord et al., 2018; van der Velden et al., 2013a; Ward et al., 2010). For the mature Arctic char, THg concentration increased with age indicating that higher THg acquisition with age was likely linked to a longer period of exposure to Hg over time, reduced elimination rates with senescence, and other age-related factors such as food consumption rates and activity costs (Rowan & Rasmussen, 1996; Trudel & Rasmussen, 2001, 2006). The importance of age for determining THg in Arctic char has similarly been reported in other studies, both from freshwater and marine environments (Gantner et al., 2010; van der Velden et al., 2013a). For the mature Arctic char, THg concentrations decreased with increasing growth rate, indicating that a greater proportion of biomass is incorporated relative to THg as a result of consumption of higher quality prey and/or switching to low-THg prey, resulting in a THg dilution effect in muscle tissue (Karimi et al., 2007; Trudel & Rasmussen, 2006; Ward et al., 2010). Overall, age and growth rate were related to THg concentrations in the mature Arctic char, but there were a lack of trends for the immature Arctic char.

In fish, THg concentrations typically increase with $\delta^{15}N$ values due to biomagnification (Kidd et al., 1995; Power et al., 2002; van der Velden et al., 2013b). For all fish, THg concentrations decreased with $\delta^{15}N$ values, and this was somewhat unexpected. High trophic level prey are often associated with high THg concentrations as a result of biomagnification (Kidd et al., 1995; Power et al., 2002), however, high $\delta^{15}N$ values associated with low THg concentrations suggests that $\delta^{15}N$ not only reflects trophic position but may be indicative of freshwater versus marine prey reliance, since marine organisms contain higher $\delta^{15}N$ and $\delta^{13}C$ values than freshwater organisms (Attrill et al., 2009; Ulrich & Tallman, 2021). Previous research shows that Hg concentrations are generally lower in marine environments than in freshwater environments (Farmer et al., 2010; Fry & Chumchal, 2012; Smylie et al., 2016; van der Velden et al., 2013b), indicating that feeding in different environments, as evidenced by $\delta^{15}N$, appears to have affected THg concentrations in the immature and mature anadromous Arctic char. There were two groups of immature Arctic char, which could be related to differences in migration history; the IM-hi group had high mean THg concentrations and low mean $\delta^{15}N$ values, and the IM-lo group had low mean THg concentrations and high mean $\delta^{15}N$ values, possibly indicating that IM-hi are first-time migrants, and IM-lo are returning migrants. Further research including $\delta^{34}S$ or otolith microchemistry would help to resolve the mechanism of the negative relationship between THg and $\delta^{15}N$, and the two groups of immature fish.

Overall, the immature Arctic char exhibited higher among-individual variability in THg concentrations and in relationships of THg with biological covariates compared to the mature Arctic char, especially since there were two distinct groups of immature Arctic char; a high-Hg group (IM-hi) and a low-Hg group (IM-lo). IM-hi were older and larger than IM-lo, indicating that IM-hi could be late age, first-time migrants, and IM-lo could be early age, repeat migrants. The high THg concentrations in IM-hi

could reflect previously feeding on high-Hg freshwater prey (e.g., Farmer et al., 2010; Fry & Chumchal, 2012; Smylie et al., 2016; van der Velden et al., 2013b), and the increasing $\delta^{15}N$ with size, likely reflects progressive marine prey dependence with size (Davidsen et al., 2020), whereas low THg concentrations and high $\delta^{15}N$ values across the range of captured sizes exhibited by IM-lo likely reflects early marine prey dependence. Further investigation and comparisons of habitat use, feeding ecology, and migration history in IM-lo and IM-hi fish is necessary to elucidate the mechanisms behind differences in THg concentrations, and in covariates of THg concentrations, observed in this study.

2.5 Conclusion

In this study, I found that i) THg concentrations and relationships between THg and biological covariates were more varied for the immature Arctic char compared to mature conspecifics; and ii) trophic ecology was important in influencing THg concentrations in both immature and mature anadromous Arctic char. This was the first study, to our knowledge, to compare THg concentrations with various biological covariates among immature and mature anadromous Arctic char. Results highlight the importance of considering maturity status when evaluating THg dynamics in anadromous Arctic char. I found that the immature Arctic char were composed of two distinct groups, and that the ecological or life history foundation of this variation deserves further study. Fish are one of the main exposure routes of THg to humans therefore understanding drivers of THg concentration in a variety of maturity groups in fish that are important to Inuit food security, is critical to informing consumption health advisories and to further our understanding of the continued safety of this food source with climate change.

2.6 Tables

Table 2.1. Mean ± standard deviations, and ranges of biological variables for immature and mature anadromous Arctic char (*Salvelinus alpinus*) caught in inner Frobisher Bay, Nunavut in 2018 and 2019. Tukey's HSD results are presented, where significant differences ($p < 0.05$) are indicated by different letters (see Table S2.2, Appendix A, for the ANOVA and Tukey's HSD test statistics).

	IM-hi (Immature)	**IM-lo (Immature)**	**MAT (Mature)**
n	37	30	46
Age (years)	10 ± 2 6 – 14 a	6 ± 1 4 – 9 b	11 ± 2 6 – 17 a
Fork length (mm)	346.27 ± 45.46 240 – 485 a	308.47 ± 49.95 220 – 408 b	459.30 ± 69.27 331 – 580 c
Round weight (g)	413.01 ± 169.25 128 – 1053 a	369.62 ± 292.85 107 – 1615 b	1132.91 ± 533.09 286 – 2201 c
Growth Rate (mm/year)	34.95 ± 4.74 26.14 – 45.71 a	50.27 ± 7.77 41.43 – 70.40 b	43.65 ± 10.67 22.12 – 73.33 c
$\delta^{13}C$ (‰)	-20.07 ± 0.59 -21.84 – -18.97 a	-19.10 ± 0.56 -20.99 – -18.02 b	-19.72 ± 0.63 -21.09 – -18.43 c
$\delta^{15}N$ (‰)	10.19 ± 1.11 8.34 – 12.43 a	13.01 ± 0.82 9.40 – 13.86 b	12.79 ± 1.59 8.55 – 14.71 b
Benthic Reliance Index	0.59 ± 0.09 0.31 – 0.77 a	0.74 ± 0.09 0.44 – 0.92 b	0.65 ± 0.10 0.43 – 0.85 c
Condition	0.96 ± 0.20 0.57 – 1.95 a	1.09 ± 0.29 0.84 – 2.47 b	1.08 ± 0.14 0.71 – 1.35 b
Gonadosomatic Index	0.23 ± 0.25 0.01 – 1.10 a	0.11 ± 0.12 0.01 – 0.44 a	0.71 ± 1.38 0.03 – 7.38 b
Hepatosomatic Index	1.49 ± 0.49 0.62 – 2.55 a	2.06 ± 0.54 0.77 – 2.88 b	2.26 ± 0.58 0.29 – 3.44 b
[THg] (ng/g dw)	379.22 ± 102.18 166.65 – 678.98 a	94.62 ± 63.27 53.57 – 387.97 b	191.33 ± 176.07 54.26 – 1052.35 c

Table 2.2. Log_{10} THg (ng/g dry weight) ANCOVA interaction terms and regression slopes for each biological variable for each immature (IM-hi; IM-lo) and mature (MAT) group of anadromous Arctic char (*Salvelinus alpinus*) caught in inner Frobisher Bay, Nunavut in 2018 and 2019.

Variable	ANCOVA interaction terms			Regressions				
	F	df	p	Maturity	Slope	Intercept	R^2_{adj}	p
Age (years)	6.203	2, 100	< 0.01	IM-hi	-0.013	2.696	0.009	> 0.05
				IM-lo	0.012	1.830	-0.025	> 0.05
				MAT	0.053	1.539	0.239	< 0.001
Fork length (mm)	5.000	2, 103	< 0.01	IM-hi	-0.001	3.038	0.217	< 0.01
				IM-lo	0.000	1.930	-0.036	> 0.05
				MAT	-0.002	3.241	0.352	< 0.001
Log_{10} weight (g)	15.487	2, 103	< 0.001	IM-hi	-0.444	3.708	0.323	< 0.001
				IM-lo	0.032	1.827	-0.033	> 0.05
				MAT	-0.813	4.614	0.455	< 0.001
Log_{10} growth rate (mm/year)	8.395	2, 102	< 0.001	IM-hi	-0.388	3.160	0.005	> 0.05
				IM-lo	-0.391	2.568	0.000	> 0.05
				MAT	-1.927	5.303	0.573	< 0.001
$\delta^{15}N$ (‰)	3.273	2, 99	< 0.05	IM-hi	-0.091	3.479	0.690	< 0.001
				IM-lo	-0.162	4.020	0.674	< 0.001
				MAT	-0.129	3.784	0.686	< 0.001
Benthic Reliance Index	5.446	2, 100	< 0.01	IM-hi	-1.033	3.172	0.571	< 0.001
				IM-lo	0.513	1.518	0.039	> 0.05
				MAT	-0.028	2.126	-0.026	> 0.05
Condition	5.614	2, 100	< 0.01	IM-hi	-0.648	3.178	0.188	< 0.01
				IM-lo	-0.079	1.975	-0.031	> 0.05
				MAT	-1.188	3.465	0.324	< 0.001
Gonadosomatic Index	0.285	2, 101	> 0.05	IM-hi	-0.055	2.574	-0.017	> 0.05
				IM-lo	-0.054	1.911	-0.035	> 0.05
				MAT	0.028	2.078	0.006	> 0.05
Hepatosomatic Index	8.316	2, 99	< 0.001	IM-hi	-0.145	2.776	0.272	< 0.001
				IM-lo	-0.017	1.940	-0.032	> 0.05
				MAT	-0.310	2.831	0.397	< 0.001

Table 2.3. Akaike's information criterion corrected for small sample size (AIC_C) for candidate models that describe variation in THg concentration (ng/g dw) in immature (IM-hi, n = 32; IM-lo, n = 27) and mature (MAT, n = 42) Arctic char. Candidate models within the 95% confidence interval set (i.e., cumulative w_i up to 0.95) are presented. K, number of parameters; RSS, residual sums of squares; Δ_i, difference in AIC_C values between the top model and model *i*; w_i, Akaike weight for model *i*; Cumul. w_i, cumulative Akaike weights starting with the top model. Age (years); BRI, benthic reliance index; FL, fork length (mm); LGR, $\log_{10}$ growth rate (mm/year); LWT, $\log_{10}$ weight (g); and $\delta^{15}N$ (‰). See Table S2.6 in Appendix A for all models ranked with AIC_C.

Maturity group	**Dependent variable**	**Candidate models**	**K**	**RSS**	**AIC_C**	**Δ_i**	**w_i**	**Cumul. w_i**
IM-hi (Immature)	Log_{10} THg	$\delta^{15}N$ + BRI + Age	5	0.082	-178.602	0.000	0.350	0.350
		$\delta^{15}N$ + BRI + LGR	5	0.082	-178.473	0.129	0.328	0.678
		$\delta^{15}N$ + BRI	4	0.096	-176.429	2.173	0.118	0.796
		$\delta^{15}N$ + BRI + FL	5	0.092	-175.074	3.527	0.060	0.856
		$\delta^{15}N$ + BRI + LWT	5	0.092	-175.069	3.533	0.060	0.916
		$\delta^{15}N$ + LGR	4	0.106	-173.191	5.410	0.023	0.939
		$\delta^{15}N$	3	0.118	-172.567	6.035	0.017	0.956
IM-lo (Immature)	Log_{10} THg	$\delta^{15}N$ + FL	4	0.152	-129.949	0.000	0.237	0.237
		$\delta^{15}N$ + LWT	4	0.153	-129.834	0.115	0.223	0.460
		$\delta^{15}N$ + Age + LWT	5	0.146	-128.107	1.843	0.094	0.554
		$\delta^{15}N$ + Age + FL	5	0.147	-127.944	2.006	0.087	0.641
		$\delta^{15}N$ + BRI + FL	5	0.151	-127.103	2.847	0.057	0.698
		$\delta^{15}N$ + BRI + LWT	5	0.152	-126.993	2.956	0.054	0.752
		FL	3	0.195	-126.059	3.891	0.034	0.785
		LWT	3	0.195	-126.056	3.893	0.034	0.819
		$\delta^{15}N$	3	0.200	-125.441	4.508	0.025	0.844
		Age + LWT	4	0.182	-125.209	4.740	0.022	0.866
		$\delta^{15}N$ + LGR	4	0.182	-125.138	4.811	0.021	0.888
		Age + FL	4	0.184	-124.812	5.138	0.018	0.906
		$\delta^{15}N$ + BRI	4	0.187	-124.468	5.481	0.015	0.921
		$\delta^{15}N$ + BRI + LGR	5	0.169	-124.131	5.818	0.013	0.934
		$\delta^{15}N$ + Age	4	0.191	-123.857	6.093	0.011	0.945
		BRI + FL	4	0.194	-123.446	6.503	0.009	0.954
MAT (Mature)	Log_{10} THg	$\delta^{15}N$ + BRI + Age	5	0.523	-172.508	0.000	0.887	0.887
		$\delta^{15}N$ + Age	4	0.644	-166.379	6.130	0.041	0.928
		$\delta^{15}N$ + BRI + LGR	5	0.608	-166.208	6.300	0.038	0.966

Table 2.4. Cumulative Akaike weights (w_i; i.e., the probability that the predictor variable is included in the top model) for variables in the 95% confidence interval set of candidate models that describe variation in THg concentration (ng/g dw) in immature (IM-hi, n = 32; IM-lo, n = 27) and mature (MAT, n = 42) Arctic char (see Table 2.3), in order from highest to lowest. Age (years); BRI, benthic reliance index; FL, fork length (mm); LGR, $\log_{10}$ growth rate (mm/year); LWT, $\log_{10}$ weight (g); and $\delta^{15}N$ (‰).

Maturity group	Variable	Cumulative w_i
IM-hi	$\delta^{15}N$	0.956
(Immature)	BRI	0.916
	LGR	0.351
	Age	0.350
	FL	0.060
	LWT	0.060
IM-lo	$\delta^{15}N$	0.837
(Immature)	FL	0.441
	LWT	0.427
	Age	0.232
	BRI	0.148
	LGR	0.034
MAT	$\delta^{15}N$	0.966
(Mature)	Age	0.928
	BRI	0.925
	LGR	0.038

2.7 Figures

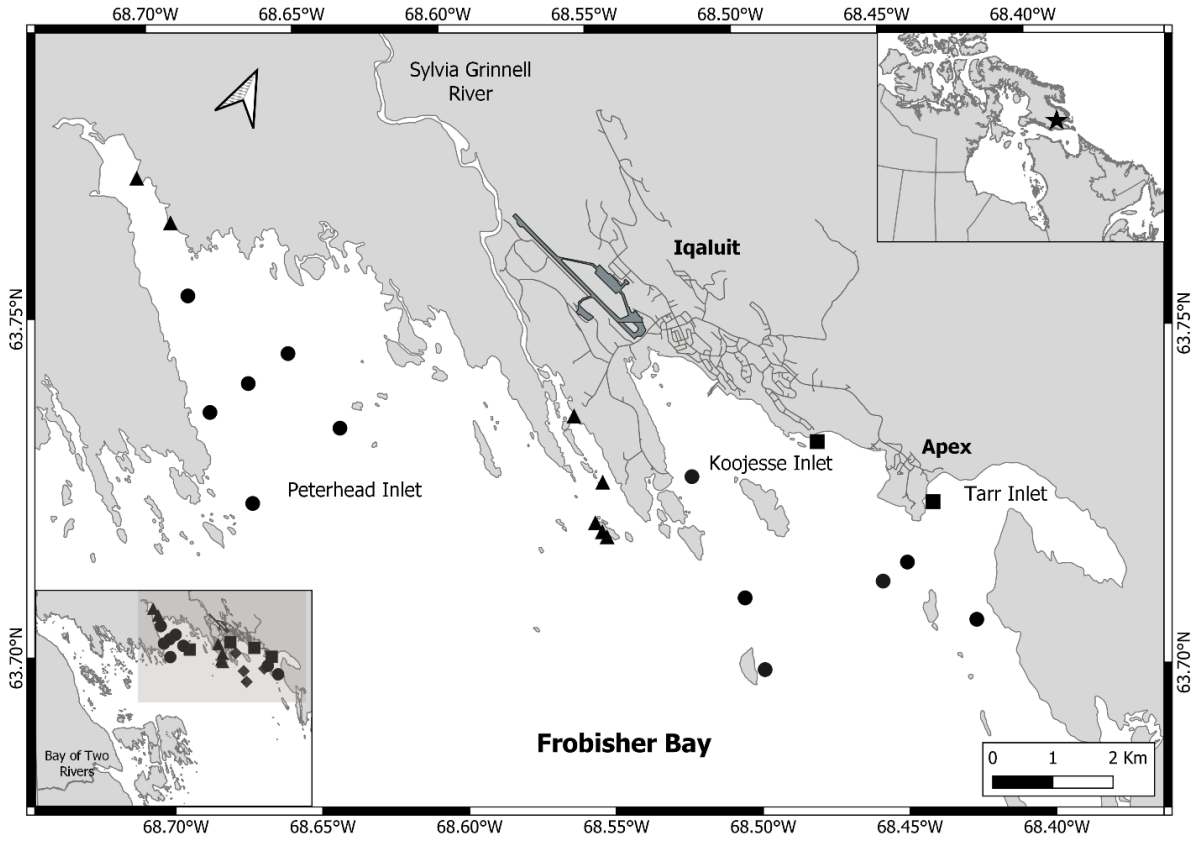

Figure 2.1. Map of inner Frobisher Bay, Nunavut. Shapes correspond to sample collection sites. Triangles, Arctic char collected in 2018 and 2019; circles, zooplankton collected in 2019; squares, gastropods collected in 2019; star, location of Frobisher Bay with respect to northeastern Canada.

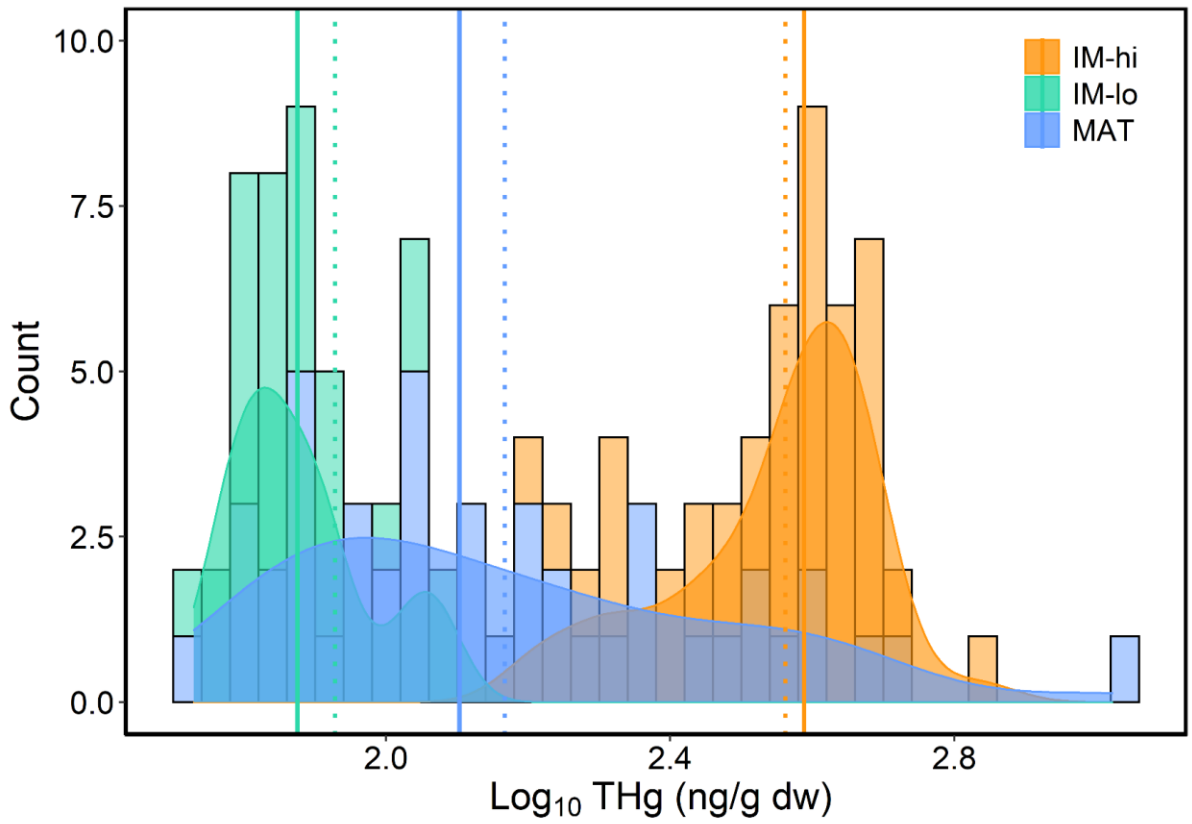

Figure 2.2. Data distribution of $\log_{10}$ THg (ng/g dry weight) concentrations for each immature (IM-hi, n = 37; IM-lo, n = 30), and mature (MAT; n = 46) group of anadromous Arctic char (*Salvelinus alpinus*) collected in 2018 and 2019 in Frobisher Bay, Nunavut. Histograms and density distributions are shown. Medians and means are given, respectively as solid and dotted vertical lines.

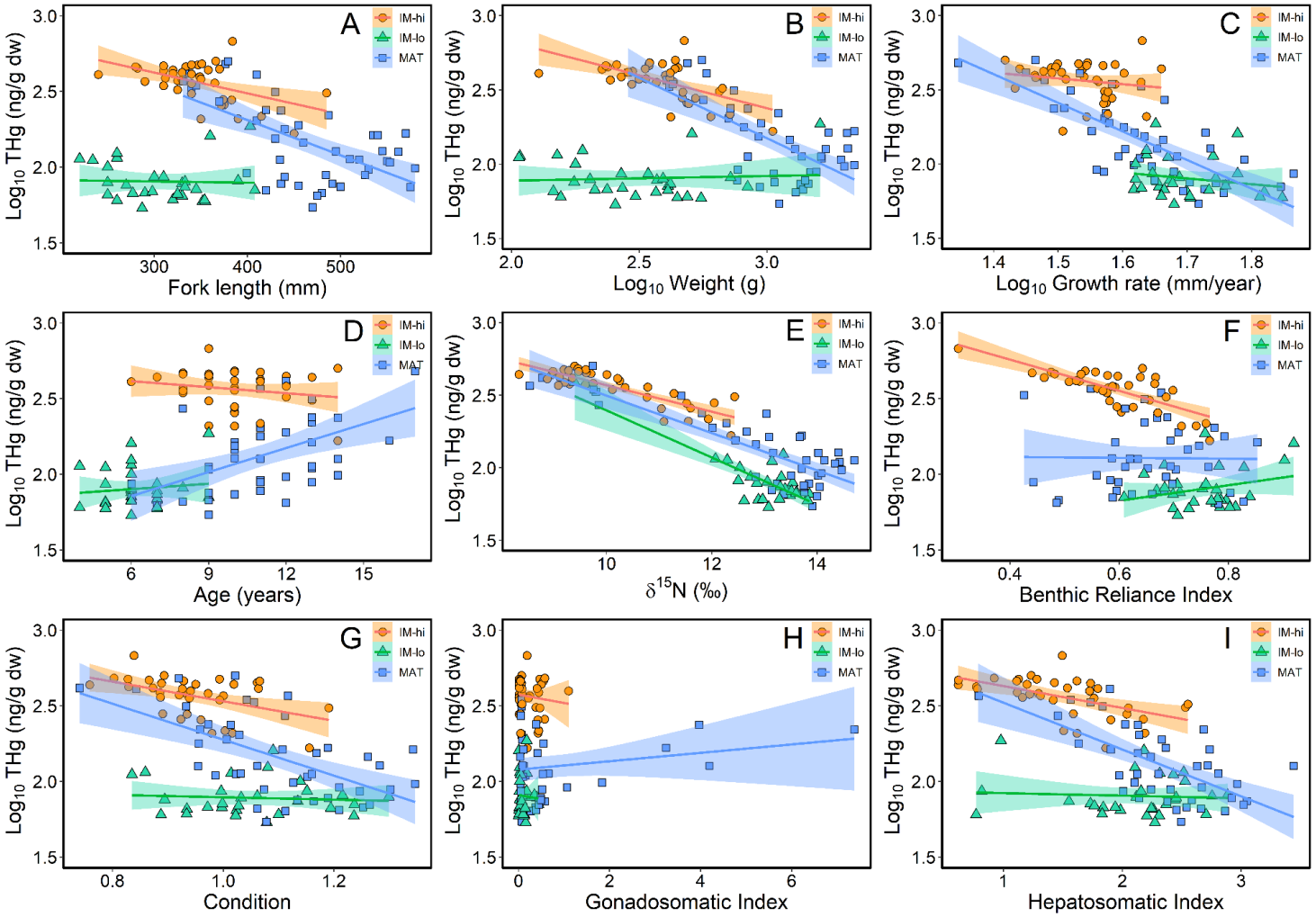

Figure 2.3. Log_{10} THg (ng/g dry weight) as a function of biological covariates for each immature (IM-hi; IM-lo) and mature (MAT) group of anadromous Arctic char (*Salvelinus alpinus*) caught in inner Frobisher Bay, Nunavut in 2018 and 2019. The 95% confidence intervals are shown. Regression summary statistics are listed in Table 2.2. A, fork length (mm); B, log_{10} weight (g); C, log_{10} growth rate (mm/year); D, age (years); E, $\delta^{15}N$ (‰); F, benthic reliance index; G, condition; H, gonadosomatic index; I, hepatosomatic index.

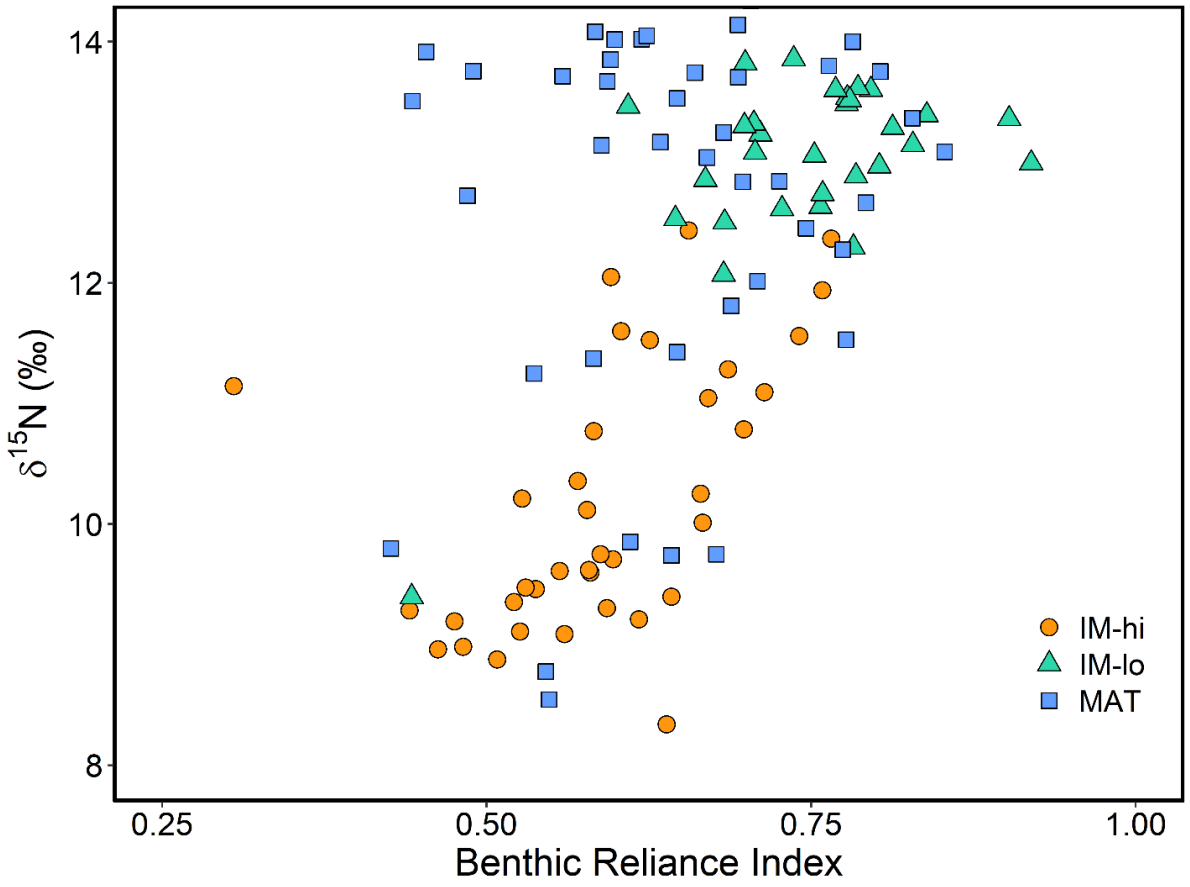

Figure 2.4. Bivariate plot of δ^{15}N (‰) and benthic reliance index (BRI) for each immature (IM-hi; IM-lo) and mature (MAT) group of anadromous Arctic char (*Salvelinus alpinus*) caught in inner Frobisher Bay, Nunavut in 2018 and 2019.

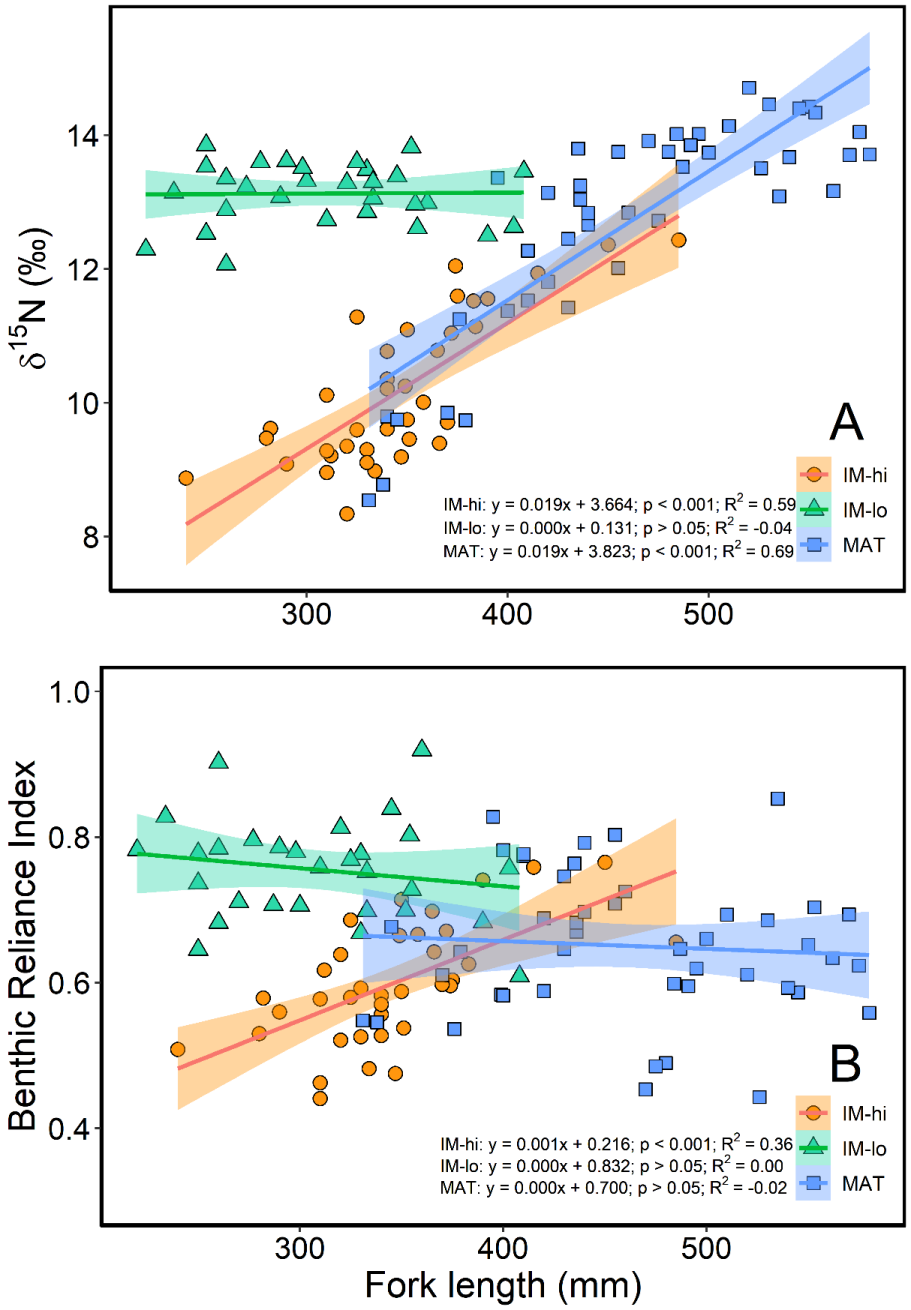

Figure 2.5. Regressions of $\delta^{15}N$ (‰) as a function of fork length (mm; A) and benthic reliance index (BRI) as a function of fork length (mm; B) for the immature (IM-hi, IM-lo) and mature (MAT) groups of anadromous Arctic char caught in inner Frobisher Bay, Nunavut in 2018 and 2019. Linear regression equations, p-values, and adjusted R^2 values for each maturity group are displayed.

Chapter 3
Mercury biomagnification in benthic, pelagic, and benthopelagic food webs in an Arctic marine ecosystem

3.1 Introduction

Mercury (Hg), a contaminant that is globally distributed via long-range atmospheric transport, is prevalent in Arctic marine ecosystems, placing Arctic marine species at risk of exposure to concentrations that may affect organismal health and fitness (Chételat et al., 2020; Dietz et al., 2009, 2019). Hg is a neurotoxin and an endrocrine disruptor that can elicit a variety of adverse health effects in humans and other organisms, such as visual impairment, ataxia, lethargy, and developmental impairment (Scheuhammer et al., 2007; Wolfe et al., 1998).

Hg is globally emitted from various natural and anthropogenic point sources, such as volcanic eruptions, artisanal and small-scale gold mining, and fossil fuel combustion (e.g., Gworek et al., 2017; UNEP, 2019b) and is transported to remote Arctic locations via long-range atmospheric processes (Bargagli et al., 2007; Chaulk et al., 2011). Once deposited in Arctic aquatic environments via wet and/or dry deposition (Kirk et al., 2012), inorganic Hg is methylated by sulfate-reducing bacteria in anoxic sediment in benthic habitats, or by marine bacteria and macroalgae in the water column in pelagic habitats, producing methyl Hg (MeHg) - the toxic, bioavailable form of Hg (Barkay & Poulain, 2007; King et al., 2000; Kirk et al., 2012). MeHg binds to thiol groups in amino acids, namely cysteine and methionine, which can lead to elevated concentrations in the muscle tissue of organisms (Lemes & Wang, 2009; Murillo-Cisneros et al., 2018). The rapid accumulation and slow excretion of MeHg in tissue proteins leads to MeHg accumulation in organisms. MeHg also biomagnifies, with concentrations of MeHg increasing through food webs with each trophic transfer (e.g., Gray, 2002; Kidd et al., 1995; Ordiano-Flores et al., 2021).

The rate at which MeHg biomagnifies is affected by food web structure (e.g., Hobson et al., 2002; Thomas et al., 2016). Food web structure can be quantified by using ratios of stable nitrogen and carbon isotopes ($\delta^{15}N$ and $\delta^{13}C$), which reflect dietary information over time and indicate trophic position and carbon sources, respectively (Fry, 2006; Hesslein et al., 1993). A variety of metrics have been developed to quantify food web structure (e.g., Layman et al., 2007; Newsome et al., 2012). When linked with Hg concentration data, stable isotope data can be used to estimate rates of biomagnification through whole food webs (e.g., Borgå et al., 2011; Jæger et al., 2009; Ordiano-Flores et al., 2021) or through food web compartments (e.g., benthic vs pelagic), which are often distinguished with $\delta^{13}C$ (Power et al., 2002). In marine ecosystems, organisms dependent on the pelagic-based (i.e., phytoplankton) food web often have lower $\delta^{13}C$ values compared to organisms that depend on the benthic-based (i.e., phytodetritus, kelp,

attached algae) food web (Deniro & Epstein, 1978; France, 1995; McMahon et al., 2006; Søreide et al., 2006; Tamelander et al., 2006; Medina-Contreras et al., 2020). Benthic communities exhibit a high diversity in functional feeding groups (e.g., Macdonald et al., 2010; Renaud et al., 2011) and exploit a wider variety of basal carbon sources compared to pelagic communities (e.g., Iken et al., 2010; Søreide et al., 2013; Tamelander et al., 2006; Medina-Contreras et al., 2022). These characteristics contribute to the complexity of the benthic food web and can weaken direct MeHg transfer between trophic levels (Rooney et al., 2006; Trussell et al., 2006), compared to the simpler pelagic food web (Reynolds, 2008).

Understanding food web structure is essential for understanding Hg biomagnification, as the roles and ecological relationships among organisms govern the efficiency with which energy and contaminants are transferred between trophic levels (e.g., Hobson et al., 2002; Rooney et al., 2006; Thomas et al., 2016; Trussell et al., 2006). Within ecosystems, benthic and pelagic food webs differentially accumulate Hg, resulting in different pathways of Hg exposure to higher trophic level consumers depending on their feeding habits (e.g., Chen et al., 2014; Post, 2002a; Power et al., 2002). The majority of studies on biomagnification rates of Hg in Arctic marine ecosystems have focused on pelagic food webs (e.g., Campbell et al., 2005; Clayden et al., 2015; Jæger et al., 2009), and few data are available for benthic food webs. Existing data indicate that benthic food webs have lower rates of biomagnification compared to pelagic food webs (e.g., Fox et al., 2014; Loseto et al., 2008). However, basal sources of production in Arctic marine environments are predicted to shift as a result of climate change, and will likely affect MeHg biomagnification rates (Jędruch et al., 2018; McKinney et al., 2015; Stern et al., 2012). Acquiring baseline data on Hg biomagnification rates in benthic and benthopelagic marine food webs, in addition to pelagic food webs, is therefore critical to understanding and predicting the possible effects of continued environmental change on Hg dynamics.

In this study, organisms were collected from the benthic, benthopelagic, and pelagic food webs of inner Frobisher Bay, near Iqaluit, Nunavut, Canada. Hg concentrations and the $\delta^{13}C$ and $\delta^{15}N$ values measured in consumers were used to determine food web structure and quantify Hg biomagnification rates. Data were then used to: (1) compare the structure of benthic, benthopelagic, and pelagic food webs; (2) determine and compare % MeHg, THg concentrations, and MeHg concentrations in food web taxa; (3) determine and compare rates of MeHg biomagnification among the benthic, benthopelagic, and pelagic food webs of inner Frobisher Bay, and compare those rates to literature values for other Arctic food webs. We hypothesized that rates of biomagnification of MeHg would differ significantly among the three food webs, and be highest in the pelagic food web and lowest in the benthic food web.

3.2 Methods

3.2.1 Study Site

Frobisher Bay is a semi-enclosed 265 km embayment located in southeastern Baffin Island in Nunavut, Canada (Deering et al., 2018; Fig. 3.1). Inner Frobisher Bay is defined as the furthest inland area of the bay, and is approximately 25 km × 70 km (63ºN; 68ºW; Deering et al., 2018; Spares et al., 2015), with depths not exceeding 300 m (Deering et al., 2018). Tidal amplitudes in the inner bay range from approximately 7 to 11 m (McCann & Dale, 1986; Spares et al., 2015). The boulder-strewn tidal flats are largely comprised of gravel and sand, which overlay a silt and clay substrate (McCann et al., 1981; McCann & Dale, 1986). The ice-free summer season generally spans from July to October (ECCC Canadian Ice Service, 2013). Iqaluit (63.7476ºN, 68.5170ºW), the capital city of Nunavut, is located in the innermost part of Frobisher Bay, on the shores of Koojesse Inlet, and has a population of approximately 7429 people (Statistics Canada, 2022).

3.2.2 Sample Collection

To quantify mercury (Hg) concentrations in the abiotic environment, seawater and surface sediment samples were collected in August 2019. Unfiltered seawater samples (n = 2) were collected following the United States Environment Protection Agency (U.S. EPA) method 1669 (U.S. EPA, 1996) from two locations in Frobisher Bay (Fig. 3.1 diamonds). Filtered seawater samples (n = 2) were collected with a peristaltic pump; water passed through acid-washed Teflon tubing and filtered through muffled (550 ºC for 20 min) quartz QMA filters. Seawater samples were preserved with 0.5% (by volume) hydrochloric acid (trace metal grade) and analyzed for total (THg) and methyl mercury (MeHg) at the Biotron Analytical Services Laboratory (Biotron) at Western University, London, Ontario. Surface sediment (n = 9) was sampled at low tide at each intertidal site (Fig. 3.1 closed squares) with a stainless-steel spoon, placed in Whirl-Pak bags, and frozen to -20 ºC.

Particulate organic matter (POM) in water was sampled with a 5 L Niskin bottle 1 m below the surface biweekly from August to September 2019 at sites in Koojesse Inlet (Fig. 3.1 closed circles). Sites in Peterhead Inlet (Fig. 3.1 open circles) were sampled once in August 2019. Once collected, seawater was filtered via suction to collect POM onto pre-combusted 21 mm, 0.7 µm GF/F glass microfibre filters (n = 41). Bulk zooplankton samples were collected biweekly at coastal sites in Koojesse Inlet (Fig. 3.1 closed circles) and Peterhead Inlet (Fig. 3.1 open circles) from August to September in 2019, using a 500 µm mesh net via 10-min horizontal tows. After each tow, the cod-end of the net was rinsed with seawater that had been filtered through 150 µm Nitex mesh. Zooplanktivorous fish and jellyfish were removed from the

sample. Zooplankton were then sorted by species and placed into sterile 20 mL borosilicate glass scintillation vials, and samples (n = 49) were subsequently frozen to -80 ºC.

Fish (n = 20 samples), invertebrates (n = 82 samples), and primary producers (kelp and periphyton; n = 19 samples) were collected from intertidal sites at low tide from Koojesse and Peterhead Inlets, as well as from Faris Island (Fig. 3.1 closed squares) in summer 2019. Free-swimming organisms (e.g., fish and amphipods) were opportunistically sampled from tidal pools using a small handheld aquarium net. Sub-surface macrobenthos (e.g., polychaetes and bivalves) were sampled with a trowel, and surface macrobenthos (e.g., anemones, barnacles, and gastropods) were scraped off rocks with a knife. *Mya truncata* bivalves (n = 24) were collected from intertidal sites in Koojesse and Peterhead Inlets and from Kituriaqannigituq (Fig. 3.1 open squares).

Fish (n = 97 samples) and invertebrates (n = 99 samples) were collected from coastal sites in Koojesse and Peterhead Inlets in the summers of 2018 and 2019 (Fig. 3.1 open and closed circles). Coastal sampling depths ranged from 15 to 56 m. Samples were collected by boat using a Van Veen Grab and a Subtidal Beam Trawl with an opening size of 99.1 cm × 50.8 cm and a cod-end mesh size of 9.5 mm. Arctic Char (*Salvelinus alpinus*, n = 119) were caught with 50 m multi-mesh gillnets (38 – 140 mm mesh sizes) at various locations in inner Frobisher Bay in summers of 2018 and 2019 (Fig. 3.1 triangles). Invertebrates and fish were identified to the lowest taxonomic resolution feasible and subsequently frozen to -80 ºC. Taxonomic identification was verified with voucher specimens that were frozen to -20 ºC or preserved in ethanol and sent to taxonomists at Université Laval, Québec. Species names accepted by the World Register of Marine Species were used (WoRMS Editorial Board, 2022).

Muscle tissue for Hg and stable isotope analyses was dissected from invertebrates of sufficient size (e.g., Caridea). Whole bodies were analyzed when invertebrates were too small to have sufficient muscle tissue dissected (e.g., Gammaridea), including all zooplankton. Organisms that were too small to be analyzed individually were combined (within taxa) to obtain sufficient sample mass for analyses. Skinless dorsal muscle tissue was excised from fish. All tissue samples were frozen to -20 ºC and, along with sediment samples, were subsequently freeze-dried (Freezone Plus 2.5 Litre Cascade Benchtop Freeze Dry Systems, Labconco, Kansas City, USA) for 48 h or until sufficiently dry. Samples were then homogenized with a glass mortar and pestle or stainless-steel scissors and transferred to acid-washed 20 mL borosilicate glass scintillation vials for subsequent laboratory analyses.

3.2.3 Stable Isotope Analysis

Prior to analyses of stable isotopes of carbon and nitrogen, inorganic carbon was removed from zooplankton and macroinvertebrate samples with an exoskeleton using drop-by-drop additions of 10% trace

metal grade hydrochloric acid (Jacob et al., 2005). Samples were dried in a fumehood at room temperature until excess acid was exhausted, followed by 24–48 h at 50 ºC in a drying oven. Once dried, the samples were re-homogenized. If hygroscopic salts were present, the samples were rinsed with ultra pure milli-q water (Milli-Q SimPak1, MilliporeSigma), placed in a drying oven at 50 ºC for 48 h, and then re-homogenized.

Dried tissue samples were weighed in tin capsules (Tin Capsules Pressed Standard Weight 5 × 3.5 mm, Elemental Microanalysis Ltd., Okehampton, UK) with an analytical balance (XP205 DeltaRange, Mettler-Toledo GmbH, Greifensee, Switzerland). Every eleventh sample was weighed in duplicate. Samples were then analyzed for $\delta^{15}N$ and $\delta^{13}C$ using a 4010 Elemental Analyzer (CNSO 4010, Costech Analytical Technologies Inc., Valencia, USA) coupled to a Delta Plus XL Continuous Flow Isotope Ratio Mass Spectrometer (Thermo Finnigan, Bremen, Germany) at the University of Waterloo Environmental Isotope Laboratory. Machine analytical precision of ± 0.2‰ for $\delta^{13}C$ and ± 0.3‰ for $\delta^{15}N$ was verified by measurement of internal laboratory standards cross-calibrated against international standards of Vienna Pee Dee Belemnite for $\delta^{13}C$ (Craig, 1957) and atmospheric nitrogen for $\delta^{15}N$ (Mariotti, 1983). Standards included International Atomic Energy Agency standards CH3 and CH6 for carbon and N1 and N2 for nitrogen. Samples of particulate organic matter (POM) were analyzed for $\delta^{13}C$ and $\delta^{15}N$ with a Delta V Plus Continuous Flow Isotope Ratio Mass Spectrometer (Thermo Finnigan, Bremen, Germany) coupled to a Carlo Erba elemental analyzer (CE NC2500, Milan, Italy) at the University of New Brunswick Stable Isotopes in Nature Laboratory. Reported machine analytical precisions were ± 0.2‰ for both $\delta^{13}C$ and $\delta^{15}N$, with measurement accuracy similarly verified using internal laboratory standards cross-calibrated against international standards. The mean relative percent difference (RPD) of all analyzed sample duplicates (n = 87) was 2.8%.

3.2.4 Mercury Analysis

Homogenized, freeze-dried tissue samples and sediment samples were weighed (25–50 mg) into nickel boats and analyzed for total mercury (THg) following U.S. EPA method 7473 (U.S. EPA, 2007) using thermal decomposition and atomic absorption spectrophotometry with a dual-cell Milestone DMA-80 Direct Mercury Analyzer (DMA80, Milestone Inc., Shelton USA, Milestone S.r.l. Sorisole, Italy) at either the University of Waterloo, Waterloo, ON or the Biotron Analytical Services Laboratory (Biotron) at Western University, London, ON. Precision was assessed by analyzing every tenth sample in duplicate. Sample measurements were accepted when the mean relative percent difference (RPD) was <10% for duplicates within each daily batch of samples analyzed. The mean RPD of all duplicates (n = 70) was 4.8%. Machine accuracy was assessed by analyzing National Research Council of Canada certified reference materials (CRMs) at the beginning, middle, and end of each batch of samples analyzed. Certified reference

materials and their acceptable percent recoveries (THg mean certified value ± S.D.) were fish protein (DORM-4; 0.412 ± 0.036 mg/kg) and lobster hepatopancreas (TORT-3; 0.292 ± 0.022 mg/kg). Sample measurements were accepted when CRM values were within 10% of their certified value (U.S. EPA, 2007). The mean method detection limit, calculated as 3 × the standard deviation of blanks, was 0.25 ng. Seawater samples were analyzed for THg following U.S. EPA method 1631 (U.S. EPA, 2002) using a Tekran model 2600 with a detection limit of 0.0014 ng at Biotron.

Methyl mercury (MeHg) concentrations were quantified in seawater, and in at least two replicates for taxonomic groupings of fish, invertebrates, and zooplankton. Individuals of similar size were chosen as replicates for fish and invertebrates. MeHg concentrations were measured following U.S. EPA method 1630 (U.S. EPA, 1998) using cold vapor atomic fluorescence spectroscopy (CVAFS) with a Tekran Model 2700 automated methylmercury analysis system at Biotron. Method detection limits for solid and aqueous samples were 0.051 ng/g, and 0.0002 ng, respectively. For each set of replicates, the average percent MeHg (% MeHg) was calculated by dividing the MeHg concentration by the THg concentration and multiplying by 100 (e.g., Burke et al., 2020). Average % MeHg for each taxon was calculated when duplicate RPD < 10 %. If RPD > 10%, two additional replicates (for that species or taxa) were sent for MeHg analysis. Taxa-specific average % MeHg was then used to estimate MeHg concentrations for all individuals analyzed for THg. For some taxa, replicates were analyzed for THg concentration but not MeHg concentration due to low sample mass. In these cases, MeHg concentration was calculated using the % MeHg value from a congeneric species. Taxa for which this was applied were: *Hiatella* sp. (% MeHg from *Hiatella arctica*), *Icelus spatula* (% MeHg from *Icelus bicornis*), *Littorina* sp. (% MeHg from *Littorina saxatilis*), *Musculus discors* (% MeHg from *Musculus niger*), and *Myoxocephalus scorpiodes* (% MeHg from *Myoxocephalus* sp.).

3.2.5 Data Analysis

All analyses were conducted in R version 4.0.5 (R Core Team, 2020) with Type I error set to $\alpha = 0.05$. Residuals were assessed for normality using the Shapiro-Wilk W test (Shapiro & Wilk, 1965), and residuals plots were visually inspected for homogeneity of variances (Zar, 2018). Data were $\log_{10}$ transformed when the assumption of normality of residuals was not met.

The filter-feeding bivalve *Mya truncata*, a relatively long-lived primary consumer, was used to assess differences in $\delta^{15}N$ baseline among sample sites: Koojesse Inlet, Peterhead Inlet, and Kituriaqannigituq. *Mya truncata* were not collected from Faris Island, so two filter-feeding bivalve species (*Hiatella arctica* and *Musculus niger*) were used to estimate $\delta^{15}N$ baseline at this site. A one-way ANOVA revealed significant among-site differences in $\delta^{15}N$ values of the primary consumers sampled ($F_{3, 22} = 24.97$,

$p < 0.001$; Table S3.1, Appendix B). $\delta^{15}N$ values were thus baseline-corrected by subtracting the average, site-specific $\delta^{15}N_{primary\ consumer}$ value from $\delta^{15}N$ values for all other taxa. The resulting adjusted $\delta^{15}N$ ($\delta^{15}N_{adj}$) values were used in all subsequent statistical analyses.

3.2.5.1 Food Web Structure

To assess food web structure and estimate habitat-specific rates of Hg biomagnification, species were classified into one of three food web categories: benthic, benthopelagic, or pelagic. Food web classifications and feeding modes (e.g., grazer, deposit feeder, suspension feeder) were assigned according to definitions published by Macdonald et al. (2010) and Jumars et al. (2015), and used by Stasko et al. (2018). To assess food web structure, Layman's community metrics (Layman et al., 2007) were calculated for each food web: $\delta^{15}N$ range (NR; diversity in trophic levels), $\delta^{13}C$ range (CR; diversity in basal carbon sources), mean distance to centroid (CD; average trophic diversity), mean nearest neighbour distance (NND; redundancy in trophic ecologies), standard deviation of nearest neighbour distance (SDNND; evenness of trophic distributions), and total area (TA; total isotopic niche space). To obtain better estimates of total occupied isotopic niche space, standard ellipse area corrected for small sample size (SEA_C), which encompasses 40% of data, and a Bayesian standard ellipse area (SEA_B) were also calculated for each food web using the SIBER package in R (Jackson et al., 2011). Values for SEA_B were calculated via 200,000 iterations with a 1000 burn-in and two chains. Posterior modal values and 95% credible intervals are reported. Proportions of food web overlap were also assessed with SIBER, an SEA_C ellipse overlap proportion >0.60 was deemed significant (e.g., Guzzo et al., 2013). Primary producers and POM were not included in analyses of food web structure because isotopic values of primary producers and POM are spatially and seasonally variable in marine systems (e.g., Hansen et al., 2012; Søreide et al., 2006).

3.2.5.2 Total and Methyl Mercury Concentrations

Mean values of THg and MeHg concentrations were calculated for each taxon. Taxa mean % MeHg values were calculated and were linearly regressed against $\delta^{15}N_{adj}$. To compare Hg concentrations among food webs, mean and range of THg and MeHg concentrations were calculated for each food web.

3.2.5.3 Biomagnification of Mercury

Trophic magnification slopes (TMS) and trophic magnification factors (TMF) were calculated for the benthic, benthopelagic, and pelagic food webs of inner Frobisher Bay. The TMS value indicates the Hg biomagnification potential of a food web, and was calculated for each food web as the slope of the linear regression of $\log_{10}$ MeHg concentrations (ng/g dry weight) and $\delta^{15}N_{adj}$ values. The TMF value indicates the average increase in Hg concentration per trophic level, and was calculated for each food web as the antilog

of the regression slope (e.g., Borgå et al., 2011; Lavoie et al., 2013). An analysis of covariance (ANCOVA) was used to compare regression slopes among food webs.

3.3 Results

3.3.1 Food Web Structure

Benthic food webs were longer, supported by more diverse carbon sources, had more trophic redundancy, and had larger niche sizes than either the benthopelagic or pelagic food webs. Range of $\delta^{15}N_{adj}$ (NR) for the benthic food web was 9.07‰ whereas ranges for the pelagic and benthopelagic food webs were 5.38‰ and 6.67‰, respectively (Table 3.1, Table 3.2, Fig. 3.2A). The $\delta^{13}C$ range of the benthic food web was > 3 times larger than either of the other two food webs. Carbon isotope values ranged from -24.08‰ to -13.63‰ (CR = 10.46‰) in the benthic food web, whereas ranges for the pelagic and benthopelagic food webs were -23.54 to -20.57‰ (CR = 2.97‰) and -19.96 to -16.81‰ (CR = 3.15‰), respectively (Table 3.1, Table 3.2, Fig. 3.2). Trophic diversity was over 1.5 times larger for the benthic (CD = 2.90) food web compared to the benthopelagic (CD = 1.89) and pelagic (CD = 1.81) food webs (Table 3.2, Fig. 3.2). Greater trophic redundancy was observed in the benthic food web (NND = 0.65) as compared to the pelagic (NND = 1.43) and benthopelagic (NND = 1.09) food webs (Table 3.2, Fig. 3.2). Similarly, benthic food webs had a more even distribution of species within the isotopic niche space (SDNND = 0.45) than the benthopelagic and pelagic (SDNND = 0.59 and 0.67, respectively) food webs (Table 3.2, Fig. 3.2). Given the larger range in both $\delta^{15}N$ and $\delta^{13}C$ values, the two-dimensional isotopic niche area of the benthic food web exceeded that of both the pelagic and benthopelagic food webs. SEA_C and SEA_B values of the benthic food web were approximately 2 times greater than for the pelagic and benthopelagic food webs (Table 3.2, Fig. 3.2B; Fig. S3.1, Appendix B). The overlap between the food webs never exceeded 0.34, with values <0.60 indicative of insignificant overlap (Guzzo et al., 2013), i.e. benthic vs benthopelagic (0.34), benthic vs pelagic (0.03) and pelagic vs benthopelagic (0.00).

3.3.2 Total and Methyl Mercury Concentrations

When considering all taxa in all food webs, percent MeHg (% MeHg) ranged from 3.4 % to 100 % (Table 3.3). Percent MeHg did not significantly increase with increasing trophic level, and $\delta^{15}N_{adj}$ explained only 9% of the observed variation in % MeHg (Linear regression, % MeHg = 3.56 ($\delta^{15}N_{adj}$) + 40.59, R^2_{adj} = 0.09, $p > 0.05$; Fig. S3.2, Appendix B) which was largely a result of several benthic species from polychaeta, ophiuroidea, and holothuriodea that had high $\delta^{15}N_{adj}$ values and low % MeHg values, and several bivalvia species that had low $\delta^{15}N_{adj}$ values and high % MeHg values. When considering the reduced matched set of species for which both THg and MeHg concentrations were available, the benthopelagic food web had the highest mean ± SE THg (262.88 ± 80.37 ng/g dw; n = 6) and MeHg (240.61 ± 79.49 ng/g

dw; n = 6) concentrations, followed by the benthic food web (THg = 93.71 ± 34.80 ng/g dw; MeHg = 73.39 ± 35.42 ng/g dw; n = 28), and the pelagic food web had the lowest mean concentrations (THg = 62.48 ± 22.61 ng/g dw; MeHg = 20.93 ± 13.07 ng/g dw; n = 4; Table 3.3). When considering the full set of taxa for which only THg data were available, the overall food web mean THg concentrations were 216.60 ± 59.20 ng/g dw (n = 9) and 98.47 ± 23.30 ng/g dw (n = 43) for the benthopelagic and benthic food webs, respectively. When considering the full set of taxa for which MeHg data were available in the pelagic food web, the overall mean MeHg concentration was 16.89 ± 8.72 ng/g dw (n = 6; Table 3.3). The benthic food web had the largest range in mean THg concentrations (979.11 ng/g dw) and MeHg concentrations (989.44 ng/g dw), followed by the benthopelagic food web (537.37 ng/g dw and 550.36 ng/g dw), and the pelagic food web (109.52 ng/g dw and 55.67 ng/g dw; Table 3.3). The benthic primary producers, periphyton (11.11 ± 1.83 ng/g dw) and kelp (*Desmarestia aculeata*, 5.71 ± 0.03 ng/g dw; *Fucus vesiculosis*, 6.99 ± 0.77 ng/g dw), had the lowest THg concentrations of all biota (Table 3.3). Seawater samples had THg concentrations below detection limit (< 0.0014 ng/L), and the mean ± SE THg concentration of sediment samples was 1.93 ± 0.45 ng/g dw.

3.3.3 Biomagnification of Mercury

The TMS and TMF values indicated that MeHg did not biomagnify in the benthic food web ($p > 0.05$; Table 3.4, Fig. 3.3), but did biomagnify in the pelagic and benthopelagic food webs ($p < 0.05$; Table 3.4, Fig. 3.3). The variation in MeHg concentrations was best explained by $\delta^{15}N_{adj}$ in the benthopelagic food web (88%), followed by the pelagic food web (79%). Only 9% of variability in MeHg concentrations in organisms in the benthic food web was explained by $\delta^{15}N_{adj}$ (Table 3.4). Contrary to what was predicted, TMS and TMF values were numerically highest in the benthopelagic food web (0.201, 1.59), intermediate in the pelagic food web (0.183, 1.52), and lowest in the benthic food web (0.079, 1.20; Table 3.4, Fig. 3.3). Estimated slopes did not statistically differ among food webs (ANCOVA, $F_{2, 34} = 1.030$, $p > 0.05$).

3.4 Discussion

Pairing food web structural analyses with biomagnification calculations informed our understanding of dietary Hg pathways in an under-studied Arctic marine environment. Relatively higher complexity in the benthic food web was revealed by a large estimated isotopic niche area and greater redundancy in two-dimensional isotopic space (lower NND). Comparison of food web structure, and calculated biomagnification values (TMS and TMF) among benthic, benthopelagic, and pelagic food webs in inner Frobisher Bay revealed that the rate of Hg biomagnification was highest in the benthopelagic food web and lowest in the benthic food web. To our knowledge, only one other marine study has simultaneously quantified and compared benthic, benthopelagic, and pelagic food webs. The benthopelagic and pelagic

food webs in a north-temperate ecosystem were found to have similar rates of Hg biomagnification that were both significantly higher than the benthic food web (Lavoie et al., 2010). Findings of Lavoie et al. (2010) contributed to the formulation of our hypothesis that biomagnification of Hg would be lowest in the benthic food web, and consistent with our hypothesis the benthic food web had the lowest rate of Hg biomagnification. However, contrary to our hypothesis, the rate of Hg biomagnification was higher in the benthopelagic food web than in the pelagic food web.

3.4.1 Food Web Structure

Understanding food web structure is essential for gaining a thorough understanding of Hg biomagnification, as trophic ecology and interspecific relationships among organisms within a food web govern the efficiency with which energy and contaminants are transferred between trophic levels (e.g., Hobson et al., 2002; Rooney et al., 2006; Thomas et al., 2016; Trussell et al., 2006). In this study, the benthic food web displayed the greatest trophic diversity (CR and NR), the greatest trophic redundancy (i.e., species occupying similar positions within the isotopic niche space, NND), and the largest isotopic niche area (SEA_C and SEA_B), relative to the pelagic and benthopelagic food webs. These results are consistent with the relatively high complexity of coastal marine benthic food webs that has been reported by others (e.g., Linnebjerg et al., 2016; McMeans et al., 2013; Polis & Strong, 1996; Reynolds, 2008; Rooney et al., 2006). In nearshore marine ecosystems, benthic food webs are fueled by diverse basal carbon sources, including both labile and refractory pelagic and sympagic phytoplankton that have undergone sedimentation (e.g., labile phytodetritus; Feder et al., 2011; McMahon et al., 2006; Tamelander et al., 2006), terrestrial organic matter delivered by rivers (e.g., Bell et al., 2016; Divine et al., 2015), and benthic macrophytes (e.g., kelp and periphyton; Tamelander et al., 2006). Pelagic food webs, in contrast, are supported primarily by sympagic and pelagic phytoplankton (e.g., POM; McMahon et al., 2006; McMeans et al., 2013; Søreide et al., 2006; Tamelander et al., 2006). A wider range in basal carbon sources available to the benthic food web supports a greater degree of trophic omnivory (i.e., wherein a consumer can use food sources from multiple trophic levels; e.g., North et al., 2014) and a greater variety of feeding modes exhibited by benthic species; for example, scavenger, deposit feeder, detritus feeder, suspension feeder, etc. (e.g., Feder et al., 2011; Iken et al., 2005; Macdonald et al., 2010). The benthic food web had the largest isotopic niche space (e.g., SEA_C) and overlapped slightly with the pelagic food web. Overlap between the pelagic and benthic food webs likely reflects the broad range in carbon sources exploited by benthic species, including pelagic-derived food sources, such as labile phytodetritus (e.g., Iken et al., 2005, 2010; Tamelander et al., 2006). The benthic food web also overlapped with the benthopelagic food web, likely indicating the exploitation of benthic prey by higher trophic level benthopelagic species. No overlap was observed between the pelagic and benthopelagic food webs. This could be due to incomplete representation

of species in the benthopelagic food web, particularly low-trophic level species, or diet seasonality and time of sampling (e.g., Papiol et al., 2013; Tamelander et al., 2006).

Consistent with other Arctic marine food web studies, we found that the benthic food web spanned more trophic levels than the pelagic and benthopelagic food webs (e.g., Feder et al., 2011; Hobson et al., 2002; Iken et al., 2005). The increased range in nitrogen isotope ratios is likely linked to the variety of feeding strategies exhibited by benthic organisms compared to the pelagic organisms measured (e.g., 8 feeding modes in collected benthic taxa; 3 feeding modes in collected pelagic taxa; 2 feeding modes in collected benthopelagic taxa), as well as a relatively greater consumption of food sources that contain microbially re-mineralized organic matter, as re-mineralization can result in higher $\delta^{15}N$ values in consumers (Hadas et al., 2009; Lovvorn et al., 2005). In agreement with previous authors, we infer that energy pathways in benthic food webs are more complex than those in pelagic (and benthopelagic) food webs due to the presence of more functional feeding groups and a wider variety of basal food sources (e.g., Sokołowski et al., 2012), and that greater food web complexity results in weaker Hg-$\delta^{15}N$ relationships.

3.4.2 Total and Methyl Mercury Concentrations

We observed substantial inter-species variability in % MeHg, which increased 29-fold from polychaeta to fish. However, % MeHg did not significantly increase with trophic level among taxa, and only 9% of variation in % MeHg was explained by $\delta^{15}N_{adj}$ when all taxa were analyzed, regardless of food web. Fish species had the highest % MeHg in each food web, which is consistent with other studies that have found higher trophic level predatory fish to have the highest muscle tissue % MeHg values among poikilotherms (e.g., Lescord et al., 2018; Loseto et al., 2008; Mason et al., 2000).

In the pelagic food web, the *Limacina* sp. pteropod had the highest THg concentration, and Arctic Cod (*Boreogadus saida*) had the highest MeHg concentration. Species with the highest THg and MeHg concentrations in the benthic and benthopelagic food webs were Arctic Staghorn Sculpin (*Gymnocanthus tricuspis*) and Twohorn Sculpin (*Icelus bicornis*), respectively. Sculpin species have been shown to have relatively high Hg concentrations in other studies. For example, in West Greenland, Shorthorn Sculpin (*Myoxocephalus scorpius*) had the highest mean THg and MeHg concentrations of all poikilotherm species studied (Rigét et al., 2007), and in the eastern Beaufort Sea, Fourhorn Sculpin (*Myoxocephalus quadricornis*) had the highest THg and MeHg concentrations of all poikilotherm species studied (Loseto et al., 2008). Sculpin are known to feed on a variety of invertebrates and fish (e.g., Landry et al., 2018), and have a large gape size relative to their body size. A large gape size allows them to consume large prey relative to their body size (Gray et al., 2017), which may result in relatively high dietary exposure to Hg, as Hg tends to increase with body size (Gewurtz et al., 2011; Somers & Jackson, 1993; Wiener et al., 1990).

The range in THg and MeHg concentrations was largest for the benthic food web and smallest for the pelagic food web. The result is likely linked to the diverse mechanisms of Hg uptake exhibited by benthic species as a result of a wide array of feeding modes and the range of physicochemical conditions, and hence Hg concentrations, experienced by infaunal and epifaunal biota (Lawrence & Mason, 2001; Tomczyk et al., 2018). Benthic communities utilize a greater diversity of carbon sources than pelagic communities (Iken et al., 2005; Lovvorn et al., 2005; McMeans et al., 2013), and exhibit various feeding strategies (e.g., Macdonald et al., 2010; Renaud et al., 2011), which can result in variability in Hg concentrations. For example, detritivores consuming coarse detrital material are exposed to low concentrations of bioavailable MeHg because MeHg is often chelated by organic matter ligands in detrital material (Ravichandran, 2004; Tomczyk et al., 2018). Filter feeders, in contrast, may be exposed to higher bioavailable MeHg concentrations as a result of consuming dissolved organic carbon-MeHg complexes linked to microbial pathways (Hall & Meyer, 1998; Qiu et al., 2001; Sánchez-Marín et al., 2016; Tomczyk et al., 2018). Many infaunal invertebrates, such as polychaetes, bivalves, and crustaceans are exposed to and take up MeHg via respiratory surfaces or from surrounding water (Goodyear & McNeill, 1999; Gray, 2002) in addition to exposure via diet. Some invertebrates moult, which eliminates a proportion of the MeHg burden (O'Callaghan & Sullivan, 2020), and further leads to variability in MeHg concentrations among benthic biota. Differing physicochemical conditions in pelagic and benthic habitats also promotes variable Hg exposures to pelagic and benthic biota. In the marine pelagic habitat, Hg methylation is reported to take place in oxygen-deficient zones, where methylation is supported by heterotrophic decomposition and primary production (Kim et al., 2017; Kirk et al., 2012; Pongratz & Heumann, 1998; Regnell & Watras, 2019). In coastal marine benthic habitats, MeHg is primarily formed by anaerobic microbial processes via sulfate reducing bacteria, archaea, and methanogens in anoxic sediments (Gworek et al., 2016; Lehnherr, 2014). Although Hg methylation (and demethylation) occurs in both pelagic and benthic habitats, sediments have MeHg concentrations that are orders of magnitude greater than seawater (e.g., Choy et al., 2009). As a result, benthic biota can be exposed to more variable MeHg concentrations depending on the microbial community present in surface sediments and on the amount of organic matter content available, which has the ability to chelate MeHg and subsequently reduce its bioavailability (Lawrence & Mason, 2001). A larger range in THg and MeHg concentrations observed for the benthic food web compared to the pelagic and benthopelagic food webs can, therefore, be attributed to benthic species exploiting a wider variety of food sources, various mechanisms of Hg accumulation and elimination that are less prevalent in pelagic or benthopelagic taxa, and being exposed to a wider range of physicochemical characteristics that result in higher variability in Hg exposure.

3.4.3 Biomagnification of Mercury

Biomagnification of MeHg, as assessed with regressions of MeHg concentrations and $\delta^{15}N_{adj}$ values, was not statistically significant in the benthic food web. Slopes (TMS) of MeHg and $\delta^{15}N_{adj}$ regressions were, however, significant for the pelagic and benthopelagic food webs. TMS values indicate the biomagnification potential of Hg in food webs, whereas TMF values represent the average increase in Hg concentration with each trophic level (Borgå et al., 2011; Lavoie et al., 2013). High TMS and TMF values indicate high rates of Hg biomagnification, and thus higher trophic level consumers are more at risk of having high Hg concentrations, which poses greater health risks to the humans who consume them (Scheuhammer et al., 2007).

The lack of a significant relationship between MeHg concentration and $\delta^{15}N_{adj}$ in the benthic food web could reflect: i) MeHg exposure via non-dietary pathways, such as induction via the gills (Goodyear & McNeill, 1999; Gray, 2002); ii) a decoupling of $\delta^{15}N_{adj}$ and trophic level (and also Hg exposure) due to enrichment of ^{15}N in microbially-mediated organic matter in benthic habitats (Lovvorn et al., 2005); iii) the wide diversity of feeding strategies exhibited by benthos (e.g., detritivores, suspension feeders; Tomczyk et al., 2018); and/or, iv) individuals feeding at multiple trophic levels (e.g., North et al., 2014), as discussed above (section 3.4.1). The pelagic and benthopelagic food webs had lower trophic redundancy compared to the benthic food web. The pelagic and benthopelagic food webs also used a more restricted range of basal carbon sources, as indicated by smaller CR values. These results suggest that the pelagic and benthopelagic food webs could be more efficient at transferring Hg than the benthic food web, and that species/taxa at a given trophic level are more likely to feed on similar food sources (with perhaps more similar Hg concentrations). In the only other comparative marine food web Hg study we are aware of, benthopelagic and pelagic food webs were found to have similar slopes that were both higher than in the benthic food web (Lavoie et al., 2010). We posit that it is important in future studies to consider MeHg biomagnification in the benthopelagic food web in addition to the pelagic food web. Benthopelagic food webs are unique in that they couple benthic and pelagic carbon sources, which is important for nutrient cycling and for the transfer of energy among food webs and habitats (Griffiths et al., 2017; Stasko et al., 2018). Benthopelagic food webs also have a unique trophic structure because they are generally composed of mobile top predator species (McMeans et al., 2013), which may make them susceptible to relatively higher rates of Hg biomagnification.

The TMFs calculated for the food webs in this study (range 1.20 – 1.59) were all lower than the TMFs calculated for other marine food webs in the Arctic (range 1.67 – 8.70; Table 3.5). This could be due to among-study variability in methods of calculation (e.g., trophic level vs $\delta^{15}N$), number of trophic links included (Borgå et al., 2011), or a result of comparatively lower efficiency in MeHg transfer through the

inner Frobisher Bay food web. Low TMF values coupled with low MeHg concentrations at the base of the food web have positive health implications for top predators (Ferriss & Essington, 2014). Lower availability of MeHg at the base of the food web could be a result of the high tidal fluctuations that are characteristic of inner Frobisher Bay. Wave action that results from the high tides in this area re-suspends sediment (Quillien et al., 2016; Schaal et al., 2008), increasing exposure of particle surface area (Heyes et al., 2004). Mixing induced by wave action introduces oxygenated waters to sediment which reduces anaerobic methylation activity (Fitzgerald et al., 2007). Furthermore, a high degree of tidal action promotes more coastal erosion (McCann & Dale, 1986), which can release more material, such as clay and other minerals that are able to bind Hg species (Jackson, 1989; Ravichandran, 2004) and make them unavailable for methylation.

In this study, the pelagic and benthopelagic food webs had higher TMS and TMF values than the benthic food web, underlining the importance of studying MeHg pathways in multiple habitats within an ecosystem. The ecological roles and relationships of organisms in food webs are susceptible to change as a result of shifts in basal sources of production in Arctic marine environments due to climate change (Jędruch et al., 2018; McKinney et al., 2015; Stern et al., 2012). Climate-induced changes to basal energy sources and food web structure could de-stabilize food webs (Griffiths et al., 2017; McMeans et al., 2013) and alter the ratio of benthic and pelagic energy flow to higher trophic level consumers, consequently altering Hg concentrations (Jędruch et al., 2018; Stern et al., 2012). The less complex food webs in this study (i.e., pelagic and benthopelagic) appeared to exploit fewer carbon sources, and higher rates of MeHg biomagnification were observed in these food webs. Acquiring data on Hg biomagnification rates of benthic, benthopelagic, and pelagic food webs will ultimately support spatial and temporal comparisons which are critical to understanding and predicting the effects of climate-induced changes to food web structure and Hg dynamics in Arctic marine environments.

3.5 Conclusion

In this study, we found that: i) the benthic food web had the highest trophic diversity and trophic niche redundancy; ii) the benthopelagic food web had the highest mean THg and MeHg concentrations, and the benthic food web had the greatest range in concentrations; and iii) MeHg biomagnification varied among spatially proximate food webs. Greater food web complexity, as indicated by high trophic diversity and redundancy among benthic organisms, appeared to reduce the efficiency by which MeHg was transferred between trophic levels, resulting in low MeHg biomagnification in the benthic food web compared to the pelagic and benthopelagic food webs. Contrary to what was hypothesized, the benthopelagic food web had a higher rate of MeHg biomagnification than the pelagic and benthic food webs, as indicated by Trophic Magnification Slopes (TMS) and Trophic Magnification Factors (TMF). The

TMS and TMF values measured in this study were lower than those reported for other Arctic marine food webs. Collectively, these results highlight the importance of understanding the structuring of multiple food webs in Arctic marine ecosystems, particularly when Hg concentrations in their constituent higher trophic level consumers are consumed by humans, and when food webs may be differentially impacted by climate change.

3.6 Tables

Table 3.1. Food web classifications, mean ± standard error $\delta^{13}C$ (‰), $\delta^{15}N$ (‰), and baseline-adjusted $\delta^{15}N$ values ($\delta^{15}N_{adj}$, ‰) for taxa collected in inner Frobisher Bay, Nunavut, in 2018 and 2019.

Taxa	Code	Food web and feeding mode[a]	Tissue[b]	n[c]	$\delta^{13}C$ (‰)	$\delta^{15}N$ (‰)	$\delta^{15}N_{adj}$ (‰)	References for food web and feeding mode classifications[f]
Primary producers								
Particulate organic matter	POM	P	WB	41	-23.0 ± 0.2	6.5 ± 0.2	-0.3 ± 0.2	_
Periphyton	ALG	B	WB	8	-17.7 ± 0.6	6.8 ± 0.7	-0.2 ± 0.7	_
Desmarestia aculeata	DES	B	WB	2	-16.8 ± 1.7	6.9 ± 0.9	0.2 ± 0.8	_
Fucus vesiculosis	FUV	B	WB	9	-14.9 ± 0.6	7.5 ± 0.5	0.5 ± 0.4	_
Invertebrata								
Annelida								
Polychaeta	POL	B	WB	11	-19.8 ± 0.5	10.9 ± 0.4	4.2 ± 0.5	_
Harmothroe imbricata	HAR	B – CA	WB	3	-17.7 ± 0.1	12.6 ± 0.3	5.7 ± 0.3	Macdonald et al., 2010
Travisia carnea	TRC	B – CA, DPF	WB	3	-17.5 ± 0.0	13.7 ± 0.4	6.8 ± 0.4	Macdonald et al., 2010
Travisia forbesii	TRF	B – CA, DPF	WB	1	-17.1	14.8	7.9	Macdonald et al., 2010
Chaetognatha	CHA	P – CA, PR	WB	14[d]	-22.0 ± 0.2	10.3 ± 0.3	3.5 ± 0.3	Pearre, 1980; Stasko et al., 2018
Cnidaria								
Actiniaria	ACT	B – CA	WB	4[d]	-19.4 ± 0.3	12.8 ± 0.2	6.0 ± 0.2	Macdonald et al., 2010; Søreide et al., 2013; Stasko et al., 2018
Halcampa arctica	HAL	B – CA	WB	15	-18.9 ± 0.3	13.7 ± 0.2	6.7 ± 0.2	Macdonald et al., 2010; Søreide et al., 2013; Stasko et al., 2018
Crustacea								
Amphipoda								
Gammaridea	GAM	BP	WB	12[d]	-20.0 ± 0.3	9.1 ± 0.2	2.2 ± 0.2	_
Anonyx sp.	ANX	B – CA, SC	WB	1[d]	-22.0	9.2	2.3	Macdonald et al., 2010
Themisto libellula	THL	P – CA	WB	10[d]	-22.0 ± 0.4	9.7 ± 0.2	2.9 ± 0.2	Søreide et al., 2013; Stasko et al., 2018; Wesławski et al., 2010
Calanoida								
Calanus sp.	CAL	P – HE	WB	18[d]	-23.5 ± 0.1	7.7 ± 0.1	0.9 ± 0.1	Conover, 1960; Falk-Petersen et al., 2009; Stasko et al., 2018
Caridea								
Argis dentata	ARG	BP – CA	TM	6[e]	-17.6 ± 0.4	14.1 ± 0.5	7.2 ± 0.5	Stasko et al., 2018
Eualus gaimardii	EUG	BP – CA, PR	TM/WB	2	-18.1 ± 1.4	12.3 ± 0.3	5.4 ± 0.3	Birkely & Gulliksen, 2003; Graeve et al., 1997; Macdonald et al., 2010; Stasko et al., 2018; Wesławski et al., 2010
Lebbeus groenlandicus	LEG	BP – CA, PR/SC	TM	9	-16.8 ± 0.1	13.4 ± 0.2	6.5 ± 0.2	Birkely & Gulliksen, 2003; Graeve et al., 1997; Macdonald et al., 2010; Søreide et al., 2013; Stasko et al., 2018; Wesławski et al., 2010
Lebbeus polaris	LEP	BP – CA, PR/SC	TM	8[e]	-19.0 ± 0.3	11.4 ± 0.3	4.5 ± 0.3	Birkely & Gulliksen, 2003; Graeve et al., 1997; Macdonald et al., 2010; Søreide et al., 2013; Stasko et al., 2018; Wesławski et al., 2010
Sabinea septemcarinata	SAB	B – OM, PR/DPF/SC	TM/WB	3	-17.5 ± 0.7	14.5 ± 1.0	7.6 ± 1.0	Birkely & Gulliksen, 2003; Stasko et al., 2018; Wesławski et al., 2010
Sclerocrangon boreas	SCB	B – CA, PR	TM	2	-17.3 ± 0.2	14.7 ± 0.1	7.8 ± 0.1	Birkely & Gulliksen, 2003; Wesławski et al., 2010
Cirripedia								

Semibalanus balanoides	SEB	B – OM, SF	WV	3[e]	-21.3 ± 0.3	7.9 ± 0.4	1.1 ± 0.4	Macdonald et al., 2010
Isopoda								
Arcturus baffini	ARB	B – OM, SF	WB	10	-21.5 ± 0.1	10.2 ± 0.2	3.3 ± 0.2	Graeve et al., 1997
Saduria sabini	SAD	B – CA	WB	3	-18.1 ± 0.3	12.1 ± 0.1	5.2 ± 0.1	Percy, 1983; Premke et al., 2003; Stasko et al., 2018
Mysidacea								
Mysis sp.	MYI	P – HE	WB	1[e]	-20.8	8.2	0.0	Stasko et al., 2018; Wesławski et al., 2010
Echinodermata								
Echinoidea								
Strongylocentrotus droebachiensis	SOD	B – HE, GR	HB	3	-24.1 ± 1.5	8.3 ± 0.1	1.4 ± 0.1	Macdonald et al., 2010
Holothuriodea								
Myriotrochus rinkii	MYR	B – OM, DPF	WB	3	-15.4 ± 0.5	11.9 ± 0.3	3.8 ± 0.3	Stasko et al., 2018; Wagstaff et al., 2014
Ophiuroidea								
Amphilepidida	AMA	B	WB	5[e]	-20.5 ± 0.2	11.9 ± 0.2	5.0 ± 0.2	_
Ophiacantha bidentata	OPH	B – OM, SF/DPF/DTF	WB	15[e]	-19.1 ± 0.1	13.9 ± 0.3	7.0 ± 0.3	Graeve et al., 1997; Piepenburg, 2005; Stasko et al., 2018
Stegophiura nodosa	STN	B	WB	8[d]	-19.7 ± 0.2	11.7 ± 0.1	4.9 ± 0.1	Piepenburg, 2005
Mollusca								
Bivalvia	BIV	B	FM/WB	3	-20.2 ± 0.1	7.8 ± 0.1	0.9 ± 0.1	_
Astarte sp.	AST	B – OM, SF	WV	6[e]	-20.6 ± 0.1	8.8 ± 0.3	1.9 ± 0.3	Aitken & Gilbert, 1996; Macdonald et al., 2010; Søreide et al., 2013; Stasko et al., 2018
Cyrtodaria kurriana	CYR	B – FF	WVS	4	-20.2 ± 0.1	8.9 ± 0.3	2.2 ± 0.2	_
Ennucula tenuis	ENT	B – OM, DPF	WV	1	-21.3	8.6	1.7	Kędra et al., 2010; Macdonald et al., 2010; North et al., 2014; Stasko et al., 2018
Hiatella sp.	HIS	B – OM, SF	FM	2	-19.4 ± 0.1	8.6 ± 0.1	1.7 ± 0.1	Macdonald et al., 2010
Hiatella arctica	HIA	B – OM, SF	FM/WVS	9	-20.0 ± 0.1	7.9 ± 0.2	1.0 ± 0.2	Macdonald et al., 2010
Macoma loveni	MAC	B – OM, DPF/SF	WV	1	-20.0	10.2	3.3	Aitken & Gilbert, 1996; Kędra et al., 2010; Macdonald et al., 2010; North et al., 2014; Søreide et al., 2013; Stasko et al., 2018
Musculus discors	MUD	B – OM, SF	FM	1	-20.6	8.1	1.2	Macdonald et al., 2010
Musculus niger	MUN	B – OM, SF	WVS	3	-19.7 ± 0.1	7.8 ± 0.3	0.5 ± 0.2	Macdonald et al., 2010
Mya truncata	MYA	B – OM, SF	WV	24	-20.7 ± 0.1	7.0 ± 0.1	0.0 ± 0.0	Macdonald et al., 2010
Nuculana pernula	NUC	B – OM, DPF	WV	1[d]	-21.8	8.5	1.6	Kędra et al., 2010; Macdonald et al., 2010; Søreide et al., 2013; Stasko et al., 2018
Gastropoda	GAS	B	FM	1[d]	-13.6	10.0	3.4	_
Buccinidae	BUC	B – CA, PR/SC	WV/FM	2	-19.0 ± 1.8	14.2 ± 1.1	7.3 ± 1.1	Himmelman & Hamel, 1993; Lavoie et al., 2010; Macdonald et al., 2010
Colus stimpsoni	COL	B – CA, PR	FM	3	-18.2 ± 0.2	14.0 ± 0.3	7.1 ± 0.3	Macdonald et al., 2010
Limacina sp.	LIM	P – OM	WB	7[d]	-21.9 ± 0.6	8.0 ± 0.4	1.4 ± 0.4	Gilmer & Harbison, 1991; Søreide et al., 2013; Stasko et al., 2018
Littorina sp.	LIS	B – HE, GR	FM	1[d]	-18.1	10.6	3.8	Olsson et al., 2007
Littorina saxatilis	LIT	B – HE, GR	FM	2[d]	-16.9 ± 1.1	10.0 ± 0.8	3.2 ± 0.8	Olsson et al., 2007
Scabrotrophon fabricii	SCA	B	WV	1	-19.2	11.5	4.6	_
Nudibranchia								
Dendronotus sp.	DEN	B – CA	WB	3	-19.5 ± 0.4	11.9 ± 0.6	5.0 ± 0.6	Macdonald et al., 2010
Nemertea	NEM	B – CA, PR	WB	1	-18.4	12.4	5.7	Macdonald et al., 2010; Stasko et al., 2018
Priapulida								
Priapulus caudatus	PRI	B – CA, PR	WB	5	-16.8 ± 0.1	13.3 ± 0.2	6.5 ± 0.2	Macdonald et al., 2010

Pisces								
Boreogadus saida	BOR	P – CA, PR	DM	60	-20.6 ± 0.1	12.2 ± 0.1	5.4 ± 0.1	Geoffroy et al., 2011; Majewski et al., 2016; Stasko et al., 2018; Whitehouse et al., 2017
Cottidae								
Artediellus atlanticus	ART	B – CA, PR	DM	1	-17.2	14.0	7.1	Coad & Reist, 2004; Whitehouse et al., 2017
Gymnocanthus tricuspis	GYT	B – CA, PR	DM	2	-19.1 ± 0.1	15.4 ± 0.4	8.7 ± 0.3	Atkinson & Percy, 1992; Coad & Reist, 2004; Stasko et al., 2018; Whitehouse et al., 2017
Icelus bicornis	ICB	BP – CA, PR	DM	4	-18.2 ± 0.2	15.8 ± 0.2	8.9 ± 0.2	Atkinson & Percy, 1992; Stasko et al., 2018
Icelus spatula	ICS	BP – CA, PR	DM	8	-18.8 ± 0.3	14.8 ± 0.2	8.1 ± 0.2	Atkinson & Percy, 1992; Coad & Reist, 2004; Stasko et al., 2018; Whitehouse et al., 2017
Myoxocephalus sp.	MYS	B – CA, PR	DM	20[e]	-18.6 ± 0.1	12.7 ± 0.2	5.7 ± 0.2	Atkinson & Percy, 1992; Coad & Reist, 2004; Whitehouse et al., 2017
Myoxocephalus scorpioides	MYO	B – CA, PR	DM	1	-17.7	14.6	8.0	Coad & Reist, 2004
Triglops pingelii	TRP	BP – CA, PR	DM	2	-19.8 ± 0.2	12.7 ± 0.1	5.9 ± 0.1	Atkinson & Percy, 1992; Coad & Reist, 2004; Stasko et al., 2018; Whitehouse et al., 2017
Gymnelus viridis	GYV	B – CA, PR	DM	17	-19.1 ± 0.2	15.9 ± 0.3	9.1 ± 0.3	Coad & Reist, 2004
Liparis fabricii	LIP	B – CA, PR	DM	2	-17.4 ± 0.0	15.1 ± 0.3	8.2 ± 0.3	Coad & Reist, 2004; Stasko et al., 2018
Salvelinus alpinus	SAL	BP – CA, PR	DM	119	-19.6 ± 0.1	12.0 ± 0.2	5.4 ± 0.2	Dempson et al., 2002; Rikardsen et al., 2007

[a]Food webs and feeding modes: B, benthic; BP, benthopelagic; P, pelagic; CA, carnivore; HE, herbivore; OM, omnivore; BR, browser; DPF, deposit feeder; DTF, detritus feeder; FF, filter feeder; GR, grazer; PR, predator; SC, scavenger; SF, suspension feeder.

[b]Tissue types analyzed: DM, dorsal muscle; FM, foot muscle; HB, half body; TM, tail muscle; WB, whole body; WV, whole viscera; WVS, whole viscera without stomach.

[c]Number of samples.

[d]Pooled replicates.

[e]Individual and pooled replicates.

[f]Dashes (i.e., –) indicate taxa for which references were not available and food web classifications were assigned according to the habitat where the taxon was collected.

Table 3.2. Layman et al. (2007) metrics for the benthic, benthopelagic, and pelagic food webs. NR, $\delta^{15}N$ range; CR, $\delta^{13}C$ range; CD, mean distance to centroid; NND, mean nearest neighbour distance; SDNND, standard deviation of nearest neighbour distance. Also included are estimates of niche size SEA_C, standard ellipse area corrected for small sample size and SEA_B, Bayesian standard ellipse area (modal value) and the associated 95% credible interval. Number of individuals (n ind.) and number of taxa (n taxa) included in each food web are listed.

Food web	**n ind.**	**n taxa**	**NR**	**CR**	**CD**	**NND**	**SDNND**	**TA**	**SEA_C**	**SEA_B**	**SEA_B 95% CI**
Benthic	210	43	9.07	10.46	2.90	0.65	0.45	48.69	13.48	12.90	9.73 – 17.83
Benthopelagic	170	9	6.67	3.15	1.89	1.09	0.59	9.53	6.36	5.27	2.72 – 11.14
Pelagic	110	6	5.38	2.97	1.81	1.43	0.67	7.80	7.65	5.42	2.31 – 14.45

Table 3.3. Mean ± standard error of total mercury (THg) and methyl mercury (MeHg) concentrations (ng/g dry weight), and percent methyl mercury (% MeHg) values for taxa collected in inner Frobisher Bay, Nunavut, in 2018 and 2019. The number of samples analyzed for THg (n_T) and the number of samples analyzed for MeHg (n_M) are listed. B, benthic; BP, benthopelagic; P, pelagic; NA, not analyzed.

Taxa	Code	Food web	n_T	n_M	THg (ng/g dw)	MeHg (ng/g dw)	% MeHg (%)
Primary producers							
Particulate organic matter	POM	P	NA	NA	NA	NA	NA
Periphyton	ALG	B	8	NA	11.11 ± 1.83	NA	NA
Desmarestia aculeata	DES	B	2	NA	5.71 ± 0.03	NA	NA
Fucus vesiculosis	FUV	B	9	NA	6.99 ± 0.77	NA	NA
Invertebrata							
Annelida							
Polychaeta	POL	B	11	NA	158.41 ± 83.87	NA	NA
Harmothroe imbricata	HAR	B	3	2	48.16 ± 6.75	31.80 ± 4.46	66.03 ± 8.29
Travisia carnea	TRC	B	3	2	39.36 ± 7.84	5.30 ± 1.06	13.46 ± 5.93
Travisia forbesii	TRF	B	1	1	31.76	1.09	3.42
Chaetognatha	CHA	P	NA	4	NA	13.22 ± 0.82	NA
Cnidaria							
Actiniaria	ACT	B	4	4	40.91 ± 7.06	26.21 ± 4.52	64.07 ± 12.05
Halcampa arctica	HAL	B	15	4	39.74 ± 2.01	25.80 ± 1.31	64.94 ± 4.62
Crustacea							
Amphipoda							
Gammaridea	GAM	BP	12	4	33.97 ± 2.70	20.97± 1.67	61.74 ± 2.77
Anonyx sp.	ANX	B	1	1	26.87	11.40	42.30
Themisto libellula	THL	P	2	2	53.98 ± 19.76	9.45 ± 1.40	19.12 ± 4.41
Calanoida							
Calanus sp.	CAL	P	NA	4	NA	4.42 ± 0.43	NA
Caridea							
Argis dentata	ARG	BP	6	NA	238.46 ± 106.47	NA	NA
Eualus gaimardii	EUG	BP	2	NA	80.32 ± 60.77	NA	NA
Lebbeus groenlandicus	LEG	BP	9	2	377.65 ± 59.57	280.48 ± 44.24	74.27 ± 1.09
Lebbeus polaris	LEP	BP	8	2	87.02 ± 12.39	74.78 ± 10.65	85.93 ± 5.83
Sabinea septemcarinata	SAB	B	3	NA	83.73 ± 32.46	NA	NA
Sclerocrangon boreas	SCB	B	2	NA	262.36 ± 111.03	NA	NA
Cirripedia							
Semibalanus balanoides	SEB	B	3	3	15.75 ± 1.41	4.32 ± 0.39	27.40 ± 5.17
Isopoda							
Arcturus baffini	ARB	B	10	2	19.44 ± 1.02	12.23 ± 0.64	62.90 ± 2.12
Saduria sabini	SAD	B	3	3	44.25 ± 3.14	23.42 ± 1.66	52.91 ± 11.13
Mysidacea							
Mysis sp.	MYI	P	1	2	13.17	6.45	49.01 ± 0.42
Echinodermata							
Echinoidea							
Strongylocentrotus droebachiensis	SOD	B	3	NA	65.00 ± 2.37	NA	NA
Holothuriodea							
Myriotrochus rinkii	MYR	B	3	3	20.92 ± 1.43	3.20 ± 0.22	15.29 ± 3.79
Ophiuroidea							
Amphilepidida	AMA	B	5	NA	33.66 ± 2.37	NA	NA
Ophiacantha bidentata	OPH	B	15	2	52.47 ± 2.34	17.60 ± 0.78	33.53 ± 3.82
Stegophiura nodosa	STN	B	8	2	23.77 ± 1.59	12.52 ± 0.84	52.69 ± 2.63
Mollusca							
Bivalvia	BIV	B	3	NA	46.68 ± 6.68	NA	NA
Astarte sp.	AST	B	6	NA	63.04 ± 3.80	NA	NA
Cyrtodaria kurriana	CYR	B	4	4	11.42 ± 3.09	8.66 ± 2.34	75.81 ± 4.60
Ennucula tenuis	ENT	B	1	NA	122.69	NA	NA
Hiatella sp.	HIS	B	2	NA	105.02 ± 32.63	70.39 ± 21.87[a]	NA
Hiatella arctica	HIA	B	9	4	29.02 ± 4.56	19.45 ± 3.05	67.02 ± 4.28
Macoma loveni	MAC	B	1	NA	69.13	NA	NA
Musculus discors	MUD	B	1	NA	81.30	34.17[a]	NA
Musculus niger	MUN	B	3	2	87.72 ± 15.92	36.87 ± 6.69	42.03 ± 0.70
Mya truncata	MYA	B	24	6	21.03 ± 1.14	10.87 ± 0.59	51.66 ± 3.83
Nuculana pernula	NUC	B	1	NA	67.86	NA	NA
Gastropoda	GAS	B	1	NA	41.22	NA	NA

Buccinidae	BUC	B	2	NA	201.70 ± 89.28	NA	NA
Colus stimpsoni	COL	B	3	NA	76.72 ± 29.25	29.25	NA
Limacina sp.	LIM	P	1	3	122.69	7.72 ± 1.16	6.30
Littorina sp.	LIS	B	1	NA	39.33	20.77[a]	NA
Littorina saxatilis	LIT	B	2	3	34.22 ± 0.79	18.07 ± 0.42	52.81 ± 1.99
Scabrotrophon fabricii	SCA	B	1	NA	158.11	NA	NA
Nudibranchia							
Dendronotus sp.	DEN	B	3	2	72.38 ± 3.86	30.88 ± 1.65	42.67 ± 1.54
Nemertea	NEM	B	1	1	63.24	37.24	58.89
Priapulida							
Priapulus caudatus	PRI	B	5	3	26.62 ± 2.55	10.67 ± 1.02	40.06 ± 4.06
Pisces							
Boreogadus saida	BOR	P	60	5	60.09 ± 3.48	60.09 ± 3.48	115.71 ± 9.08[b]
Cottidae							
Artediellus atlanticus	ART	B	1	NA	160.22	NA	NA
Gymnocanthus tricuspis	GYT	B	2	2	990.53 ± 299.79	990.53 ± 299.79	101.02 ± 5.00[b]
Icelus bicornis	ICB	BP	4	4	571.33 ± 138.03	571.33 ± 138.03	100.90 ± 7.32[b]
Icelus spatula	ICS	BP	8	NA	285.06 ± 60.62	285.06 ± 60.62[a]	NA
Myoxocephalus sp.	MYS	B	20	7	58.49 ± 12.01	56.21 ± 10.27	98.38 ± 10.94
Myoxocephalus scorpioides	MYO	B	1	NA	220.26	216.70 [a]	NA
Triglops pingelii	TRP	BP	2	NA	53.32 ± 2.14	NA	NA
Gymnelus viridis	GYV	B	17	4	219.84 ± 11.89	192.44 ± 10.41	87.54 ± 3.43
Liparis fabricii	LIP	B	2	2	159.91 ± 2.12	126.24 ± 1.67	78.94 ± 1.90
Salvelinus alpinus	SAL	BP	119	8	222.26 ± 15.74	211.02 ± 14.94	94.94 ± 5.27

[a]Taxa whose MeHg concentration was calculated with the % MeHg value from a congener species.

[b]Taxa whose % MeHg exceeded 100 % due to analytical error and therefore mean ± standard error MeHg concentration was deemed equivalent to the mean ± standard error THg concentration.

Table 3.4. Trophic magnification slopes (TMS), trophic magnification factors (TMF), and regression results of $\log_{10}$ MeHg (ng/g dw) and $\delta^{15}N_{adj}$ (‰) for the benthic (n = 28 taxa), benthopelagic (n = 6 taxa), and pelagic (n = 6 taxa) food webs. Regression slopes did not differ significantly from one another (ANCOVA, $F_{2, 34} = 1.030$, $p > 0.05$).

Food web	**TMS**	**TMS SE**	**TMF**	**Intercept**	**R^2_{adj}**	**p**
Benthic	0.079	0.041	1.20	1.004	0.09	> 0.05
Benthopelagic	0.201	0.032	1.59	1.000	0.88	< 0.01
Pelagic	0.183	0.042	1.52	0.606	0.79	< 0.05

Table 3.5. Summary of reported trophic magnification slopes (TMS) and trophic magnification factors (TMF), and indices of how factors were calculated ($\delta^{15}N$ or TL, trophic level; TEF, trophic enrichment factor; unit of mercury (Hg) measurement, dry weight (dw), wet weight (ww)) for several Arctic marine food webs. Locations are listed in order from west to east. Values reported in this study are highlighted in bold. NA, not available.

Location	Sampling year	Food web	Biota included	$\delta^{15}N$/ TL	TEF	Hg unit	TMS		TMF		References
							THg	MeHg	THg	MeHg	
Chukchi Sea, Alaska	2009 – 2010	Benthic	Invertebrates	$\delta^{15}N$	NA	ng/g dw	0.100	0.190	NA	NA	Fox et al., 2014
Beaufort Sea, NWT	2002 – 2004, 2006	Epibenthic	Invertebrates, Fish, Mammals	$\delta^{15}N$	NA	µg/g dw	0.232	0.254	NA	NA	Loseto et al., 2008
		Pelagic	Zooplankton, Fish, Mammals	$\delta^{15}N$	NA	µg/g dw	0.254	0.311	NA	NA	
Nasaruvaalik Island, NU	2011	Pelagic	Jellyfish, Zooplankton, Invertebrates, Fish	$\delta^{15}N$	NA	ng/g dw	0.036	0.157	1.37	3.96	Clayden et al., 2015
			Jellyfish, Zooplankton, Invertebrates, Fish, Seabirds	$\delta^{15}N$	NA	ng/g dw	0.095	0.267	2.13	7.65	
Lancaster Sound, NU	1988 – 1990	Not specified	POM, Zooplankton, Invertebrates, Fish, Seabirds, Mammals, *Ursus maritimus*	$\delta^{15}N$	NA	µg/g dw	0.200	NA	1.58	NA	Atwell et al., 1998
Pond Inlet, NU	2005 – 2008, 2010	Not specified	Zooplankton, Invertebrates, Fish	TL	3.4	ng/g dw	0.450	0.760	2.82	5.70	van der Velden et al., 2013
Northwater Polynya	1998	Pelagic	Algae, Zooplankton, Fish, Seabirds, *Phoca hispida*	$\delta^{15}N$	NA	µg/g ww	0.197	0.223	1.57	1.67	Campbell et al., 2005
Frobisher Bay, Iqaluit, NU	2004, 2010	Not specified	Zooplankton, Invertebrates, Fish	TL	3.4	ng/g dw	0.44	0.75	2.77	5.57	van der Velden et al., 2013
Frobisher Bay, Iqaluit, NU	**2018 – 2019**	**Benthic**	**Invertebrates, Fish**	**$\delta^{15}N$**	**NA**	**ng/g dw**	**NA**	**0.079**	**NA**	**1.20**	**This study**
		Benthopelagic	**Invertebrates, Fish**	**$\delta^{15}N$**	**NA**	**ng/g dw**	**NA**	**0.201**	**NA**	**1.59**	
		Pelagic	**Zooplankton, Fish**	**$\delta^{15}N$**	**NA**	**ng/g dw**	**NA**	**0.183**	**NA**	**1.52**	
West Greenland	2003 – 2004	Not specified	Zooplankton, Invertebrates, Fish, Seabirds, Mammals	$\delta^{15}N$	NA	mg/kg dw	0.183	0.339	NA	NA	Rigét et al., 2007
Kongsfjorden, Svalbard, Norway	2005 – 2006	Pelagic	Fish, Seabirds	TL	3.4	µg/g ww	NA	NA	4.87	NA	Jæger et al., 2009
	2007	Pelagic	Zooplankton, Fish, Seabirds	TL	3.8	ng/g dw	NA	0.941	NA	8.70	Ruus et al., 2015

3.7 Figures

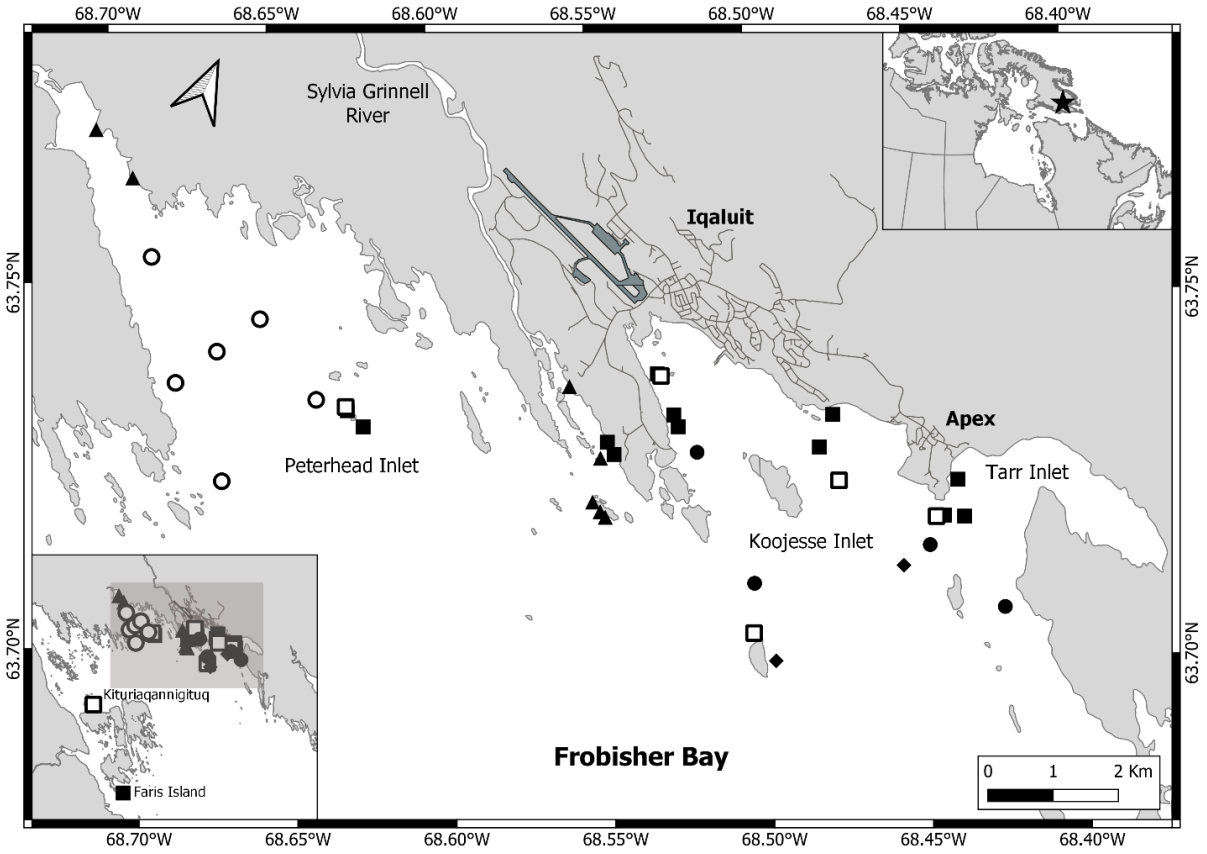

Figure 3.1. Map of inner Frobisher Bay, Nunavut. Shapes correspond to sampling sites: open circles, coastal invertebrates, fish, zooplankton, and POM sampled in 2019; closed circles, coastal invertebrates, and fish sampled in 2018 and 2019, and zooplankton and POM sampled in 2019; diamonds, coastal invertebrates and fish sampled in 2018 and 2019, and zooplankton, POM, and seawater sampled in 2019; open squares, *Mya truncata* (MYA) sampled in 2019; closed squares, intertidal invertebrates, fish, and sediment sampled in 2019; triangles, *Salvelinus alpinus* (SAL) sampled in 2018 and 2019.

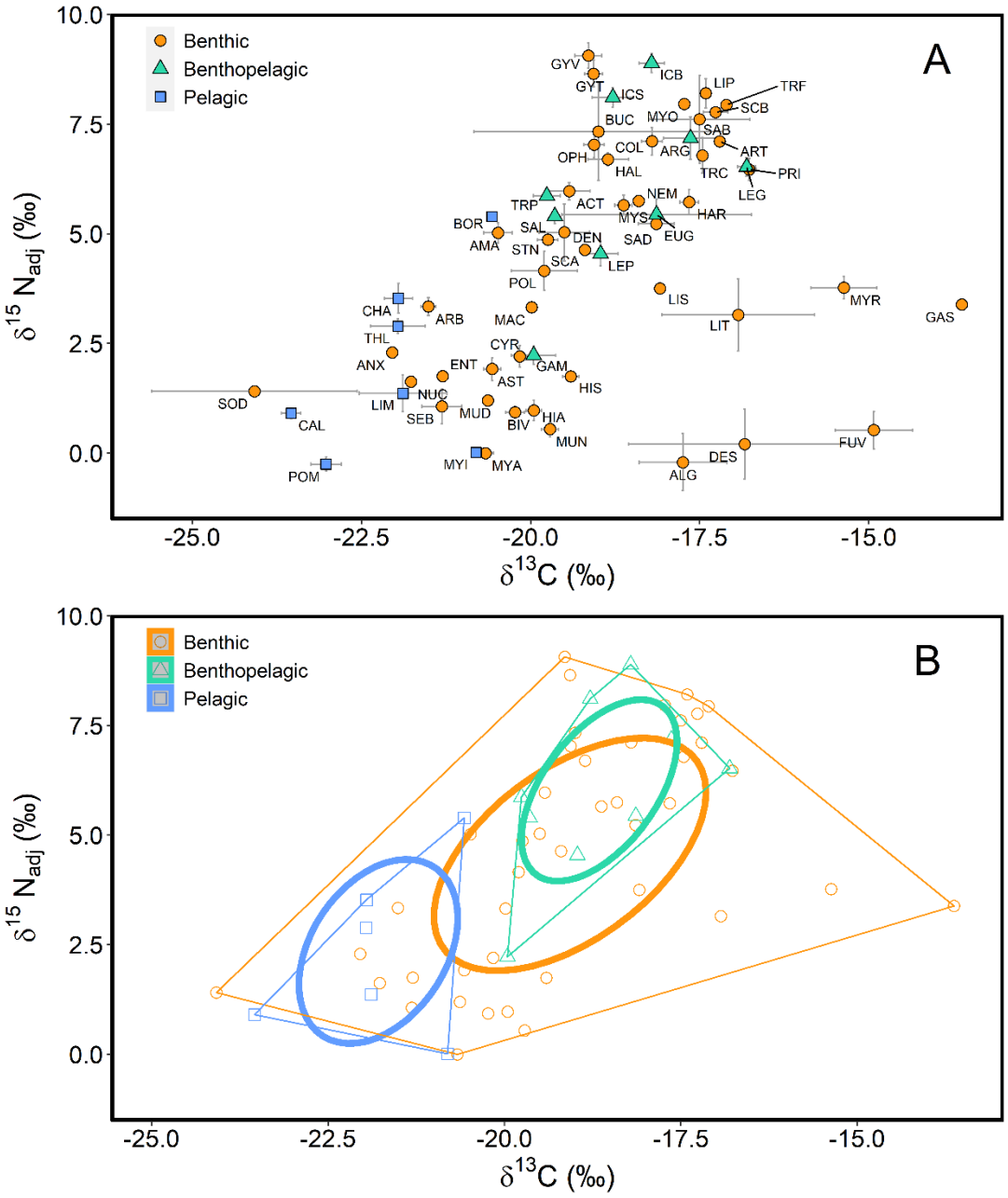

Figure 3.2. A) Bivariate plot of mean and standard error of baseline-adjusted $\delta^{15}N_{adj}$ (‰) and $\delta^{13}C$ (‰) for taxa collected in inner Frobisher Bay, Nunavut, in 2018 and 2019. Labels refer to codes listed in Table 3.1. Additional information for organisms with low $\delta^{15}N$ values and less negative $\delta^{13}C$ values (lower right of bivariate plot) is provided in Appendix B (see Supplementary Information, SI 3.1). B) Standard ellipse areas corrected for small sample size (SEA_C; thick lines) and convex hulls representing Total Area (TA; thin lines) for each food web.

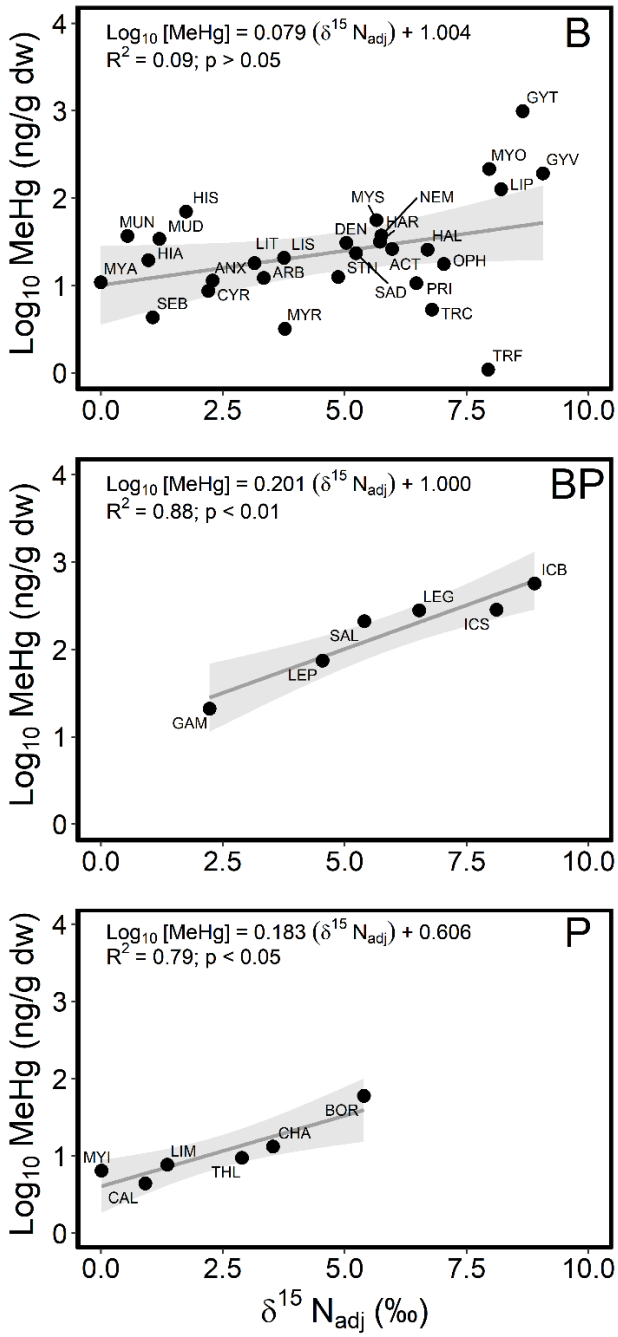

Figure 3.3. Linear regressions and 95% confidence intervals for slopes (grey area) of mean $\delta^{15}N_{adj}$ (‰) values and $\log_{10}$ MeHg (ng/g dw) concentrations for taxa collected in inner Frobisher Bay, Nunavut, in 2018 and 2019. B, benthic food web; BP, benthopelagic food web; P, pelagic food web. Labels refer to codes listed in Table 3.1.

Chapter 4
Conclusion

4.1 Summary of Findings

Mercury (Hg) is a heavy metal that can affect the quality and safety of subsistence food sources in the Canadian North (Chételat et al., 2020; Dietz et al., 2009, 2019; Douglas et al., 2012). Canada's Arctic Indigenous peoples are at an elevated risk of Hg exposure due to cultural and dietary dependence on Arctic wildlife (Priest & Usher, 2004). The Arctic environment is rapidly changing as a result of climate change (CCCR, 2019; IPCC, 2013), and it is unclear what the net effects of climate change on Hg concentrations in wildlife will be (AMAP, 2011). Gathering baseline information on Hg concentrations and bioaccumulation in Arctic ecosystems is critical so that we can understand how Hg accumulation and concentrations are changing over time, and so that processes responsible for change can be elucidated. The research presented in this thesis includes some of the first comprehensive Hg baseline data for Nunavut's inner Frobisher Bay organisms. The research was conducted in collaboration with Canada's Coastal Environmental Baseline Program (DFO, 2020a, 2020b). Hg concentration data were acquired for a variety of fish and invertebrates, and used to assess Hg bioaccumulation in anadromous Arctic char, a staple food source of Inuit, as well as Hg biomagnification in the benthic, pelagic, and benthopelagic food webs of inner Frobisher Bay.

In Chapter 2, I investigated inter-individual variability in total Hg (THg) accumulation in anadromous Arctic char (*Salvelinus alpinus*), and sought to elucidate drivers of this variability. The objective of the study was to determine whether mean THg concentrations and relationships between THg concentrations and biological variables (e.g., age, fork length, weight, growth rate, $\delta^{15}N$, benthic reliance index based on $\delta^{13}C$, condition, hepatosomatic index, and gonadosomatic index) differed between immature and mature Arctic char. THg concentrations and stable isotope ratios, $\delta^{15}N$ and $\delta^{13}C$, were analyzed in 119 samples of Arctic char captured in several locations in inner Frobisher Bay in 2018 and 2019. Relationships between THg concentrations and biological variables differed among maturity groups for 8 of the 9 variables assessed, and stronger relationships (i.e., greater explained variation in the data) were found for mature Arctic char. Results of the study suggest there is greater inter-individual variability in factors affecting THg accumulation in immature anadromous Arctic char than in mature anadromous Arctic char. Findings also indicated that knowledge of maturity and frequency of marine migrations (i.e., feeding environment) are important when assessing Hg concentrations in anadromous Arctic char.

In Chapter 3, I investigated food web structure and methyl Hg (MeHg) biomagnification in the benthic, benthopelagic, and pelagic food webs of inner Frobisher Bay. The objectives of the study were to

determine and compare food web structure and MeHg biomagnification rates in the three food webs, and compare the biomagnification rates to literature estimates for other Arctic marine food webs. Stable isotope data ($\delta^{15}N$ and $\delta^{13}C$) were paired with mercury concentrations (THg, MeHg, % MeHg) for 62 taxa collected from various pelagic and intertidal locations in inner Frobisher Bay. Metrics that quantify food web structure (i.e., Layman's metrics; Layman et al., 2007) and the standard ellipse area (Jackson et al., 2011) were employed to describe food web structures. The biomagnification rates were calculated from regressions of $\log_{10}$ MeHg concentrations on $\delta^{15}N$. A lower rate of MeHg biomagnification was exhibited in the more complex benthic food web, and higher rates were exhibited in the less complex pelagic and benthopelagic food webs. Results suggest that higher food web complexity, as indicated by high trophic diversity and ecological niche redundancy among benthic organisms, reduced the efficiency of MeHg transfer between trophic levels.

4.2 Relevance of Findings

Combined, results from Chapter 2 and Chapter 3 highlight that Hg dynamics are complex and a variety of biological and ecological factors influence the resulting Hg concentrations found in organisms. Chapter 2 focused on species-specific biological factors that affect Hg concentrations, whereas Chapter 3 focused on how ecological factors, specifically the complexity of species interactions, affect rates of Hg biomagnification in food webs. Together, the two chapters provide insight into variables that affect Hg bioaccumulation and biomagnification in Arctic marine organisms, and in Arctic char in particular. I found that habitat and trophic ecology are key factors in governing Hg accumulation within and among species and ultimately impact Hg concentrations in Arctic marine ecosystems.

Understanding the ecological roles and relationships within and among species of an ecosystem can help to elucidate mechanisms of Hg transfer. Bottom-up controls, such as habitat and prey choice, exert a strong influence on the accumulation of Hg concentrations in biota (Ferriss & Essington, 2014; Stern et al., 2012). Investigations of Hg accumulation in lower trophic level organisms, such as invertebrates, are essential for understanding pathways of Hg exposure to higher trophic level organisms, such as Arctic char, which are an essential dietary mainstay for many Inuit. Acquisition of Hg data for both invertebrates and fish can provide critical baseline information that allows spatial and temporal comparisons, and which can facilitate a more nuanced understanding of how Hg bioaccumulation and biomagnification processes might change with a shifting climate. Such information may also help inform governmental policy to ensure that appropriate mitigation measures are implemented.

The results presented in this thesis not only explored the different biological factors that influence Hg concentrations in the anadromous Arctic char, but also provided insight into the broader food web(s)

and species aggregations that Arctic char are associated with throughout the summer season. This broadened our understanding of Arctic char prey and sympatric marine fish species and how that might influence Hg concentrations. Chapter 3 demonstrated the importance of understanding which food web prey are associated with and how that might affect Hg concentrations; for example, if Arctic char were to consume a greater proportion of benthic species, they would likely have lower Hg concentrations, and if they were to consume a greater proportion of pelagic species, they would likely have higher Hg concentrations. Furthermore, Hg concentrations in the anadromous Arctic char and coastal marine fish and invertebrates were all below the Health Canada guideline of 0.5 ppm (Health Canada, 2007; Table S4.1, Appendix C), and the Hg biomagnification rates calculated for the food webs of inner Frobisher Bay (Chapter 3) were all below biomagnification rates calculated for other Arctic marine food webs (Table 3.5). These results suggest that the inner Frobisher Bay anadromous Arctic char and marine taxa sampled in this study are currently safe for consumption in regards to Hg concentrations.

4.3 Climate Change

Climate change has the potential to alter Hg dynamics and pathways of energy transfer in food webs. The Arctic is warming at three times the global rate (CCCR, 2019), and the consequent environmental changes influence the global cycling of Hg (e.g., Krabbenhoft & Sunderland, 2013) as well as organismal and food web ecology (CACAR, 2012; Kędra et al., 2015). As temperatures are rising, climate-induced permafrost thaw is increasing the bioavailability of legacy Hg deposits (Amos et al., 2013; Obrist et al., 2018; UNEP 2019b), and thus coastal erosion coupled with increased river discharge from melting ice will introduce higher quantities of terrestrial organic matter and Hg to coastal marine ecosystems (Jonsson et al., 2017; Paranjape & Hall, 2017). Increasing temperatures could also increase rates of microbially-mediated mercury methylation (e.g., Monperrus et al., 2007; Ramlal et al., 1993; Yang et al., 2016), which would increase the amount of bioavailable MeHg to organisms. Climate change also imposes indirect changes to food web structure and may alter the efficiency with which energy, and Hg, are transferred among organisms (McKinney et al., 2015; Stern et al., 2012).

In Chapter 3, greater food web complexity was associated with lower MeHg biomagnification; this demonstrated that rates of MeHg biomagnification are influenced by food web structure, and therefore altered species assemblages and predator-prey interactions will likely alter energy and MeHg transfer among species. Warmer temperatures and reduced sea ice in the Arctic (CCCR, 2019; Comiso et al., 2008) are expected to change food web structures, such as via shifts in the vertical migration of species due to changes in temperature and salinity stratification (Greene et al., 2008), the introduction of invasive species (Chan et al., 2019), and/or reduced benthopelagic coupling resulting in reduced nutrient and energy transfer among food web compartments (Griffiths et al., 2017). Changes to energy pathways in food webs could

therefore alter rates of MeHg biomagnification in Arctic marine benthic, pelagic, and benthopelagic food webs, leading to either higher or lower MeHg concentrations in top predators.

In Chapter 2, feeding environment (indicated by $\delta^{15}N$) was one of the most important factors influencing THg concentrations in both immature and mature anadromous Arctic char, with greater marine prey reliance (i.e., higher $\delta^{15}N$ values) associated with lower THg concentrations. Predicted fluctuations in Arctic river discharge (McClelland et al., 2006; Peterson et al., 2002) could pose a barrier to marine migration for anadromous Arctic char (Prowse et al., 2006; Reist et al., 2006), potentially resulting in higher THg concentrations, similar to those observed in non-anadromous Arctic char (e.g., Lockhart et al., 2005; Swanson et al., 2011b; van der Velden et al., 2013a), and potentially leading to greater differences in THg concentrations between immature and mature individuals.

Therefore, climate-induced changes to ecosystems could increase Hg bioaccumulation and biomagnification. Many Arctic marine mammals, birds, and fish have already been reported to exceed Hg toxicity thresholds (Dietz et al., 2013), presenting a risk to the fitness of those species and a health risk to the humans who consume them. Due to the high degree of uncertainty related to how climate change will impact the rate and extent of Hg bioaccumulation and biomagnification in Arctic biota it is essential to acquire baseline data to monitor spatial and temporal variation in Hg concentrations. Baselines will inform policy and governmental action towards Hg emission reductions and climate action.

4.4 Policy

Climate change effects are inducing a greater need for policy to implement actions to reduce Hg emissions. Anthropogenic activities have released approximately 1.54 million tonnes of Hg into the environment (Streets et al., 2017), which has increased atmospheric Hg concentrations by 450 % above natural levels (UNEP, 2019b) and, during the past 150 years, the amount of Hg in the Arctic has increased 10-fold (UNEP, 2019b). The research presented in this thesis acquired a comprehensive Hg baseline for inner Frobisher Bay organisms, in collaboration with Canada's Coastal Environmental Baseline Program (DFO, 2020a, 2020b). Baseline programs and Hg monitoring programs are important for obtaining data that can be used to elucidate spatial and temporal trends in the abundance and distribution of Hg, which can be used to inform future national and international management and regulations concerning Hg (e.g., Selin et al., 2018), as well as decisions regarding consumption guidelines. Although the work in this thesis helped to establish a Hg baseline for inner Frobisher Bay organisms, there is still a lack of data concerning Hg in humans (i.e., biomonitoring). Biomonitoring should be done in the future, especially given the importance of Arctic char and other country foods as subsistence food sources. Quantifying relationships between Hg

concentrations in food animals, consumption rates in humans, and concentrations of Hg in human demographic groups with different sensitivities would be helpful in guiding future policy.

4.5 Future Research

The research presented in this thesis compared factors affecting THg bioaccumulation in immature and mature anadromous Arctic char (Chapter 2), and determined and compared MeHg biomagnification in three spatially-proximate Arctic food webs (Chapter 3). Although this and other research has provided insight into mechanisms of Hg bioaccumulation and biomagnification, there are still many knowledge gaps pertaining to Hg dynamics in Arctic char and coastal marine food webs. Accordingly, I propose future research should focus on: i) Hg accumulation in immature anadromous Arctic char, and ii) MeHg biomagnification in benthic, benthopelagic, and pelagic food webs in other coastal Arctic marine ecosystems.

In Chapter 2, the immature Arctic char showed more variability than mature Arctic char in THg concentrations. Relationships linking THg with biological variables used to explain Hg bioaccumulation were also weaker for immature Arctic char. Feeding environment (i.e., freshwater vs marine), as indicated by $\delta^{15}N$, had a strong influence on Hg bioaccumulation in both the immature and mature anadromous Arctic char. Anadromous parr and smolts have been reported to feed on freshwater prey and surface insects prior to and after marine migrations, whereas mature veteran migrants generally do not (Rikardsen et al., 2002, 2003). Relative recent reliance on freshwater vs marine prey sources has the potential to affect Hg concentrations in immature anadromous Arctic char since freshwater prey contain higher Hg concentrations than marine prey (e.g., Farmer et al., 2010; Fry & Chumchal, 2012; Smylie et al., 2016). Therefore, it would be informative to acquire information on: i) annual freshwater feeding habits of immature anadromous Arctic char parr and pre-smolts; ii) overwinter freshwater feeding habits of immature smolts; iii) age at first migration of immature and mature Arctic char; iv) number and duration of marine migrations by immature Arctic char; v) use of feeding habitats proximate to freshwater discharge of immature and mature Arctic char; vi) whether maturity status (i.e., immature vs mature) is an important factor that contributes to among-individual variation in THg concentrations and relationships of THg concentrations with biological variables in other populations of anadromous Arctic char; and vii) whether an increased resolution of maturity status (e.g., immature, mature, ripe, spent) would elucidate further differences in THg concentrations and trends in anadromous Arctic char.

In Chapter 3, the incorporation of stable isotope food web structure metrics alongside MeHg biomagnification analyses proved to be an informative method for understanding how food web structure affects MeHg biomagnification. Furthermore, the study of MeHg pathways in multiple food webs within

an ecosystem is important for understanding how species interactions affect biomagnification of MeHg. Food web structures are expected to shift with climate change (Stern et al., 2012), therefore acquiring data on benthic, benthopelagic and pelagic food webs is important for reference, particularly as Arctic benthic food webs have been poorly studied relative to pelagic food webs, which have been the focus of most large Arctic marine Hg biomagnification studies (e.g., see Chapter 3, Table 3.5). Future studies should also emphasize acquiring Hg data for lower trophic level organisms because they exert a bottom-up control on Hg biomagnification and affect Hg concentrations in higher trophic level organisms (e.g., Ferriss & Essington, 2014). Improved sampling and stable isotope analyses of the benthos, when coupled with Hg analyses, would facilitate additional characterization of spatially proximate benthic, benthopelagic, and pelagic food webs for other Arctic coastal marine ecosystems and help to establish the generality of the differences among the food webs for Hg biomagnification.

Continued monitoring of Hg concentrations in Arctic char and Arctic marine biota is strongly suggested, particularly as climate change effects impact food web structures and increase the bioavailability of legacy Hg deposits (McKinney et al., 2015; Obrist et al., 2018; Stern et al., 2012). Monitoring Hg concentrations in fish that have high cultural and dietary value to Indigenous peoples is particularly important. Continued interdisciplinary collaboration among Indigenous peoples, scientists, and stakeholders such as studies in association with the Arctic Monitoring and Assessment Program (AMAP) and the Northern Contaminants Program (NCP; AMAP, 2011; CACAR, 2012), will be critical for ensuring the continued health of humans reliant on fish for nutritional reasons and for informing government policy.

4.6 Concluding Summary

Future Hg concentrations in Arctic biota will be linked to anthropogenic Hg emission reductions and climate-induced environmental changes. Investigating the inter-individual variability of Hg concentrations in anadromous Arctic char coupled with an examination of the Hg biomagnification in three spatially proximate food webs has broadened the scope of understanding of Hg dynamics in Arctic marine ecosystems. The research presented in this thesis was connected to the Iqaluit Coastal Environmental Baseline Program and aimed to establish a comprehensive Hg baseline and elucidate factors affecting Hg bioaccumulation (Chapter 2) and Hg biomagnification (Chapter 3) in Frobisher Bay fish and invertebrates. By acquiring species-level and food web-level Hg data, a comprehensive baseline has been established that will be integral to improving understanding of the future impacts of changing Hg bioavailability in Arctic marine ecosystems.

References

Aitken, A. E., & Gilbert, R. (1996). Marine Mollusca from Expedition Fiord, Western Axel Heiberg Island, Northwest Territories, Canada. *Arctic*, *49*(1), 29–43. https://doi.org/10.14430/arctic1181

Alvarez, M. del C., Murphy, C. A., Rose, K. A., McCarthy, I. D., & Fuiman, L. A. (2006). Maternal body burdens of methylmercury impair survival skills of offspring in Atlantic croaker (*Micropogonias undulatus*). *Aquatic Toxicology, 80*(4), 329–337. https://doi.org/10.1016/j.aquatox.2006.09.010

AMAP. (2011). AMAP Assessment 2011: Mercury in the Arctic. Arctic Monitoring and Assessment Programme (AMAP). Oslo, Norway. xiv + 193 pp.

Amos, H.M., Jacob, D.J., Streets, D.G., & Sunderland, E.M. (2013). Legacy impacts of all-time anthropogenic emissions on the global mercury cycle. *Global Biogeochemical Cycles, 27*, 410–412. https://doi.org/10.1002/gbc.20040

Amundsen, P. A. (1995). Feeding strategy of Arctic charr (*Salvelinus alpinus*): general opportunist, but individual specialist. *Nordic Journal of Freshwater Research, 71*, 150–156.

Atkinson, E. G., & Percy, J. A. (1992). Diet comparison among demersal marine fish from the Canadian Arctic. *Polar Biology*, *11*, 567-573. https://doi.org/10.1007/BF00237950

Attrill, M. J., Rundle, S. D., Fraser, A., & Power, M. (2009). Oligochaetes as a possible entry route for terrigenous organic carbon into estuarine benthic food webs. *Marine Ecology Progress Series*, *384*, 147–157. https://doi.org/10.3354/meps08019

Atwell, L., Hobson, K. A., & Welch, H. E. (1998). Biomagnification and bioaccumulation of mercury in an Arctic marine food web: insights from stable nitrogen isotope analysis. *Canadian Journal of Fisheries and Aquatic Sciences, 55*(5), 1114–1121. https://doi.org/10.1139/f98-001

Barber, W.E., & McFarlane, G.A. (1987). Evaluation of three techniques to age Arctic char from Alaskan and Canadian waters. *Transactions of the American Fisheries Society 116*(6), 874–881. 10.1577/1548-8659(1987)116<874:EOTTTA>2.0.CO;2

Bargagli, R., Monaci, F., & Bucci, C. (2007). Environmental biogeochemistry of mercury in Antarctic ecosystems. *Soil Biology and Biochemistry, 39*(1), 352–360. https://doi.org/10.1016/j.soilbio.2006.08.005

Barkay, T., & Poulain, A. J. (2007). Mercury (micro)biogeochemistry in polar environments. *FEMS Microbiology Ecology*, *59*(2), 232–241. https://doi.org/10.1111/j.1574-6941.2006.00246.x

Barst, B. D., Drevnick, P. E., Muir, D. C. G., Gantner, N., Power, M., Köck, G., Chéhab, N., Swanson, H., Rigét, F., & Basu, N. (2019). Screening-level risk assessment of methylmercurfor non-anadromous Arctic char (*Salvelinus alpinus*). *Environmental Toxicology and Chemistry, 38*(3), 489–502. https://doi.org/10.1002/etc.4341

Beckvar, N., Dillon, T. M., & Read, L. B. (2005). Approaches for linking whole-body fish tissue residues of mercury or DDT to biological effects thresholds. *Environmental Toxicology and Chemistry, 24*(8), 2094–2105. https://doi.org/10.1897/04-284R.1

Bell, L. E., Bluhm, B. A., & Iken, K. (2016). Influence of terrestrial organic matter in marine food webs of the Beaufort Sea shelf and slope. *Marine Ecology Progress Series, 550*, 1–24. https://doi.org/10.3354/meps11725

Birkely, S. R., & Gulliksen, B. (2003). Feeding ecology in five shrimp species (Decapoda, Caridea) from an Arctic fjord (Isfjorden, Svalbard), with emphasis on *Sclerocrangon boreas* (Phipps, 1774). *Crustaceana*, *76*(6), 699–715. https://doi.org/10.1163/156854003322381513

Bloom, N. S. (1992). On the Chemical Form of Mercury in Edible Fish and Marine Invertebrate Tissue. *Canadian Journal of Fisheries and Aquatic Sciences, 49*(5), 1010–1017. https://doi.org/10.1139/f92-113

Boivin, T.G., & Power, G. (1990). Winter condition and proximate composition of anadromous arctic charr (*Salvelinus alpinus*) in eastern Ungava Bay, Quebec. *Canadian Journal of Zoology, 68*(11), 2284–2289. https://doi.org/10.1139/z90-319

Borgå, K., Kidd, K. A., Muir, D. C. G., Berglund, O., Conder, J. M., Gobas, F. A. P. C., Kucklick, J., Malm, O., & Powell, D. E. (2011). Trophic Magnification Factors: Considerations of Ecology, Ecosystems, and Study Design. *Integrated Environmental Assessment and Management, 8*(1), 64–84. https://doi.org/10.1002/ieam.244

Branfireun, B. A., Cosio, C., Poulain, A. J., Riise, G., & Bravo, A. G. (2020). Mercury cycling in freshwater systems - An updated conceptual model. *Science of the Total Environment, 745*. https://doi.org/10.1016/j.scitotenv.2020.140906

Burke, S. M., Zimmerman, C. E., Laske, S. M., Koch, J. C., Derry, A. M., Guernon, S., Branfireun, B. A., & Swanson, H. K. (2020). Fish growth rates and lake sulphate explain variation in mercury levels in ninespine stickleback (*Pungitius pungitius*) on the Arctic Coastal Plain of Alaska. *Science of the Total Environment, 743*. https://doi.org/10.1016/j.scitotenv.2020.140564

Burnham, K. P., & Anderson, D. R. (2002). Model Selection and Multimodel Inference: A Practical Information-Theoretic Approach. 2nd Edition. Springer-Verlag, New York, NY, USA.

Cabana, G., & Rasmussen, J. B. (1994). Modelling food chain structure and contaminant bioaccumulation using stable nitrogen isotopes. *Letters to Nature, 372*, 255–257. https://doi.org/10.1038/372255a0

CACAR. (2012). Canadian Arctic Contaminants Assessment Report III: Mercury in Canada's North. Northern Contaminants Program, Aboriginal Affairs and Northern Development Canada, Ottawa, Canada. xv + 276.

Campbell, L. M., Norstrom, R. J., Hobson, K. A., Muir, D. C. G., Backus, S., & Fisk, A. T. (2005). Mercury and other trace elements in a pelagic Arctic marine food web (Northwater Polynya, Baffin Bay*). Science of the Total Environment, 351-352*, 247–263. https://doi.org/10.1016/j.scitotenv.2005.02.043

CCCR. (2019). Canada's Changing Climate Report, (ed.) Bush, E. & Lemmen, D.S. Government of Canada, Ottawa, Ontario. 444 p.

Chan, F. T., Stanislawczyk, K., Sneekes, A. C., Dvoretsky, A., Gollasch, S., Minchin, D., David, M., Jelmert, A., Albretsen, J., & Bailey, S. A. (2019). Climate change opens new frontiers for marine species in the Arctic: Current trends and future invasion risks. *Global Change Biology, 25*(1), 25–38. https://doi.org/10.1111/gcb.14469

Chaulk, A., Stern, G. A., Armstrong, D., Barber, D. G., & Wang, F. (2011). Mercury Distribution and Transport Across the Ocean-Sea-Ice-Atmosphere Interface in the Arctic Ocean. *Environmental Science and Technology, 45*(5), 1866–1872. https://doi.org/10.1021/es103434c

Chellappa, S., Huntingford, F.A., Strang, R.H.C., Thomson, R.Y. (1995). Condition factor and hepatosomatic index as estimates of energy status in male three-spined stickleback. *Journal of Fish Biology, 47*, 775–787. https://doi.org/10.1111/j.1095-8649.1995.tb06002.x

Chen, C. Y., Borsuk, M. E., Bugge, D. M., Hollweg, T., Balcom, P. H., Ward, D. M., Williams, J., & Mason, R. P. (2014). Benthic and Pelagic Pathways of Methylmercury Bioaccumulation in Estuarine Food Webs of the Northeast United States. *PLoS ONE, 9*(2). https://doi.org/10.1371/journal.pone.0089305

Chételat, J., Ackerman, J. T., Eagles-Smith, C. A., & Hebert, C. E. (2020). Methylmercury exposure in wildlife: A review of the ecological and physiological processes affecting contaminant concentrations and their interpretation. *Science of the Total Environment*, *711*. https://doi.org/10.1016/j.scitotenv.2019.135117

Chouvelon, T., Cresson, P., Bouchoucha, M., Brach-Papa, C., Bustamante, P., Crochet, S., Marco-Miralles, F., Thomas, B., & Knoery, J. (2018). Oligotrophy as a major driver of mercury bioaccumulation in medium-to high-trophic level consumers: A marine ecosystem-comparative study. *Environmental Pollution, 233*, 844–854. https://doi.org/10.1016/j.envpol.2017.11.015

Choy, C. A., Popp, B. N., Kaneko, J. J., & Drazen, J. C. (2009). The influence of depth on mercury levels in pelagic fishes and their prey. *Proceedings of the National Academy of Sciences of the United States of America*, *106*(33), 13865–13869. https://doi.org/10.1073/pnas.0900711106

Clayden, M. G., Arsenault, L. M., Kidd, K. A., O'Driscoll, N. J., & Mallory, M. L. (2015). Mercury bioaccumulation and biomagnification in a small Arctic polynya ecosystem. *Science of the Total Environment, 509–510*, 206–215. https://doi.org/10.1016/j.scitotenv.2014.07.087

Coad, B. W., & Reist, J. D. (2004). Annotated List of the Arctic Marine Fishes of Canada. *Canadian Manuscript Report of Fisheries and Aquatic Sciences* 2674. iv + 112 p.

Comiso, J.C., Parkinson, C.L., Gersten, R., & Stock, L. (2008). Accelerated decline in the Arctic sea ice cover. *Geophysical Research Letters, 35*(1). https://doi.org/10.1029/2007GL0319

Conover, R. J. (1960). The Feeding Behavior and Respiration of Some Marine Planktonic Crustacea. *Biological Bulletin*, *119*(3), 399–415. https://doi.org/10.2307/1539258

Craig, H. (1957). Isotopic standards for carbon and oxygen and correction factors for mass-spectrometric analysis of carbon dioxide. *Geochimica et Cosmochimica Acta*, *12*(1–2), 133–149. https://doi.org/https://doi.org/10.1016/0016-7037(57)90024-8

Cresson, P., Travers-Trolet, M., Rouquette, M., Timmerman, C.-A., Giraldo, C., Lefebvre, S., Ernande, B. (2017). Underestimation of chemical contamination in marine fish muscle tissue can be reduced by considering variable wet:dry weight ratios. *Marine Pollution Bulletin, 123*(1–2), 279–285. https://doi.org/10.1016/j.marpolbul.2017.08.046

Crump, K. L., & Trudeau, V. L. (2009). Mercury-induced reproductive impairment in fish. *Environmental Toxicology and Chemistry, 28*(5), 895–907. https://doi.org/10.1897/08-151.1

Dang, F. & Wang, W.-X. (2012). Why mercury concentration increases with fish size? Biokinetic explanation. *Environmental Pollution, 163*, 192–198. 10.1016/j.envpol.2011.12.026

Davidsen, J. G., Power, M., Knudsen, R., Sjursen, A. D., Kjærstad, G., Rønning, L., & Arnekleiv, J. V. (2020). Marine trophic niche use and life history diversity among Arctic charr *Salvelinus alpinus* in southwestern Greenland. *Journal of Fish Biology, 96*(3), 681–692. https://doi.org/10.1111/jfb.14261

Deering, R., Misiuk, B., Bell, T., Forbes, D. L., Edinger, E., Tremblay, T., Telka, A., Aitken, A., & Campbell, C. (2018). Characterization of the seabed and postglacial sediments of inner Frobisher Bay, Baffin Island, Nunavut. *Canada-Nunavut Geoscience Office,* 139–152. http://cngo.ca/summary-of-activities/2018/

Dempson, J. B., Shears, M., & Bloom, M. (2002). Spatial and temporal variability in the diet of anadromous Arctic charr, *Salvelinus alpinus*, in northern Labrador. *Environmental Biology of Fishes, 64*(1), 49–62. https://doi.org/10.1023/A:1016018909496

Deniro, M. J., & Epstein, S. (1978). Influence of diet on the distribution of carbon isotopes in animals. *Geochimica et Cosmochimica Acta, 42*(5), 495–506. https://doi.org/10.1016/0016-7037(78)90199-0

DeNiro, M. J., & Epstein, S. (1981). Influence of diet on the distribution of nitrogen isotopes in animals. *Geochimica et Cosmochimica Acta, 45*, 341–351.

DFO. (2020a). Coastal Environmental Baseline Program. Fisheries and Oceans Canada. [Accessed: March 1, 2022]. https://www.dfo-mpo.gc.ca/science/environmental-environnement/cebp-pdecr/index-eng.html

DFO. (2020b) Coastal Environmental Baseline Program projects in Iqaluit, Nunavut. Baseline mercury levels in Frobisher Bay fish and invertebrates. Fisheries and Oceans Canada. [Accessed: March 1, 2022]. https://www.dfo-mpo.gc.ca/science/environmental-environnement/cebp-pdecr/projects/iqaluit-eng.html

DFO. (2020c). Canada's Oceans Protection Plan. Transport Canada. [Accessed: March 1, 2022]. https://tc.canada.ca/en/initiatives/oceans-protection-plan/canada-s-oceans-protection-plan

Diaz-Somoano, M., Unterberger, S., & Hein, K. R. G. (2007). Mercury emission control in coal-fired plants: The role of wet scrubbers. *Fuel Processing Technology, 88*(3), 259–263. https://doi.org/10.1016/j.fuproc.2006.10.003

Dietz, R., Outridge, P. M., & Hobson, K. A. (2009). Anthropogenic contributions to mercury levels in present-day Arctic animals – A review. *Science of the Total Environment, 407*(24), 6120–6131. https://doi.org/10.1016/j.scitotenv.2009.08.036

Dietz, R., Sonne, C., Basu, N., Braune, B., O'Hara, T., Letcher, R. J., Scheuhammer, T., Andersen, M., Andreasen, C., Andriashek, D., Asmund, G., Aubail, A., Baagøe, H., Born, E. W., Chan, H. M., Derocher, A. E., Grandjean, P., Knott, K., Kirkegaard, M., … Aars, J. (2013). What are the toxicological effects of mercury in Arctic biota? *Science of the Total Environment, 443*, 775–790. https://doi.org/10.1016/j.scitotenv.2012.11.046

Dietz, R., Letcher, R. J., Desforges, J. P., Eulaers, I., Sonne, C., Wilson, S., Andersen-Ranberg, E., Basu, N., Barst, B. D., Bustnes, J. O., Bytingsvik, J., Ciesielski, T. M., Drevnick, P. E., Gabrielsen, G. W., Haarr, A., Hylland, K., Jenssen, B. M., Levin, M., McKinney, M. A., … Víkingsson, G. (2019). Current state of knowledge on biological effects from contaminants on arctic wildlife and fish. *Science of the Total Environment*, *696*. https://doi.org/10.1016/j.scitotenv.2019.133792

Ding C., & Li, Z. (2022). Research on the shipping network structure under the influence of Arctic routes. *GeoJournal, 87*, 1027–1045. https://doi.org/10.1007/s10708-020-10296-z

Divine, L. M., Iken, K., & Bluhm, B. A. (2015). Regional benthic food web structure on the Alaska Beaufort Sea shelf. *Marine Ecology Progress Series, 531*, 15–32. https://doi.org/10.3354/meps11340

Douglas, T. A., Loseto, L. L., MacDonald, R. W., Outridge, P., Dommergue, A., Poulain, A., Amyot, M., Barkay, T., Berg, T., Chetelat, J., Constant, P., Evans, M., Ferrari, C., Gantner, N., Johnson, M. S., Kirk, J., Kroer, N., Larose, C., Lean, D., … Zdanowicz, C. M. (2012). The fate of mercury in Arctic terrestrial and aquatic ecosystems, a review. *Environmental Chemistry, 9*(4), 321–355. https://doi.org/10.1071/EN11140

Doyon, J.-F., Schetagne, R., & Verdon, R. (1998). Different mercury bioaccumulation rates between sympatric populations of dwarf and normal lake whitefish (*Coregonus clupeaformis*) in the La Grande complex watershed, James Bay, Québec. *Biogeochemistry, 40,* 203–216.

Dunbar, M. J. (1956). The *Calanus* Expeditions in the Canadian Arctic, 1947 to 1955. *Arctic, 9*(3), 178 – 190. http://www.jstor.org/stable/40506717

Dutil, J.-D. (1986). Energetic Constraints and Spawning Interval in the Anadromous Arctic Charr (*Salvelinus alpinus*). *Copeia, 4*, 945–955. https://doi.org/10.2307/1445291

Eagles-Smith, C. A., Ackerman, J. T., Julie, Y., & Adelsbach, T. L. (2009). Mercury demethylation in waterbird livers: Dose-response thresholds and differences among species. *Environmental Toxicology and Chemistry, 28*(3), 568–577. https://doi.org/10.1897/08-245.1

ECCC Canadian Ice Service. (2013). Sea Ice Climatic Atlas for the Northern Canadian Waters 1981-2010. Environment and Climate Change Canada: Canadian Ice Service. Break-up (JL02) – Freeze-up (OC29): https://iceweb1.cis.ec.gc.ca/30Atlas/page1.xhtml?region=AR&lang=en# [Accessed: March 1, 2022].

Erasmus, V. N., Iitembu, J.A., Hamutenya, S., Gamatham, J. (2019). Evidences of possible influences of methylmercury concentrations on condition factor and maturation of *Lophius vomerinus* (Cape monkfish). *Marine Pollution Bulletin, 146*, 33–38. https://doi.org/10.1016/j.marpolbul.2019.05.060

Evans, M. S., Muir, D. C. G., Keating, J., & Wang, X. (2015). Anadromous char as an alternate food choice to marine animals: A synthesis of Hg concentrations, population features and other influencing factors. *Science of the Total Environment, 509–510*, 175–194. https://doi.org/10.1016/j.scitotenv.2014.10.074

Falk-Petersen, S., Mayzaud, P., Kattner, G., & Sargent, J. R. (2009). Lipids and life strategy of Arctic *Calanus*. *Marine Biology Research, 5*(1), 18–39. https://doi.org/10.1080/17451000802512267

Farmer, T. M., Wright, R. A., & DeVries, D. R. (2010). Mercury Concentration in Two Estuarine Fish Populations across a Seasonal Salinity Gradient. *Transactions of the American Fisheries Society*, *139*(6), 1896–1912. https://doi.org/10.1577/t09-194.1

Farris, F. F., Dedrick, R. L., Allen, P. V., & Smith, J. C. (1993). Physiological Model for the Pharmacokinetics of Methyl Mercury in the Growing Rat. *Toxicology and Applied Pharmacology, 119*(1), 74–90. https://doi.org/10.1006/taap.1993.1046

Feder, H. M., Iken, K., Blanchard, A. L., Jewett, S. C., & Schonberg, S. (2011). Benthic food web structure in the southeastern Chukchi Sea: an assessment using $\delta^{13}C$ and $\delta^{15}N$ analyses. *Polar Biology*, *34*, 521–532. https://doi.org/10.1007/s00300-010-0906-9

Ferriss, B. E., & Essington, T. E. (2014). Does trophic structure dictate mercury concentrations in top predators? A comparative analysis of pelagic food webs in the Pacific Ocean. *Ecological Modelling*, *278,* 18–28. https://doi.org/10.1016/j.ecolmodel.2014.01.029

Fitzgerald, W. F., Lamborg, C. H., & Hammerschmidt, C. R. (2007). Marine Biogeochemical Cycling of Mercury. *Chemical Reviews, 107*(2), 641–662. https://doi.org/10.1021/cr050353m

Fox, A. L., Hughes, E. A., Trocine, R. P., Trefry, J. H., Schonberg, S. V., McTigue, N. D., Lasorsa, B. K., Konar, B., & Cooper, L. W. (2014). Mercury in the northeastern Chukchi Sea: Distribution patterns in seawater and sediments and biomagnification in the benthic food web. *Deep-Sea Research Part II: Topical Studies in Oceanography, 102*, 56–67. https://doi.org/10.1016/j.dsr2.2013.07.012

France, R. L. (1995). Differentiation between littoral and pelagic food webs in lakes using stable carbon isotopes. *Limnology and Oceanography, 40*(7), 1310–1313. https://doi.org/10.4319/lo.1995.40.7.1310

Fry, B. (2006). Stable Isotope Ecology. Springer Science+Business Media, LLC, New York, NY, vii + 297.

Fry, B., & Chumchal, M. M. (2012). Mercury bioaccumulation in estuarine food webs. *Ecological Applications, 22*(2), 606–623. https://doi.org/10.1890/11-0921.1

Fry, B., & Sherr, E. B. (1984). $\delta^{13}C$ measurements as indicators of carbon flow in marine and freshwater ecosystems. *Contributions in Marine Science, 27*, 13–47.

Gallagher, C. P., & Dick, T. A. (2010). Historical and Current Population Characteristics and Subsistence Harvest of Arctic Char from the Sylvia Grinnell River, Nunavut, Canada. *North American Journal of Fisheries Management, 30*(1), 126–141. https://doi.org/10.1577/m09-027.1

Gantner, N., Muir, D. C., Power, M., Iqaluk, D., Reist, J. D., Babaluk, J. A., Meili, M., Borg, H., Hammar, J., Michaud, W., Dempson, B., & Solomon, K. R. (2010). Mercury concentrations in landlocked arctic char (*Salvelinus alpinus*) from the Canadian arctic. Part II: Influence of lake biotic and abiotic characteristics on geographic trends in 27 populations. *Environmental Toxicology and Chemistry, 29*(3), 633–643. https://doi.org/10.1002/etc.96

Geoffroy, M., Robert, D., Darnis, G., & Fortier, L. (2011). The aggregation of polar cod (*Boreogadus saida*) in the deep Atlantic layer of ice-covered Amundsen Gulf (Beaufort Sea) in winter. *Polar Biology*, *34*, 1959–1971. https://doi.org/10.1007/s00300-011-1019-9

Gewurtz, S. B., Bhavsar, S. P., & Fletcher, R. (2011). Influence of fish size and sex on mercury/PCB concentration: Importance for fish consumption advisories. *Environment International, 37*(2), 425–434. https://doi.org/10.1016/j.envint.2010.11.005

Gilmer, R. W., & Harbison, G. R. (1991). Diet of *Limacina helicina* (Gastropoda: Thecosomata) in Arctic waters in midsummer. *Marine Ecology Progress Series*, *77*, 125–134. https://doi.org/10.3354/meps077125

Glantz, S.A., & Slinker, B.K. (2001). Primer of Applied Regression and Analysis of Variance. 2nd ed. McGraw-Hill, New York. 949 pp.

Goodyear, K. L., & McNeill, S. (1999). Bioaccumulation of heavy metals by aquatic macro-invertebrates of different feeding guilds: a review. *Science of the Total Environment*, *229*(1–2), 1–19. https://doi.org/10.1016/S0048-9697(99)00051-0

Graeve, M., Kattner, G., & Piepenburg, D. (1997). Lipids in Arctic benthos: does the fatty acid and alcohol composition reflect feeding and trophic interactions? *Polar Biology*, *18*, 53–61. https://doi.org/10.1007/s003000050158

Grainger, E. H. (1953). On the Age, Growth, Migration, Reproductive Potential and Feeding Habits of the Arctic Char (*Salvelinus alpinus*) of Frobisher Bay, Baffin Island. *Journal of the Fisheries Research Board of Canada, 10*(6), 326–370. https://doi.org/10.1139/f53-023

Gray, B. P., Norcross, B. L., Beaudreau, A. H., Blanchard, A. L., & Seitz, A. C. (2017). Food habits of Arctic staghorn sculpin (*Gymnocanthus tricuspis*) and shorthorn sculpin (*Myoxocephalus scorpius*) in the northeastern Chukchi and western Beaufort Seas. *Deep-Sea Research Part II: Topical Studies in Oceanography, 135*, 111–123. https://doi.org/10.1016/j.dsr2.2016.05.013

Gray, J. S. (2002). Biomagnification in marine systems: The perspective of an ecologist. *Marine Pollution Bulletin, 45*(1–12), 46–52. https://doi.org/10.1016/S0025-326X(01)00323-X

Greene, C.H., Pershing, A.J., Cronin, T.M., & Ceci, N. (2008). Arctic climate change and its impacts on the ecology of the North Atlantic. *Ecology, 89*(11), 24–38. https://doi.org/10.1890/07-0550.1

Grieb, T. M., Bowie, G. L., Driscoll, C. T., Gloss, S. P., Schofield, C. L., & Porcella, D. B. (1990). Factors affecting mercury accumulation in fish in the upper Michigan peninsula. *Environmental Toxicology and Chemistry, 9*(7), 919–930. https://doi.org/10.1002/etc.5620090710

Griffiths, J. R., Kadin, M., Nascimento, F. J. A., Tamelander, T., Törnroos, A., Bonaglia, S., Bonsdorff, E., Brüchert, V., Gårdmark, A., Järnström, M., Kotta, J., Lindegren, M., Nordström, M. C., Norkko, A., Olsson, J., Weigel, B., Žydelis, R., Blenckner, T., Niiranen, S., & Winder, M. (2017). The importance of benthic–pelagic coupling for marine ecosystem functioning in a changing world. *Global Change Biology*, *23*(6), 2179–2196. https://doi.org/10.1111/gcb.13642

Gross, M. R., Coleman, R. M., & McDowall, R. M. (1988). Aquatic productivity and the evolution of diadromous fish migration. *Science, 239*(4845), 1291–1293. https://doi.org/10.1126/science.239.4845.1291

Guzzo, M. M., Haffner, G. D., Legler, N. D., Rush, S. A., & Fisk, A. T. (2013). Fifty years later: trophic ecology and niche overlap of a native and non-indigenous fish species in the western basin of Lake Erie. *Biological Invasions, 15*, 1695–1711. https://doi.org/10.1007/s10530-012-0401-z

Gworek, B., Bemowska-Kałabun, O., Kijeńska, M., & Wrzosek-Jakubowska, J. (2016). Mercury in Marine and Oceanic Waters—a Review. *Water, Air, and Soil Pollution, 227*(10), 1–19. https://doi.org/10.1007/s11270-016-3060-3

Gworek, B., Dmuchowski, W., Baczewska, A. H., Brągoszewska, P., Bemowska-Kałabun, O., & Wrzosek-Jakubowska, J. (2017). Air Contamination by Mercury, Emissions and Transformations—a Review. *Water, Air, and Soil Pollution, 228(*123). https://doi.org/10.1007/s11270-017-3311-y

Hadas, O., Altabet, M. A., & Agnihotri, R. (2009). Seasonally varying nitrogen isotope biogeochemistry of particulate organic matter in Lake Kinneret, Israel. *Limnology and Oceanography, 54*(1), 75–85. https://doi.org/10.4319/lo.2009.54.1.0075

Hair, J.F., Jr., Black, W.C., Babin, B.J., Anderson, R.E., & Tatham, R.L. (2006). Multivariate Data Analysis. 6th ed. Prentice Hall, Upper Saddle River, NJ. 899 pp.

Hall, B. D., Bodaly, R. A., Fudge, R. J. P., Rudd, J. W. M., & Rosenberg, D. M. (1997). Food as the dominant pathway of methylmercury uptake by fish. *Water, Air, and Soil Pollution, 100*(1–2). https://doi.org/10.1023/a:1018071406537

Hall, R. O., & Meyer, J. L. (1998). The Trophic Significance of Bacteria in a Detritus-Based Stream Food Web. *Ecology, 79*(6), 1995–2012. https://www.jstor.org/stable/176704

Hammerschmidt, C. R., Wiener, J. G., Frazier, B. E., & Rada, R. G. (1999). Methylmercury Content of Eggs in Yellow Perch Related to Maternal Exposure in Four Wisconsin Lakes. *Environmental Science and Technology, 33*(7), 999–1003. https://doi.org/10.1021/es980948h

Hansen, J. H., Hedeholm, R. B., Sünksen, K., Christensen, J. T., & Grønkjær, P. (2012). Spatial variability of carbon ($\delta^{13}C$) and nitrogen ($\delta^{15}N$) stable isotope ratios in an Arctic marine food web. *Marine Ecology Progress Series, 467*, 47–59. https://doi.org/10.3354/meps09945

Harris, R. C., & Bodaly, R. A. (1998). Temperature, growth and dietary effects on fish mercury dynamics in two Ontario lakes. *Biogeochemistry, 40*, 175–187. https://doi.org/10.1023/A:1005986505407

Health Canada. (2007). Human Health Risk Assessment of Mercury in Fish and Health Benefits of Fish Consumption. Health Canada, Ottawa.

Hebbali, Aravind. (2020). olsrr: Tools for Building OLS Regression Models. R package version 0.5.3. https://CRAN.R-project.org/package=olsrr

Hesslein, R. H., Hallard, K. A., & Ramlal, P. (1993). Replacement of Sulfur, Carbon, and Nitrogen in Tissue of Growing Broad Whitefish (*Coregonus nasus*) in Response to a Change in Diet Traced by $\delta^{34}S$, $\delta^{13}C$, and $\delta^{15}N$. *Canadian Journal of Fisheries and Aquatic Sciences, 50*(10), 2071–2076. https://doi.org/10.1139/f93-230

Heyes, A., Miller, C., & Mason, R. P. (2004). Mercury and methylmercury in Hudson River sediment: Impact of tidal resuspension on partitioning and methylation. *Marine Chemistry*, *90*(1-4), 75–89. https://doi.org/10.1016/j.marchem.2004.03.011

Himmelman, J. H., & Hamel, J. R. (1993). Diet, behaviour and reproduction of the whelk *Buccinum undatum* in the northern Gulf of St. Lawrence, eastern Canada. *Marine Biology*, *116*, 423–430. https://doi.org/10.1007/BF00350059

Hobson, K. A., & Welch, H. E. (1992). Determination of trophic relationships within a high Arctic marine food web using $\delta^{13}C$ and $\delta^{15}N$ analysis. *Marine Ecology Progress Series, 84*(1), 9–18. https://doi.org/10.3354/meps084009

Hobson, K. A., Fisk, A., Karnovsky, N., Holst, M., Gagnon, J.-M., & Fortier, M. (2002). A stable isotope ($\delta^{13}C$, $\delta^{15}N$) model for the North Water food web: Implications for evaluating trophodynamics and the flow of energy and contaminants. *Deep-Sea Research Part II: Topical Studies in Oceanography*, *49*(22-23), 5131–5150. https://doi.org/10.1016/S0967-0645(02)00182-0

Hogstrand, C., & Haux, C. (1991). Binding and detoxification of heavy metals in lower vertebrates with reference to metallothionein. *Comparative Biochemistry and Phyiology Part C: Comparative Pharmacology, 100*(1-2), 137–141. https://doi.org/10.1016/0742-8413(91)90140-O

Htun-Han, M. (1978). The reproductive biology of the dab *Limanda limanda* (L.) in the North Sea: gonosomatic index, hepatosomatic index and condition factor. *Journal of Fish Biology, 13*(3), 369–378. https://doi.org/10.1111/j.1095-8649.1978.tb03445.x

Hughes, W. L. (1957). A Physicochemical Rationale for the Biological Activity of Mercury and its Compounds. *Annals of the New York Academy of Sciences, 65*(5), 454–460. https://doi.org/10.1111/j.1749-6632.1956.tb36650.x

Hunter, J. G. (1976). Arctic char and hydroelectric power in the Sylvia Grinnell River. Fisheries Research Board of Canada.

Iken, K., Bluhm, B. A., & Gradinger, R. (2005). Food web structure in the high Arctic Canada Basin: evidence from $\delta^{13}C$ and $\delta^{15}N$ analysis. *Polar Biology, 28*, 238–249. https://doi.org/10.1007/s00300-004-0669-2

Iken, K., Bluhm, B., & Dunton, K. (2010). Benthic food-web structure under differing water mass properties in the southern Chukchi Sea. *Deep-Sea Research Part II: Topical Studies in Oceanography*, *57*(1–2), 71–85. https://doi.org/10.1016/j.dsr2.2009.08.007

IPCC. (2013). Summary for Policymakers. In: Climate Change 2013: The Physical Science Basis. Contribution of Working Group I to the Fifth Assessment Report of the Intergovernmental Panel on Climate Change [Stocker, T.F., D. Qin, G.-K. Plattner, M. Tignor, S.K. Allen, J. Boschung, A. Nauels, Y. Xia, V. Bex and P.M. Midgley (eds.)]. Cambridge University Press, Cambridge, United Kingdom and New York, NY, USA.

Jackson, A. L., Inger, R., Parnell, A. C., & Bearhop, S. (2011). Comparing isotopic niche widths among and within communities: SIBER – Stable Isotope Bayesian Ellipses in R. *Journal of Animal Ecology*, *80*(3), 595–602. https://doi.org/10.1111/j.1365-2656.2011.01806.x

Jackson, T.A. (1989). The influence of clay minerals, oxides, and humic matter on the methylation and demethylation of mercury by micro-organisms in freshwater sediments. *Applied Organometallic Chemistry*, *3*(1), 1–30. https://doi.org/10.1002/aoc.590030103

Jacob, U., Mintenbeck, K., Brey, T., Knust, R., & Beyer, K. (2005). Stable isotope food web studies: a case for standardized sample treatment. *Marine Ecology Progress Series*, *287*, 251–253. https://doi.org/10.3354/meps287251

Jæger, I., Hop, H., & Gabrielsen, G. W. (2009). Biomagnification of mercury in selected species from an Arctic marine food web in Svalbard. *Science of the Total Environment, 407*(16), 4744–4751. https://doi.org/10.1016/j.scitotenv.2009.04.004

Jardine, T. D., Hunt, R. J., Faggotter, S. J., Valdez, D., Burford, M. A., & Bunn, S. E. (2013). Carbon from periphyton supports fish biomass in waterholes of a wet-dry tropical river. *River Research and Applications, 29*, 560–573. https://doi.org/10.1002/rra

Jędruch, A., Bełdowska, M., & Graca, B. (2018). Seasonal variation in accumulation of mercury in the benthic macrofauna in a temperate coastal zone (Gulf of Gdańsk). *Ecotoxicology and Environmental Safety*, *164*, 305–316. https://doi.org/10.1016/j.ecoenv.2018.08.040

Jobling, M., Jørgensen, E.H., Siikavuopio, S.I. (1993). The influence of previous feeding regime on the compensatory growth response of maturing and immature Arctic charr, *Salvelinus alpinus*. *Journal of Fish Biology, 43*, 409–419. https://doi.org/10.1111/j.1095-8649.1993.tb00576.x

Jobling, M., Tveiten, H., & Hatlen, B. (1998). Cultivation of Arctic charr: an update. *Aquaculture International, 6*(3), 181–196. https://doi.org/10.1023/A:1009246509657

Johnson L. (1980). The arctic char, *Salvelinus alpinus*. In E.K. Balon (Ed.), *Charrs, Salmonid Fishes of the Genus Salvelinus* (pp. 15–98). Dr. W. Junk Publishers, Hague, Netherlands.

Jonsson, B., & Jonsson, N. (1993). Partial migration: niche shift versus sexual maturation in fishes. *Reviews in Fish Biology and Fisheries, 3*(4), 348–365. https://doi.org/10.1007/BF00043384

Jonsson, S., Andersson, A., Nilsson, M.B., Skyllberg, U., Lundberg, E., Schaefer, J.K., Åkerblom, S., & Björn, E. (2017). Terrestrial discharges mediate trophic shifts and enhance methylmercury accumulation in estuarine biota. *Science Advances, 3*(1). https://www.science.org/doi/10.1126/sciadv.1601239

Jørgensen, E.H., Johansen, S.J.S., Jobling, M. (1997). Seasonal patterns of growth, lipid deposition and lipid depletion in anadromous Arctic charr. *Journal of Fish Biology, 51,* 312-326. https://doi.org/10.1111/j.1095-8649.1997.tb01668.x

Jumars, P. A., Dorgan, K. M., & Lindsay, S. M. (2015). Diet of Worms Emended: An Update of Polychaete Feeding Guilds. *Annual Review of Marine Science, 7*, 497–520. https://doi.org/10.1146/annurev-marine-010814-020007

Kahilainen, K. K., Thomas, S. M., Keva, O., Hayden, B., Knudsen, R., Eloranta, A. P., Tuohiluoto, K., Amundsen, P. A., Malinen, T., & Järvinen, A. (2016). Seasonal dietary shift to zooplankton influences stable isotope ratios and total mercury concentrations in Arctic charr (*Salvelinus alpinus* (L.)). *Hydrobiologia, 783*(1), 47–63. https://doi.org/10.1007/s10750-016-2685-y

Kahilainen, K. K., Thomas, S. M., Nystedt, E. K. M., Keva, O., Malinen, T., & Hayden, B. (2017). Ecomorphological divergence drives differential mercury bioaccumulation in polymorphic European whitefish (*Coregonus lavaretus*) populations of subarctic lakes. *Science of the Total Environment, 599–600*, 1768–1778.

Karimi, R., Chen, C. Y., Pickhardt, P. C., Fisher, N. S., & Folt, C. L. (2007). Stoichiometric controls of mercury dilution by growth. *Proceedings of the National Academy of Sciences, 104*(18), 7477–7482. https://doi.org/10.1073/pnas.0611261104

Kaufman, L., & Rousseeuw, P.J. (1990). Finding Groups in Data: An Introduction to Cluster Analysis. *John Wiley & Sons, Inc.* 10.1002/9780470316801

Kędra, M., Gromisz, S., Jaskuła, R., Legezyńska, J., Maciejewska, B., Malec, E., Opanowski, A., Ostrowska, K., Włodarska-Kowalczuk, M., & Wesławski, J. M. (2010). Soft bottom macrofauna of an All Taxa Biodiversity Site: Hornsund (77°N, Svalbard). *Polish Polar Research*, *31*(4), 309–326. 10.2478/v10183−010−0008−y

Kędra, M., Moritz, C., Choy, E. S., David, C., Degen, R., Duerksen, S., Ellingsen, I., Górska, B., Grebmeier, J. M., Kirievskaya, D., van Oevelen, D., Piwosz, K., Samuelsen, A., & Węsławski, J. M. (2015). Status and trends in the structure of Arctic benthic food webs. *Polar Research, 34*(1). https://doi.org/10.3402/polar.v34.23775

Keva, O., Hayden, B., Harrod, C., & Kahilainen, K. K. (2017). Total mercury concentrations in liver and muscle of European whitefish (*Coregonus lavaretus* (L.)) in a subarctic lake - Assessing the factors driving year-round variation. *Environmental Pollution, 231*, 1518–1528. https://doi.org/10.1016/j.envpol.2017.09.012

Kidd, K. A., Hesslein, R. H., Fudge, R. J. P., & Hallard, K. A. (1995). The influence of trophic levels as measured by $\delta^{15}N$ on mercury concentrations in freshwater organisms. *Water, Air, and Soil Pollution*, *80*, 1011–1015. 10.1007/978-94-011-0153-0_110

Kim, H., Soerensen, A. L., Hur, J., Heimbürger, L.-E., Hahm, D., Rhee, T. S., Noh, S., & Han, S. (2017). Methylmercury Mass Budgets and Distribution Characteristics in the Western Pacific Ocean. *Environmental Science and Technology, 51*(3), 1186–1194. https://doi.org/10.1021/acs.est.6b04238

King, J. K., Kostka, J. E., Frischer, M. E., & Saunders, F. M. (2000). Sulfate-Reducing Bacteria Methylate Mercury at Variable Rates in Pure Culture and in Marine Sediments. *Applied and Environmental Microbiology, 66*(6), 2430–2437. https://doi.org/10.1128/AEM.66.6.2430-2437.2000

Kirk, J. L., Lehnherr, I., Andersson, M., Braune, B. M., Chan, L., Dastoor, A. P., Durnford, D., Gleason, A. L., Loseto, L. L., Steffen, A., & St. Louis, V. L. (2012). Mercury in Arctic marine ecosystems: Sources, pathways and exposure. *Environmental Research*, *119*, 64–87. https://doi.org/10.1016/j.envres.2012.08.012

Klemetsen, A., Amundsen, P. A., Dempson, J. B., Jonsson, B., Jonsson, N., O'Connell, M. F., & Mortensen, E. (2003). Atlantic salmon *Salmo salar* L., brown trout *Salmo trutta* L. and Arctic charr *Salvelinus alpinus* (L.): A review of aspects of their life histories. *Ecology of Freshwater Fish, 12*(1), 1–59. https://doi.org/10.1034/j.1600-0633.2003.00010.x

Knudsen, R., Siwertsson, A., Adams, C. E., Garduño-Paz, M., Newton, J., & Amundsen, P.-A. (2011). Temporal stability of niche use exposes sympatric Arctic charr to alternative selection pressures. *Evolutionary Ecology, 25*(3), 589–604. https://doi.org/10.1007/s10682-010-9451-9

Krabbenhoft, D. P., & Sunderland, E. M. (2013). Global change and mercury. *Science, 341*(6153), 1457–1458. https://doi.org/10.1126/science.1242838

Kristofferson, A.H., & Sopuck, R. D. (1983). The Effects of Exploitation on the Arctic Charr Population of the Sylvia Grinnell River, Northwest Territories. Fisheries and Oceans Canada.

Landry, J. J., Fisk, A. T., Yurkowski, D. J., Hussey, N. E., Dick, T., Crawford, R. E., & Kessel, S. T. (2018). Feeding ecology of a common benthic fish, shorthorn sculpin (*Myoxocephalus scorpius*) in the high arctic. *Polar Biology, 41*(10), 2091–2102. https://doi.org/10.1007/s00300-018-2348-8

Lavoie, R. A., Hebert, C. E., Rail, J.-F., Braune, B. M., Yumvihoze, E., Hill, L. G., & Lean, D. R. S. (2010). Trophic structure and mercury distribution in a Gulf of St. Lawrence (Canada) food web using stable isotope analysis. *Science of the Total Environment, 408*(22), 5529–5539. https://doi.org/10.1016/j.scitotenv.2010.07.053

Lavoie, R. A., Jardine, T. D., Chumchal, M. M., Kidd, K. A., & Campbell, L. M. (2013). Biomagnification of Mercury in Aquatic Food Webs: A Worldwide Meta-Analysis. *Environmental Science and Technology, 47*(23), 13385–13394. https://doi.org/10.1021/es403103t

Lawrence, A. L., & Mason, R. P. (2001). Factors controlling the bioaccumulation of mercury and methylmercury by the estuarine amphipod *Leptocheirus plumulosus*. *Environmental Pollution*, *111*(2), 217–231. https://doi.org/10.1016/S0269-7491(00)00072-5

Layman, C. A., Arrington, D. A., Montaña, C. G., & Post, D. M. (2007). Can stable isotope ratios provide for community-wide measures of trophic structure? *Ecology*, *88*(1), 42–48. https://doi.org/10.1890/0012-9658(2007)88[42:CSIRPF]2.0.CO;2

Layman, C. A., Araujo, M. S., Boucek, R., Hammerschlag-Peyer, C. M., Harrison, E., Jud, Z. R., Matich, P., Rosenblatt, A. E., Vaudo, J. J., Yeager, L. A., Post, D. M., & Bearhop, S. (2012). Applying stable isotopes to examine food-web structure: An overview of analytical tools. *Biological Reviews, 87*(3), 545–562. https://doi.org/10.1111/j.1469-185X.2011.00208.x

Le Cren, E.D. (1951). The length-weight relationship and seasonal cycle in gonad weight and condition in the perch (*Perca fluviatilis*). *Journal of Animal Ecology, 20*(2), 201–219.

Lehnherr, I., St. Louis, V. L., Hintelmann, H., & Kirk, J. L. (2011). Methylation of inorganic mercury in polar marine waters. *Nature Geoscience, 4*(5), 298–302. https://doi.org/10.1038/ngeo1134

Lehnherr, I. (2014). Methylmercury biogeochemistry: a review with special reference to Arctic aquatic ecosystems. *Environmental Reviews, 22*(3), 229–243. https://doi.org/10.1139/er-2013-0059

Lemes, M., & Wang, F. (2009). Methylmercury speciation in fish muscle by HPLC-ICP-MS following enzymatic hydrolysis. *Journal of Analytical Atomic Spectrometry, 24*(5), 663–668. https://doi.org/10.1039/b819957b

Lescord, G. L., Johnston, T. A., Branfireun, B. A., & Gunn, J. M. (2018). Percentage of Methylmercury in the Muscle Tissue of Freshwater Fish Varies with Body Size and Age Among Species. *Environmental Toxicology and Chemistry, 37*(10), 2682–2691. https://doi.org/10.1002/etc.4233

Lindberg, S., Bullock, R., Ebinghaus, R., Engstrom, D., Feng, X., Fitzgerald, W., Pirrone, N., Prestbo, E., & Seigneur, C. (2007). A Synthesis of Progress and Uncertainties in Attributing the Sources of Mercury in Deposition. *Ambio, 36*(1), 19–32. https://doi.org/10.1579/0044-7447(2007)36[19:ASOPAU]2.0.CO;2

Linnebjerg, J. F., Hobson, K. A., Fort, J., Nielsen, T. G., Møller, P., Wieland, K., Born, E. W., Rigét, F. F., & Mosbech, A. (2016). Deciphering the structure of the West Greenland marine food web using stable isotopes ($\delta^{13}C$, $\delta^{15}N$). *Marine Biology*, *163*(11). https://doi.org/10.1007/s00227-016-3001-0

Lockhart, W. L., Stern, G. A., Low, G., Hendzel, M., Boila, G., Roach, P., Evans, M. S., Billeck, B. N., DeLaronde, J., Friesen, S., Kidd, K., Atkins, S., Muir, D. C. G., Stoddart, M., Stephens, G., Stephenson, S., Harbicht, S., Snowshoe, N., Grey, B., … DeGraff, N. (2005). A history of total mercury in edible muscle of fish from lakes in northern Canada. *Science of the Total Environment*, *351–352*, 427–463. https://doi.org/10.1016/j.scitotenv.2004.11.027

Loewen, T. N., Gillis, D., & Tallman, R. F. (2010). Maturation, growth and fecundity of Arctic charr, *Salvelinus alpinus* (L.), life-history variants co-existing in lake systems of Southern Baffin Island, Nunavut, Canada. *Hydrobiologia, 650*(1), 193–202. https://doi.org/10.1007/s10750-010-0242-7

Loseto, L. L., Stern, G. A., Deibel, D., Connelly, T. L., Prokopowicz, A., Lean, D. R. S., Fortier, L., & Ferguson, S. H. (2008). Linking mercury exposure to habitat and feeding behaviour in

Beaufort Sea beluga whales. *Journal of Marine Systems*, *74*(3–4), 1012–1024. https://doi.org/10.1016/j.jmarsys.2007.10.004

Lovvorn, J. R., Cooper, L. W., Brooks, M. L., De Ruyck, C. C., Bump, J. K., & Grebmeier, J. M. (2005). Organic matter pathways to zooplankton and benthos under pack ice in late winter and open water in late summer in the north-central Bering Sea. *Marine Ecology Progress Series*, *291*, 135–150. https://doi.org/10.3354/meps291135

Macdonald, T.A., Burd, B.J., Macdonald, V.I., & van Roodselaar, A. (2010). Taxonomic and Feeding Guild Classification for the Marine Benthic Macroinvertebrates of the Strait of Georgia, British Columbia. *Canadian Technical Report of Fisheries and Aquatic Sciences* 2874, iv + 63 p. publications.gc.ca/pub?id=9.571522&sl=0

Madenjian, C.P., Keir, M.J., & Whittle, D.M. (2011). Sexual difference in mercury concentrations in lake trout (*Salvelinus namaycush*) from Lake Ontario. *Chemosphere, 83*, 903–908. https://doi.org/10.1016/j.chemosphere.2011.02.053

Madenjian, C.P., Blanchfield, P.J., Hrenchuk, L.E., Van Walleghem, J.L.A. (2014). Mercury Elimination Rates for Adult Northern Pike *Esox lucius*: Evidence for Sex Effect. *Bulletin of Environmental Contamination and Toxicology, 93*, 144–148. https://doi.org/10.1007/s00128-014-1256-z

Majewski, A. R., Walkusz, W., Lynn, B. R., Atchison, S., Eert, J., & Reist, J. D. (2016). Distribution and diet of demersal Arctic Cod, *Boreogadus saida*, in relation to habitat characteristics in the Canadian Beaufort Sea. *Polar Biology*, *39*(6), 1087–1098. https://doi.org/10.1007/s00300-015-1857-y

Mariotti, A. (1983). Atmospheric nitrogen is a reliable standard for natural ^{15}N abundance measurements. *Nature*, *303*, 685–687. https://doi.org/10.1038/303685a0

Martyniuk, M. A. C., Couture, P., Tran, L., Beaupré, L., & Power, M. (2020). Seasonal variation of total mercury and condition indices of Arctic charr (*Salvelinus alpinus*) in Northern Québec, Canada. *Science of the Total Environment, 738*. https://doi.org/10.1016/j.scitotenv.2020.139450

Mason, R. P., Laporte, J.-M., & Andres, S. (2000). Factors Controlling the Bioaccumulation of Mercury, Methylmercury, Arsenic, Selenium, and Cadmium by Freshwater Invertebrates and Fish. *Archives of Environmental Contamination and Toxicology, 38*(3), 283–297. https://doi.org/10.1007/s002449910038

McCann, S. B., & Dale, J. E. (1986). Sea Ice Breakup and Tidal Flat Processes, Frobisher Bay, Baffin Island. *Physical Geography, 7*(2), 168–180. https://doi.org/10.1080/02723646.1986.10642289

McCann, S. B., Dale, J. E., & Hale, P. B. (1981). Subarctic tidal flats in areas of large tidal range, southern Baffin Island, eastern Canada. *Geographie Physique et Quaternaire*, *35*(2), 183–204. https://doi.org/10.7202/1000436ar

McClelland, J. W., Déry, S. J., Peterson, B. J., Holmes, R. M., & Wood, E. F. (2006). A pan-arctic evaluation of changes in river discharge during the latter half of the 20th century. *Geophysical Research Letters, 33*(6), 2–5. https://doi.org/10.1029/2006GL025753

McCutchan, J. H., Lewis Jr., W. M., Kendall, C., & McGrath, C. C. (2003). Variation in trophic shift for stable isotope ratios of carbon, nitrogen, and sulfur. *Oikos, 102*, 378–390. https://doi.org/10.1111/j.0030-1299.2005.erratum_1.x

McDowall, R. M. (2008). Why are so many boreal freshwater fishes anadromous? Confronting "conventional wisdom." *Fish and Fisheries, 9*(2), 208–213. https://doi.org/10.1111/j.1467-2979.2008.00271.x

McKinney, M. A., Pedro, S., Dietz, R., Sonne, C., Fisk, A. T., Roy, D., Jenssen, B. M., & Letcher, R. J. (2015). A review of ecological impacts of global climate change on persistent organic pollutant and mercury pathways and exposures in arctic marine ecosystems. *Current Zoology, 61*(4), 617–628. https://doi.org/10.1093/czoolo/61.4.617

McMahon, K. W., Ambrose, W. G. J., Johnson, B. J., Sun, M.-Y., Lopez, G. R., Clough, L. M., & Carroll, M. L. (2006). Benthic community response to ice algae and phytoplankton in Ny Ålesund, Svalbard. *Marine Ecology Progress Series*, *310*, 1–14. https://doi.org/10.3354/meps310001

McMeans, B. C., Rooney, N., Arts, M. T., & Fisk, A. T. (2013). Food web structure of a coastal Arctic marine ecosystem and implications for stability. *Marine Ecology Progress Series*, *482*, 17–28. https://doi.org/10.3354/meps10278

Medina-Contreras, D., Arenas-González, F., Cantera-Kintz, J., Sánchez-González, A., & Giraldo, A. (2020). Food web structure and isotopic niche in a fringe macro-tidal mangrove system, Tropical Eastern Pacific. *Hydrobiologia, 847*(15), 3185–3199. https://doi.org/10.1007/s10750-020-04295-x

Medina-Contreras, D., Arenas, F., Cantera-Kintz, J., Sánchez, A., & Lázarus, J.-F. (2022). Carbon sources supporting macrobenthic crustaceans in tropical eastern pacific mangroves. *Food Webs, 30*, e00219. https://doi.org/10.1016/j.fooweb.2022.e00219

Minamata. (2021). Progress Report 2020: Overview of the Minamata Convention on Mercury activities. *Secretariat of the Minamata Convention on Mercury, Geneva, Switzerland*, pp. 27.

Monperrus, M., Tessier, E., Amouroux, D., Leynaert, A., Huonnic, P., & Donard, O. F. X. (2007). Mercury methylation, demethylation and reduction rates in coastal and marine surface waters of the Mediterranean Sea. *Marine Chemistry, 107*(1), 49–63. https://doi.org/10.1016/j.marchem.2007.01.018

Montoya, J.P. (2007). Chapter 7: Natural abundance of ^{15}N in marine planktonic ecosystems. In Stable Isotopes in Ecology and Environmental Science, 2nd Edition, Michener R. & Lajtha, K., Blackwell Publishing Ltd.

Moore, J. W., & Moore, I. A. (1974). Food and growth of arctic char, *Salvelinus alpinus* (L.), in the Cumberland Sound area of Baffin Island. *Journal of Fish Biology, 6*, 79–92.

Mukherjee, A.B. (1999). Advanced technology available for the abatement of mercury pollution in the metallurgical industry. In R. Ebinghaus, R.R. Turner, L.D. de Lacerda, O. Vasiliev, W. Salomons (Eds.), *Mercury Contaminated Sites: Characterization, Risk Assessment and Remediation* (pp. 131 – 142). Springer-Verlag Berlin Heidelberg. https://doi.org/10.1007/978-3-662-03754-6_6

Mulder, I. M., Morris, C. J., Dempson, J. B., Fleming, I. A., & Power, M. (2018). Overwinter thermal habitat use in lakes by anadromous arctic char. *Canadian Journal of Fisheries and Aquatic Sciences, 75*(12), 2343–2353. https://doi.org/10.1139/cjfas-2017-0420

Mulder, I. M., Morris, C. J., Dempson, B. J., Fleming, I. A., & Power, M. (2020). Marine temperature and depth use by anadromous Arctic char correlates to body size and diel period. *Canadian Journal of Fisheries and Aquatic Sciences, 77*(5), 882–893. https://doi.org/10.1139/cjfas-2019-0097

Murdoch, A., Dempson, J. B., Martin, F., & Power, M. (2015). Temperature-growth patterns of individually tagged anadromous Arctic charr *Salvelinus alpinus* in Ungava and Labrador, Canada. *Ecology of Freshwater Fish, 24*(2), 193–203. https://doi.org/10.1111/eff.12133

Murillo-Cisneros, D. A., O'Hara, T. M., Castellini, J. M., Sánchez-González, A., Elorriaga-Verplancken, F. R., Marmolejo-Rodríguez, A. J., Marín-Enríquez, E., & Galván-Magaña, F. (2018). Mercury concentrations in three ray species from the Pacific coast of Baja California Sur, Mexico: Variations by tissue type, sex and length. *Marine Pollution Bulletin, 126*, 77–85. https://doi.org/10.1016/j.marpolbul.2017.10.060

Newsome, S. D., Yeakel, J. D., Wheatley, P. V., & Tinker, M. T. (2012). Tools for quantifying isotopic niche space and dietary variation at the individual and population level. *Journal of Mammalogy, 93*(2), 329–341. https://doi.org/10.1644/11-MAMM-S-187.1

North, C. A., Lovvorn, J. R., Kolts, J. M., Brooks, M. L., Cooper, L. W., & Grebmeier, J. M. (2014). Deposit-feeder diets in the Bering Sea: potential effects of climatic loss of sea ice-related microalgal blooms. *Ecological Applications, 24*(6), 1525–1542. https://doi.org/10.1890/13-0486.1

O'Callaghan, I., & Sullivan, T. (2020). Shedding the load: moulting as a cause of variability in whole-body metal concentrations. *Journal of Crustacean Biology, 40*(6), 725–733. https://doi.org/10.1093/jcbiol/ruaa077

Obrist, D., Agnan, Y., Jiskra, M., Olson, C. L., Colegrove, D. P., Hueber, J., Moore, C. W., Sonke, J. E., & Helmig, D. (2017). Tundra uptake of atmospheric elemental mercury drives Arctic mercury pollution. *Nature, 547*(7662), 201–204. https://doi.org/10.1038/nature22997

Obrist, D., Kirk, J. L., Zhang, L., Sunderland, E. M., Jiskra, M., & Selin, N. E. (2018). A review of global environmental mercury processes in response to human and natural perturbations:

Changes of emissions, climate, and land use. *Ambio, 47*(2). https://doi.org/10.1007/s13280-017-1004-9

Olsson, M., Svärdh, L., & Toth, G. B. (2007). Feeding behaviour in *Littorina littorea*: the red seaweed *Osmundea ramosissima* may not prevent trematode infection. *Marine Ecology Progress Series*, *348*, 221–228. https://doi.org/10.3354/meps07048

Ordiano-Flores, A., Galván-Magaña, F., Sánchez-González, A., Soto-Jiménez, M. F., & Páez-Osuna, F. (2021). Mercury, selenium, and stable carbon and nitrogen isotopes in the striped marlin *Kajikia audax* and blue marlin *Makaira nigricans* food web from the Gulf of California. *Marine Pollution Bulletin, 170*, 112657. https://doi.org/10.1016/j.marpolbul.2021.112657

Outridge, P.M., Mason, R.P., Wang, F., Guerrero, S., & Heimbürger-Boavida, L.E. (2018). Updated Global and Oceanic Mercury Budgets for the United Nations Global Mercury Assessment 2018. *Environmental Science & Technology, 52*(20), 11466–11477. https://doi.org/10.1021/acs.est.8b01246

Papiol, V., Cartes, J.E., Fanelli, E., & Rumolo, P. (2013). Food web structure and seasonality of slope megafauna in the NW Mediterranean elucidated by stable isotopes: Relationship with available food sources. *Journal of Sea Research, 77,* 53–69. https://doi.org/10.1016/j.seares.2012.10.002

Paranjape, A. R., & Hall, B. D. (2017). Recent advances in the study of mercury methylation in aquatic systems. *Facets, 2*(1), 85–119. https://doi.org/10.1139/facets-2016-0027

Peacor, S.D., Bence, J.R., & Pfister, C.A. (2007). The effect of size-dependent growth and environmental factors on animal size variability. *Theoretical Population Biology, 71*, 80–94. https://doi.org/10.1016/j.tpb.2006.08.005

Pearre, S, J. (1980). Feeding by Chaetognatha: The Relation of Prey Size to Predator Size in Several Species. *Marine Ecology Progress Series, 3*, 125–134. https://doi.org/10.3354/meps003125

Percy, J. A. (1983). Distribution of Arctic Marine Isopods of the *Mesidotea* (= Saduria) Complex in Relation to Depth, Temperature, and Salinity in the Southern Beaufort Sea. *Arctic, 36*(4), 341–349. https://www.jstor.org/stable/40509593

Peterson, B. J., Holmes, R. M., McClelland, J. W., Vörösmarty, C. J., Lammers, R. B., Shiklomanov, A. I., Shiklomanov, I. A., & Rahmstorf, S. (2002). Increasing river discharge to the Arctic Ocean. *Science, 298*(5601), 2171–2173. https://doi.org/10.1126/science.1077445

Piepenburg, D. (2005). Recent research on Arctic benthos: common notions need to be revised. *Polar Biology, 28*(10), 733–755. https://doi.org/10.1007/s00300-005-0013-5

Polis, G. A., & Strong, D. R. (1996). Food Web Complexity and Community Dynamics. *The American Naturalist*, *147*(5), 813–846. https://www.jstor.org/stable/2463091

Pongratz, R., & Heumann, K. G. (1998). Production of methylated mercury and lead by polar macroalgae - A significant natural source for atmospheric heavy metals in clean room

compartments. *Chemosphere, 36*(9), 1935–1946. https://doi.org/10.1016/S0045-6535(97)10078-9

Post, D. M. (2002a). The long and short of food-chain length. *Trends in Ecology & Evolution*, *17*(6), 269–277. https://doi.org/10.1016/S0169-5347(02)02455-2

Post, D. M. (2002b). Using Stable Isotopes to Estimate Trophic Position: Models, Methods, and Assumptions. *Ecology, 83*(3), 703–718. https://doi.org/10.2307/3071875

Power, M., & Reist, J.D. (2018). *Salvelinus alpinus*. In B.W. Coad & J.D. Reist (Eds.) *Marine fishes of Arctic Canada* (pp. 283 – 289). University of Toronto Press. http://www.jstor.org/stable/10.3138/j.ctt1x76h0b

Power, M., Klein, G. M., Guiguer, K. R. R. A., & Kwan, M. K. H. (2002). Mercury accumulation in the fish community of a sub-Arctic lake in relation to trophic position and carbon sources. *Journal of Applied Ecology*, *39*(5), 819–830. https://doi.org/10.1046/j.1365-2664.2002.00758.x

Power, M., Reist, J. D., & Dempson, J. B. (2008). Fish in high-latitude Arctic lakes. In W.F. Vincent & J. Laybourn-Parry (Eds.), *Polar Lakes and Rivers: Limnology of Arctic and Antarctic Aquatic Ecosystems* (pp. 249 – 268). Oxford University Press. 10.1093/acprof:oso/9780199213887.001.0001

Premke, K., Muyakshin, S., Klages, M., & Wegner, J. (2003). Evidence for long-range chemoreceptive tracking of food odour in deep-sea scavengers by scanning sonar data. *Journal of Experimental Marine Biology and Ecology*, *285–286*, 283–294. https://doi.org/10.1016/S0022-0981(02)00533-6

Priest, H., & Usher, P. J. (2004). The Nunavut Wildlife Harvest Study. Nunavut Wildlife Management Board, February.

Prowse, T. D., Wrona, F. J., Reist, J. D., Gibson, J. J., Hobbie, J. E., Lévesque, L. M. J., & Vincent, W. F. (2006). Climate change effects on hydroecology of arctic freshwater ecosystems. *Ambio, 35*(7), 347–358. https://doi.org/10.1579/0044-7447(2006)35[347:CCEOHO]2.0.CO;2

Qiu, J.-W., Qian, P.-Y., & Wang, W.-X. (2001). Contribution of dietary bacteria to metal accumulation in the slipper limpet. *Aquatic Microbial Ecology, 25*(2), 151–161. https://doi.org/10.3354/ame025151

Quillien, N., Nordström, M. C., Schaal, G., Bonsdorff, E., & Grall, J. (2016). Opportunistic basal resource simplifies food web structure and functioning of a highly dynamic marine environment. *Journal of Experimental Marine Biology and Ecology, 477*, 92–102. https://doi.org/10.1016/j.jembe.2016.01.010

R Core Team (2020). R: A language and environment for statistical computing. R Foundation for Statistical Computing, Vienna, Austria. https://www.r-project.org/

Ramlal, P. S., Kelly, C. A., Rudd, J. W. M., & Furutani, A. (1993). Sites of methyl mercury production in remote Canadian Shield lakes. *Canadian Journal of Fisheries and Aquatic Sciences, 50*(5), 972–979. https://doi.org/10.1139/f93-112

Ramos-Osuna, M., Patiño-Mejía, C., Ruelas-Inzunza, J., Escobar-Sánchez, O. (2020). Bioaccumulation of mercury in *Haemulopsis elongatus* and *Pomadasys macracanthus* from the SE Gulf of California: condition indexes and health risk assessment. *Environmental Monitoring and Assessment, 192*(11). 10.1007/s10661-020-08599-2

Ravichandran, M. (2004). Interactions between mercury and dissolved organic matter - a review. *Chemosphere*, 55(3), 319–331. https://doi.org/10.1016/j.chemosphere.2003.11.011

Regnell, O., & Watras, C. J. (2019). Microbial Mercury Methylation in Aquatic Environments: A Critical Review of Published Field and Laboratory Studies. *Environmental Science and Technology, 53*(1), 4–19. https://doi.org/10.1021/acs.est.8b02709

Reist, J. D., Wrona, F. J., Prowse, T. D., Power, M., Dempson, J. B., King, J. R., & Beamish, R. J. (2006). An Overview of Effects of Climate Change on Selected Arctic Freshwater and Anadromous Fishes. *Ambio, 35*(7), 381–387. https://doi.org/10.1579/0044-7447(2006)35[381:AOOEOC]2.0.CO;2

Renaud, P. E., Tessmann, M., Evenset, A., & Christensen, G. N. (2011). Benthic food-web structure of an Arctic fjord (Kongsfjorden, Svalbard). *Marine Biology Research*, *7*(1), 13–26. https://doi.org/10.1080/17451001003671597

Reynolds, C. S. (2008). A Changing Paradigm of Pelagic Food Webs. *International Review of Hydrobiology*, 93(4–5), 517–531. https://doi.org/10.1002/iroh.200711026

Riget, F., Asmund, G., & Aastrup, P. (2000). Mercury in Arctic char (*Salvelinus alpinus*) populations from Greenland. *Science of the Total Environment, 245*(1–3), 161–172. https://doi.org/10.1016/S0048-9697(99)00441-6

Rigét, F., Møller, P., Dietz, R., Nielsen, T. G., Asmund, G., Strand, J., Larsen, M. M., & Hobson, K. A. (2007). Transfer of mercury in the marine food web of West Greenland. *Journal of Environmental Monitoring*, *9*(8), 877–883. https://doi.org/10.1039/b704796g

Rikardsen, A. H., Amundsen, P. A., Bjørn, P. A., & Johansen, M. (2000). Comparison of growth, diet and food consumption of sea-run and lake-dwelling arctic charr. *Journal of Fish Biology, 57*(5), 1172–1188. https://doi.org/10.1006/jfbi.2000.1380

Rikardsen, A. H., Amundsen, P. A., & Bodin, P. J. (2002). Foraging behaviour changes of Arctic charr during smolt migration in northern Norway. *Journal of Fish Biology, 60*(2), 489–491. https://doi.org/10.1006/jfbi.2001.1840

Rikardsen, A. H., Amundsen, P. A., & Bodin, P. J. (2003). Growth and diet of anadromous Arctic charr after their return to freshwater. *Ecology of Freshwater Fish, 12*(1), 74–80. https://doi.org/10.1034/j.1600-0633.2003.00001.x

Rikardsen, A. H., Dempson, J. B., Amundsen, P. A., Bjørn, P. A., Finstad, B., & Jensen, A. J. (2007). Temporal variability in marine feeding of sympatric Arctic charr and sea trout. *Journal of Fish Biology*, *70*(3), 837–852. https://doi.org/10.1111/j.1095-8649.2007.01345.x

Rooney, N., McCann, K., Gellner, G., & Moore, J. C. (2006). Structural asymmetry and the stability of diverse food webs. *Nature*, *442*, 265–269. https://doi.org/10.1038/nature04887

Rounick, J. S., & Winterbourn, M. J. (1986). Stable Carbon Isotopes and Carbon Flow in Ecosystems. *BioScience, 36*(3), 171–177. https://doi.org/10.2307/1310304

Rousseeuw, P.J. (1987). Silhouettes: a graphical aid to the interpretation and validation of cluster analysis. *Journal of Computational and Applied Mathematics, 20*, 53 – 65.

Roux, M. J., Tallman, R. F., & Lewis, C. W. (2011). Small-scale Arctic charr Salvelinus alpinus fisheries in Canada's Nunavut: Management challenges and options. *Journal of Fish Biology, 79*(6), 1625–1647. https://doi.org/10.1111/j.1095-8649.2011.03092.x

Rowan, D.J., & Rasmussen, J.B. (1996). Measuring the bioenergetic cost of fish activity in situ using a globally dispersed radiotracer (^{137}Cs). *Canadian Journal of Fisheries and Aquatic Sciences, 53*, 734–745. https://doi.org/10.1139/f95-046

Ruus, A., Øverjordet, I. B., Braaten, H. F. V., Evenset, A., Christensen, G., Heimstad, E. S., Gabrielsen, G. W., & Borgå, K. (2015). Methylmercury biomagnification in an Arctic pelagic food web. *Environmental Toxicology and Chemistry, 34*(11), 2636–2643. https://doi.org/10.1002/etc.3143

Sackett, D. K., Aday, D. D., Rice, J. A., & Cope, W. G. (2013). Maternally transferred mercury in wild largemouth bass, *Micropterus salmoides*. *Environmental Pollution, 178*, 493–497. https://doi.org/10.1016/j.envpol.2013.03.046

Sánchez-Marín, P., Aierbe, E., Lorenzo, J. I., Mubiana, V. K., Beiras, R., & Blust, R. (2016). Dynamic modeling of copper bioaccumulation by *Mytilus edulis* in the presence of humic acid aggregates. *Aquatic Toxicology, 178*, 165–170. https://doi.org/10.1016/j.aquatox.2016.07.021

Schaal, G., Riera, P., & Leroux, C. (2008). Trophic coupling between two adjacent benthic food webs within a man-made intertidal area: A stable isotopes evidence. *Estuarine, Coastal and Shelf Science, 77*(3), 523–534. https://doi.org/10.1016/j.ecss.2007.10.008

Scheuhammer, A. M., Meyer, M. W., Sandheinrich, M. B., & Murray, M. W. (2007). Effects of Environmental Methylmercury on the Health of Wild Birds, Mammals, and Fish. *Ambio*, *36*(1), 12–19. https://doi.org/10.1579/0044-7447(2007)36[12:EOEMOT]2.0.CO;2

Scheuhammer, A., Braune, B., Man Chan, H., Frouin, H., Krey, A., Letcher, R., Loseto, L., Noël, M., Ostertag, S., Ross, P., Wayland, M. (2015). Recent progress on our understanding of the biological effects of mercury in fish and wildlife in the Canadian Arctic. *Science of the Total Environment, 509-510*, 91–103. https://doi.org/10.1016/j.scitotenv.2014.05.142

Schmidt, S. N., Olden, J. D., Solomon, C. T., & Vander Zanden, M. J. (2007). Quantitative approaches to the analysis of stable isotope food web data. *Ecology, 88*(11), 2793–2802. https://doi.org/10.1890/07-0121.1

Selin, H., Keane, S.E., Wang, S., Selin, N.E., Davis, K., Bally, D. (2018). Linking science and policy to support the implementation of the Minamata Convention on Mercury. *Ambio, 47*, 198 – 215. https://doi.org/10.1007/s13280-017-1003-x

Shapiro, S.S., Wilk, M.B. (1965). An analysis of variance test for normality (complete samples). *Biometrika, 52*(3-4)*,* 591 – 611. https://www.jstor.org/stable/2333709

Smylie, M. S., McDonough, C. J., Reed, L. A., & Shervette, V. R. (2016). Mercury bioaccumulation in an estuarine predator: Biotic factors, abiotic factors, and assessments of fish health. *Environmental Pollution, 214*, 169–176. https://doi.org/10.1016/j.envpol.2016.04.007

Snyder, D.E. (1983). Fisheries Technique, (Nielsen, L.A. and Johnson, D.L., eds). Southern Printing Company Inc. Blacksburg, Virginia.

Sokołowski, A., Wołowicz, M., Asmus, H., Asmus, R., Carlier, A., Gasiunaité, Z., Grémare, A., Hummel, H., Lesutiené, J., Razinkovas, A., Renaud, P. E., Richard, P., & Kędra, M. (2012). Is benthic food web structure related to diversity of marine macrobenthic communities? *Estuarine, Coastal and Shelf Science, 108*, 76–86. https://doi.org/10.1016/j.ecss.2011.11.011

Somers, K. M., & Jackson, D. A. (1993). Adjusting Mercury Concentration for Fish-Size Covariation: A Multivariate Alternative to Bivariate Regression. *Canadian Journal of Fisheries and Aquatic Sciences, 50*(11), 2388–2396. https://doi.org/10.1139/f93-263

Søreide, J. E., Carroll, M. L., Hop, H., Ambrose, W. G., Hegseth, E. N., & Falk-Petersen, S. (2013). Sympagic-pelagic-benthic coupling in Arctic and Atlantic waters around Svalbard revealed by stable isotopic and fatty acid tracers. *Marine Biology Research*, *9*(9), 831–850. https://doi.org/10.1080/17451000.2013.775457

Søreide, J. E., Hop, H., Carroll, M. L., Falk-Petersen, S., & Hegseth, E. N. (2006). Seasonal food web structures and sympagic-pelagic coupling in the European Arctic revealed by stable isotopes and a two-source food web model. *Progress in Oceanography, 71*(1), 59–87. https://doi.org/10.1016/j.pocean.2006.06.001

Spares, A. D., Stokesbury, M. J. W., O'Dor, R. K., & Dick, T. A. (2012). Temperature, salinity and prey availability shape the marine migration of Arctic char, *Salvelinus alpinus*, in a macrotidal estuary. *Marine Biology, 159*(8), 1633–1646. https://doi.org/10.1007/s00227-012-1949-y

Spares, A. D., Stokesbury, M. J. W., Dadswell, M. J., O'Dor, R. K., & Dick, T. A. (2015). Residency and movement patterns of Arctic charr *Salvelinus alpinus* relative to major estuaries. *Journal of Fish Biology*, *86*(6), 1754–1780. https://doi.org/10.1111/jfb.12683

Stasko, A. D., Bluhm, B. A., Michel, C., Archambault, P., Majewski, A., Reist, J. D., Swanson, H., & Power, M. (2018). Benthic-pelagic trophic coupling in an Arctic marine food web along vertical water mass and organic matter gradients. *Marine Ecology Progress Series, 594*, 1–19. https://doi.org/10.3354/meps12582

Statistics Canada. (2022). Iqaluit [City], Nunavut (table). Census Profile. *2021 Census*. Statistics Canada Catalogue no. 98-316-X2021001. Ottawa. Released February 9, 2022. https://www12.statcan.gc.ca/census-recensement/2021/dp-pd/prof/index.cfm?Lang=E [accessed February 23, 2022].

Stern, G. A., Macdonald, R. W., Outridge, P. M., Wilson, S., Chételat, J., Cole, A., Hintelmann, H., Loseto, L. L., Steffen, A., Wang, F., & Zdanowicz, C. (2012). How does climate change influence arctic mercury? *Science of the Total Environment, 414*, 22–42. https://doi.org/10.1016/j.scitotenv.2011.10.039

Stock, B. C., Jackson, A. L., Ward, E. J., Parnell, A. C., Phillips, D. L., & Semmens, B. X. (2018). Analyzing mixing systems using a new generation of Bayesian tracer mixing models. *PeerJ, 6*. https://doi.org/10.7717/peerj.5096

Streets, D. G., Horowitz, H. M., Jacob, D. J., Lu, Z., Levin, L., Ter Schure, A. F. H., & Sunderland, E. M. (2017). Total Mercury Released to the Environment by Human Activities. *Environmental Science and Technology, 51*(11), 5969–5977. https://doi.org/10.1021/acs.est.7b00451

Sunderland, E.M., & Selin, N.E. (2013). Future trends in environmental mercury concentrations: implications for prevention strategies. *Environmental Health, 12*(2), https://doi.org/10.1186/1476-069X-12-2

Swanson, H. K., & Kidd, K. A. (2010). Mercury concentrations in arctic food fishes reflect the presence of anadromous arctic charr (*Salvelinus alpinus*), species, and life history. *Environmental Science and Technology, 44*(9), 3286–3292. https://doi.org/10.1021/es100439t

Swanson, H. K., Kidd, K. A., & Reist, J. D. (2011a). Quantifying importance of marine prey in the diets of two partially anadromous fishes. *Canadian Journal of Fisheries and Aquatic Sciences, 68*(11), 2020–2028. https://doi.org/10.1139/f2011-111

Swanson, H., Gantner, N., Kidd, K. A., Muir, D. C. G., & Reist, J. D. (2011b). Comparison of mercury concentrations in landlocked, resident, and sea-run fish (*Salvelinus* spp.) from Nunavut, Canada. *Environmental Toxicology and Chemistry, 30*(6), 1459–1467. https://doi.org/10.1002/etc.517

Symonds, M. R. E., & Moussalli, A. (2011). A brief guide to model selection, multimodel inference and model averaging in behavioural ecology using Akaike's information criterion. *Behavioral Ecology and Sociobiology, 65*(1), 13–21. https://doi.org/10.1007/s00265-010-1037-6

Tamelander, T., Renaud, P. E., Hop, H., Carroll, M. L., Ambrose, W. G. J., & Hobson, K. A. (2006). Trophic relationships and pelagic-benthic coupling during summer in the Barents Sea

Marginal Ice Zone, revealed by stable carbon and nitrogen isotope measurements. *Marine Ecology Progress Series, 310*, 33–46. https://doi.org/10.3354/meps310033

Thomas, S. M., Kiljunen, M., Malinen, T., Eloranta, A. P., Amundsen, P. A., Lodenius, M., & Kahilainen, K. K. (2016). Food-web structure and mercury dynamics in a large subarctic lake following multiple species introductions. *Freshwater Biology*, *61*(4), 500–517. https://doi.org/10.1111/fwb.12723

Thompson, S. (2005). Chapter 3: Sustainability and Vulnerability: Aboriginal Arctic Food Security in a Toxic World (F. Berkes (ed.)). University of Calgary Press.

Tomczyk, N. J., Parr, T. B., Gray, E., Iburg, J., & Capps, K. A. (2018). Trophic Strategies Influence Metal Bioaccumulation in Detritus-Based, Aquatic Food Webs. *Environmental Science and Technology*, *52*(20), 11886–11894. https://doi.org/10.1021/acs.est.8b04009

Tran, L., Reist, J. D., & Power, M. (2015). Total mercury concentrations in anadromous Northern Dolly Varden from the northwestern Canadian Arctic: A historical baseline study. *Science of the Total Environment, 509–510*, 154–164. https://doi.org/10.1016/j.scitotenv.2014.04.099

Trudel, M., & Rasmussen, J.B. (2001). Predicting Mercury Concentrations in Fish Using Mass Balance Models. *Ecological Applications, 11*(2), 517–529. https://doi.org/10.2307/3060906

Trudel, M., & Rasmussen, J. B. (2006). Bioenergetics and mercury dynamics in fish: a modelling perspective. *Canadian Journal of Fisheries and Aquatic Sciences, 63*(8), 1890–1902. https://doi.org/10.1139/f06-081

Trussell, G. C., Ewanchuk, P. J., & Matassa, C. M. (2006). The fear of being eaten reduces energy transfer in a simple food chain. *Ecology*, *87*(12), 2979–2984. https://doi.org/10.1890/0012-9658(2006)87[2979:TFOBER]2.0.CO;2

Tukey, J.W. (1953). The problem of multiple comparisons. Department of Statistics, Princeton University (unpublished).

Tveiten, H., Johnsen, H. K., & Jobling, M. (1996). Influence of maturity status on the annual cycles of feeding and growth in Arctic charr reared at constant temperature. *Journal of Fish Biology, 48*(5), 910–924. https://doi.org/10.1111/j.1095-8649.1996.tb01486.x

U.S. EPA. (1996). Method 1669: Sampling Ambient Water for Trace Metals at EPA Water Quality Criteria Levels. U.S. Environmental Protection Agency, iv + 35.

U.S. EPA. (1998). Method 1630: Methly Mercury in Water by Distillation, Aqueous Ethylation, Purge and Trap, and Cold Vapor Atomic Fluorescence Spectrometry. U.S. Environmental Protection Agency, iv + 46.

U.S. EPA. (2002). Method 1631, Revision E: Mercury in Water by Oxidation, Purge and Trap, and Cold Vapor Atomic Fluorescence Spectrometry. U.S. Environmental Protection Agency, v + 38.

U.S. EPA. (2007). Method 7473: Mercury in Solids and Solutions by Thermal Decomposition, Amalgamation, and Atomic Absorption Spectrophotometry. U.S. Environmental Protection Agency, 17.

Ulrich, K.L., & Tallman, R.F. (2021). Multi-indicator evidence for habitat use and trophic strategy segregation of two sympatric forms of Arctic char from the Cumberland Sound region of Nunavut, Canada. *Arctic Science, 7*, 512–544. https://doi.org/10.1139/as-2019-0039

UNEP. (2019a). Minamata Convention on Mercury. United Nations Environment Programme, pp. 72.

UNEP. (2019b). Global Mercury Assessment 2018. United Nations Environment Programme, Chemicals and Health Branch Geneva, Switzerland. ISBN: 978-92-807-3744-8

UNEP. (2021). Progress Report 2020: Overview of the Minamata Convention on Mercury activities. Secretariat of the Minamata Convention of Mercury, United Nations, pp 27.

van der Velden, Shannon, Reist, J. D., Babaluk, J. A., & Power, M. (2012). Biological and life-history factors affecting total mercury concentrations in Arctic charr from Heintzelman Lake, Ellesmere Island, Nunavut. *Science of the Total Environment, 433*, 309–317. https://doi.org/10.1016/j.scitotenv.2012.06.055

van der Velden, S., Evans, M. S., Dempson, J. B., Muir, D.C.G., & Power, M. (2013a). Comparative analysis of total mercury concentrations in anadromous and non-anadromous Arctic charr (*Salvelinus alpinus*) from eastern Canada. *Science of the Total Environment, 447*, 438–449. https://doi.org/10.1016/j.scitotenv.2012.12.092

van der Velden, S., Dempson, J. B., Evans, M.S., Muir, D.C.G., & Power, M. (2013b). Basal mercury concentrations and biomagnification rates in freshwater and marine food webs: Effects on Arctic charr (*Salvelinus alpinus*) from eastern Canada. *Science of the Total Environment, 444*, 531–542. https://doi.org/10.1016/j.scitotenv.2012.11.099

Vander Zanden, M. J., Vadeboncoeur, Y., & Chandra, S. (2011). Fish Reliance on Littoral-Benthic Resources and the Distribution of Primary Production in Lakes. *Ecosystems, 14*(6), 894–903. https://doi.org/10.1007/s10021-011-9454-6

VanGerwen-Toyne, M., Lewis, C., Tallman, R. F., Martin, Z., & Moore, J.-S. (2013). Information to support the assessment of Arctic Char (*Salvelinus alpinus*) in the Sylvia Grinnell River, Nunavut, 2009 – 2011. *DFO Canadian Science Advisory Secretariat*, Doc. 2013/109, vi + 19p.

Wagstaff, M. C., Howell, K. L., Bett, B. J., Billett, D. S. M., Brault, S., Stuart, C. T., & Rex, M. A. (2014). β-diversity of deep-sea holothurians and asteroids along a bathymetric gradient (NE Atlantic). *Marine Ecology Progress Series*, *508*, 177–185. https://doi.org/10.3354/meps10877

Ward, D. M., Nislow, K. H., Chen, C. Y., & Folt, C. L. (2010). Rapid, Efficient Growth Reduces Mercury Concentrations in Stream-Dwelling Atlantic Salmon. *Transactions of the American Fisheries Society, 139*(1), 1–10. https://doi.org/10.1577/t09-032.1

Wesche, S. D., & Chan, H. M. (2010). Adapting to the Impacts of Climate Change on Food Security among Inuit in the Western Canadian Arctic. *EcoHealth, 7*(3), 361–373. https://doi.org/10.1007/s10393-010-0344-8

Wesławski, J. M., Opanowski, A., Legezyńska, J., Maciejewska, B., Włodarska-Kowalczuk, M., & Kędra, M. (2010). Hidden diversity in Arctic crustaceans. How many roles can a species play? *Polish Polar Research*, *31*(3), 205–216. 10.2478/v10183−010−0001−5

Whitehouse, G. A., Buckley, T. W., & Danielson, S. L. (2017). Diet compositions and trophic guild structure of the eastern Chukchi Sea demersal fish community. *Deep-Sea Research Part II: Topical Studies in Oceanography*, *135*, 95–110. https://doi.org/10.1016/j.dsr2.2016.03.010

WHO. (1990). Environmental health criteria 101: methylmercury. World Health Organization, Geneva, Switzerland.

Wiener, J. G., Martini, R. E., Sheffy, T. B., & Glass, G. E. (1990). Factors Influencing Mercury Concentrations in Walleyes in Northern Wisconsin Lakes. *Transactions of the American Fisheries Society, 119*(5), 862–870. https://doi.org/10.1577/1548-8659(1990)119<0862:fimciw>2.3.co;2

Wolfe, M. F., Schwarzbach, S., & Sulaiman, R. A. (1998). Effects of mercury on wildlife: a comprehensive review. *Environmental Toxicology and Chemistry*, *17*(2), 146–160. https://doi.org/10.1002/etc.5620170203

WoRMS Editorial Board. (2022). World Register of Marine Species. Available from https://www.marinespecies.org at VLIZ. Accessed 2022-01-04. doi:10.14284/170

Yang, Z., Fang, W., Lu, X., Sheng, G.-P., Graham, D. E., Liang, L., Wullschleger, S. D., & Gu, B. (2016). Warming increases methylmercury production in an Arctic soil. *Environmental Pollution, 214*, 504–509. https://doi.org/10.1016/j.envpol.2016.04.069

Zar, J.H. (2018). Biostatistical Analysis (Fifth ed.). Pearson Education Inc., Upper Saddle River, NJ.

Appendices

Appendix A – Chapter 2

Table S2.1. Two-way Analysis of Variance (ANOVA) results for the immature groups, IM-hi (n = 37) and IM-lo (n = 30), of anadromous Arctic char caught in inner Frobisher Bay, Nunavut.

Variable	$\delta^{15}N$			Age		
	F value	**df**	**p-value**	**F value**	**df**	**p-value**
Sex	1.330	1, 63	> 0.05	0.032	1, 63	> 0.05
Collection site	0.931	3, 54	> 0.05	2.120	3, 54	> 0.05
Collection year	0.308	1, 63	> 0.05	4.884	1, 63	< 0.05
Collection month	1.270	1, 62	> 0.05	4.347	1, 62	< 0.05
Collection date	0.787	5, 50	> 0.05	3.125	5, 50	< 0.05

Table S2.2. Analysis of Variance (ANOVA) and Tukey's Honestly Significant Difference (HSD) test statistics for results presented in Table 2.1.

Variable	ANOVA Results			Tukey's HSD Results		
	F	df	p	IM-lo – IM-hi	MAT – IM-hi	MAT – IM-lo
Age (years)	69.98	2, 104	< 0.001	< 0.001	> 0.05	< 0.001
Fork length (mm)	73.45	2, 110	< 0.001	< 0.05	< 0.001	< 0.001
Log_{10} weight (g)	73.12	2, 109	< 0.001	< 0.05	< 0.001	< 0.001
Log_{10} growth rate (mm/year)	40.39	2, 105	< 0.001	< 0.001	< 0.001	< 0.001
$\delta^{13}C$ (‰)	26.17	2, 108	< 0.001	< 0.001	< 0.05	< 0.001
$\delta^{15}N$ (‰)	83.13	2, 107	< 0.001	< 0.001	< 0.001	> 0.05
Benthic Reliance Index	26.17	2, 108	< 0.001	< 0.001	< 0.05	< 0.001
Condition	17.93	2, 105	< 0.001	< 0.01	< 0.001	> 0.05
Gonadosomatic Index	5.007	2, 110	< 0.01	> 0.05	< 0.05	< 0.05
Hepatosomatic Index	31.61	2, 104	< 0.001	< 0.001	< 0.001	> 0.05
[THg] (ng/g dw)	108.9	2, 106	< 0.001	< 0.001	< 0.001	< 0.001

Table S2.3. Pearson correlation coefficient results for IM-hi (n = 32). The upper value is the correlation coefficient (i.e., r) and the lower value is the p-value. Significant correlations (i.e., $p < 0.05$) are highlighted in bold and underlined. Age (years); BRI, benthic reliance index; FL, fork length (mm); GSI, gonadosomatic index; HSI, hepatosomatic index; K, condition; LGR, $\log_{10}$ growth rate (mm/year); LTHG, $\log_{10}$ THg (ng/g dw); LWT, $\log_{10}$ weight (g); and $\delta^{15}N$ (‰).

	LTHG	**FL**	**LWT**	**LGR**	**Age**	**K**	**BRI**	**$\delta^{15}N$**	**GSI**	**HSI**
LTHG	1.00 -	**-0.65** **< 0.001**	**-0.69** **< 0.001**	-0.31 > 0.05	-0.19 > 0.05	**-0.43** **< 0.05**	**-0.76** **< 0.001**	**-0.87** **< 0.001**	-0.13 > 0.05	**-0.63** **< 0.001**
FL		1.00 -	**0.97** **< 0.001**	-0.07 > 0.05	**0.70** **< 0.001**	0.14 > 0.05	**0.68** **< 0.001**	**0.76** **< 0.001**	0.24 > 0.05	**0.57** **< 0.001**
LWT			1.00 -	-0.04 > 0.05	**0.65** **< 0.001**	**0.35** **< 0.05**	**0.72** **< 0.001**	**0.79** **< 0.001**	0.25 > 0.05	**0.68** **< 0.001**
LGR				1.00 -	**-0.76** **< 0.001**	0.15 > 0.05	0.08 > 0.05	0.19 > 0.05	-0.02 > 0.05	0.16 > 0.05
Age					1.00 -	-0.01 > 0.05	**0.39** **< 0.05**	0.34 > 0.05	0.16 > 0.05	0.24 > 0.05
K						1.00 -	**0.42** **< 0.05**	**0.37** **< 0.05**	0.06 > 0.05	**0.53** **< 0.01**
BRI							1.00 -	**0.69** **< 0.001**	0.15 > 0.05	**0.54** **< 0.01**
$\delta^{15}N$								1.00 -	0.19 > 0.05	**0.70** **< 0.001**
GSI									1.00 -	**0.37** **< 0.05**
HSI										1.00 -

Table S2.4. Pearson correlation coefficient results for IM-lo (n = 27). The upper value is the correlation coefficient (i.e., r) and the lower value is the p-value. Significant correlations (i.e., $p < 0.05$) are highlighted in bold and underlined. Age (years); BRI, benthic reliance index; FL, fork length (mm); GSI, gonadosomatic index; HSI, hepatosomatic index; K, condition; LGR, $\log_{10}$ growth rate (mm/year); LTHG, $\log_{10}$ THg (ng/g dw); LWT, $\log_{10}$ weight (g); and $\delta^{15}N$ (‰).

	LTHG	**FL**	**LWT**	**LGR**	**Age**	**K**	**BRI**	**$\delta^{15}N$**	**GSI**	**HSI**
LTHG	1.00 -	**-0.48** **< 0.05**	**-0.48** **< 0.05**	-0.33 > 0.05	-0.17 > 0.05	-0.14 > 0.05	0.10 > 0.05	**-0.46** **< 0.05**	-0.04 > 0.05	0.21 > 0.05
FL		1.00 -	**0.98** **< 0.001**	0.24 > 0.05	**0.67** **< 0.001**	**0.48** **< 0.05**	-0.34 > 0.05	0.12 > 0.05	**0.39** **< 0.05**	0.16 > 0.05
LWT			1.00 -	0.18 > 0.05	**0.70** **< 0.001**	**0.62** **< 0.001**	-0.34 > 0.05	0.12 > 0.05	**0.41** **< 0.05**	0.17 > 0.05
LGR				1.00 -	**-0.55** **< 0.01**	-0.17 > 0.05	0.05 > 0.05	0.15 > 0.05	-0.14 > 0.05	-0.31 > 0.05
Age					1.00 -	**0.53** **< 0.01**	-0.34 > 0.05	-0.02 > 0.05	**0.47** **< 0.05**	0.34 > 0.05
K						1.00 -	-0.27 > 0.05	-0.01 > 0.05	**0.52** **< 0.01**	0.25 > 0.05
BRI							1.00 -	0.26 > 0.05	**-0.45** **< 0.05**	-0.23 > 0.05
$\delta^{15}N$								1.00 -	-0.20 > 0.05	-0.29 > 0.05
GSI									1.00 -	0.31 > 0.05
HSI										1.00 -

Table S2.5. Pearson correlation coefficient results for MAT (n = 42). The upper value is the correlation coefficient (i.e., r) and the lower value is the p-value. Significant correlations (i.e., $p < 0.05$) are highlighted in bold and underlined. Age (years); BRI, benthic reliance index; FL, fork length (mm); GSI, gonadosomatic index; HSI, hepatosomatic index; K, condition; LGR, $\log_{10}$ growth rate (mm/year); LTHG, $\log_{10}$ THg (ng/g dw); LWT, $\log_{10}$ weight (g); and $\delta^{15}N$ (‰).

	LTHG	**FL**	**LWT**	**LGR**	**Age**	**K**	**BRI**	**$\delta^{15}N$**	**GSI**	**HSI**
LTHG	1.00 -	**-0.51** **< 0.001**	**-0.62** **< 0.001**	**-0.73** **< 0.001**	**0.41** **< 0.01**	**-0.58** **< 0.001**	0.01 > 0.05	**-0.80** **< 0.001**	0.12 > 0.05	**-0.50** **< 0.001**
FL		1.00 -	**0.97** **< 0.001**	**0.34** **< 0.05**	0.28 > 0.05	**0.37** **< 0.05**	0.02 > 0.05	**0.77** **< 0.001**	0.16 > 0.05	0.28 > 0.05
LWT			1.00 -	**0.46** **< 0.01**	0.15 > 0.05	**0.57** **< 0.001**	0.04 > 0.05	**0.82** **< 0.001**	0.10 > 0.05	**0.32** **< 0.05**
LGR				1.00 -	**-0.79** **< 0.001**	**0.59** **< 0.001**	0.15 > 0.05	**0.52** **< 0.001**	-0.22 > 0.05	0.24 > 0.05
Age					1.00 -	**-0.36** **< 0.05**	-0.13 > 0.05	-0.02 > 0.05	**0.35** **< 0.05**	-0.04 > 0.05
K						1.00 -	-0.01 > 0.05	**0.46** **< 0.01**	-0.19 > 0.05	0.24 > 0.05
BRI							1.00 -	0.17 > 0.05	-0.03 > 0.05	0.03 > 0.05
$\delta^{15}N$								1.00 -	0.16 > 0.05	**0.50** **< 0.001**
GSI									1.00 -	0.24 > 0.05
HSI										1.00 -

Table S2.6. Akaike's information criterion corrected for small sample size (AIC_C) for all ranked candidate models that describe variation in THg concentration (ng/g dw) in immature (IM-hi, n = 32; IM-lo, n = 27) and mature (MAT, n = 42) Arctic char. Candidate models within the 95% confidence interval set (i.e., cumulative w_i up to 0.95) are highlighted in bold and underlined. K, number of parameters; RSS, residual sums of squares; Δ_i, difference in AIC_C values between the top model and model *i*; w_i, Akaike weight for model *i*; Age (years); BRI, benthic reliance index; FL, fork length (mm); HSI, hepatosomatic index; K, Fulton's condition factor; LGR, $\log_{10}$ growth rate (mm/year); LWT, $\log_{10}$ weight (g); and $\delta^{15}N$ (‰).

Maturity group	Dependent variable	Candidate models	K	RSS	AIC_C	Δ_i	w_i
IM-hi (Immature)	Log_{10} THg	**$\delta^{15}N$ + BRI + Age**	**5**	**0.082**	**-178.602**	**0.000**	**0.350**
		$\delta^{15}N$ + BRI + LGR	**5**	**0.082**	**-178.473**	**0.129**	**0.328**
		$\delta^{15}N$ + BRI	**4**	**0.096**	**-176.429**	**2.173**	**0.118**
		$\delta^{15}N$ + BRI + FL	**5**	**0.092**	**-175.074**	**3.527**	**0.060**
		$\delta^{15}N$ + BRI + LWT	**5**	**0.092**	**-175.069**	**3.533**	**0.060**
		$\delta^{15}N$ + LGR	**4**	**0.106**	**-173.191**	**5.410**	**0.023**
		$\delta^{15}N$	**3**	**0.118**	**-172.567**	**6.035**	**0.017**
		$\delta^{15}N$ + Age	4	0.111	-171.812	6.789	0.012
		$\delta^{15}N$ + K	4	0.111	-171.755	6.847	0.011
		$\delta^{15}N$ + Age + LWT	5	0.106	-170.491	8.111	< 0.01
		$\delta^{15}N$ + Age + FL	5	0.107	-170.127	8.475	< 0.01
		$\delta^{15}N$ + FL	4	0.117	-170.010	8.592	< 0.01
		$\delta^{15}N$ + LWT	4	0.118	-169.943	8.659	< 0.01
		BRI + Age + FL	5	0.147	-159.875	18.727	< 0.01
		BRI + Age + LWT	5	0.151	-159.184	19.418	< 0.01
		BRI + LGR	4	0.183	-155.763	22.839	< 0.01
		BRI + LWT	4	0.193	-154.071	24.530	< 0.01
		BRI + FL	4	0.195	-153.670	24.932	< 0.01
		BRI	3	0.214	-153.382	25.219	< 0.01
		Age + LWT	4	0.202	-152.607	25.995	< 0.01
		K + BRI	4	0.207	-151.893	26.708	< 0.01
		BRI + Age	4	0.207	-151.763	26.839	< 0.01
		Age + FL	4	0.216	-150.467	28.134	< 0.01
		LWT	3	0.263	-146.813	31.789	< 0.01
		FL	3	0.286	-144.123	34.479	< 0.01
		HSI	3	0.304	-142.197	36.405	< 0.01
		K + HSI	4	0.297	-140.234	38.367	< 0.01
		K + HSI + GSI	5	0.293	-137.881	40.721	< 0.01
		K	3	0.408	-132.752	45.850	< 0.01
		K + Age	4	0.389	-131.608	46.994	< 0.01
		K + GSI	4	0.402	-130.557	48.045	< 0.01
		LGR	3	0.451	-129.519	49.083	< 0.01
		Age	3	0.482	-127.405	51.197	< 0.01
		GSI	3	0.491	-126.815	51.786	< 0.01

IM-lo (Immature)	Log_{10} THg	**$\delta^{15}N$ + FL**	**4**	**0.152**	**-129.949**	**0.000**	**0.237**
		$\delta^{15}N$ + LWT	**4**	**0.153**	**-129.834**	**0.115**	**0.223**
		$\delta^{15}N$ + Age + LWT	**5**	**0.146**	**-128.107**	**1.843**	**0.094**
		$\delta^{15}N$ + Age + FL	**5**	**0.147**	**-127.944**	**2.006**	**0.087**
		$\delta^{15}N$ + BRI + FL	**5**	**0.151**	**-127.103**	**2.847**	**0.057**
		$\delta^{15}N$ + BRI + LWT	**5**	**0.152**	**-126.993**	**2.956**	**0.054**
		FL	**3**	**0.195**	**-126.059**	**3.891**	**0.034**
		LWT	**3**	**0.195**	**-126.056**	**3.893**	**0.034**
		$\delta^{15}N$	**3**	**0.200**	**-125.441**	**4.508**	**0.025**
		Age + LWT	**4**	**0.182**	**-125.209**	**4.740**	**0.022**
		$\delta^{15}N$ + LGR	**4**	**0.182**	**-125.138**	**4.811**	**0.021**
		Age + FL	**4**	**0.184**	**-124.812**	**5.138**	**0.018**
		$\delta^{15}N$ + BRI	**4**	**0.187**	**-124.468**	**5.481**	**0.015**
		$\delta^{15}N$ + BRI + LGR	**5**	**0.169**	**-124.131**	**5.818**	**0.013**
		$\delta^{15}N$ + Age	**4**	**0.191**	**-123.857**	**6.093**	**0.011**
		BRI + FL	**4**	**0.194**	**-123.446**	**6.503**	**0.009**
		BRI + LWT	4	0.194	-123.439	6.511	0.009
		$\delta^{15}N$ + K	4	0.194	-123.389	6.561	0.009
		BRI + Age + LWT	5	0.181	-122.208	7.741	< 0.01
		LGR	3	0.227	-121.993	7.956	< 0.01
		$\delta^{15}N$ + BRI + Age	5	0.184	-121.907	8.043	< 0.01
		BRI + Age + FL	5	0.184	-121.819	8.130	< 0.01
		HSI	3	0.243	-120.129	9.820	< 0.01
		Age	3	0.247	-119.739	10.211	< 0.01
		BRI + LGR	4	0.224	-119.620	10.329	< 0.01
		K	3	0.249	-119.434	10.516	< 0.01
		BRI	3	0.252	-119.180	10.770	< 0.01
		GSI	3	0.254	-118.960	10.990	< 0.01
		K + HSI	4	0.233	-118.467	11.483	< 0.01
		K + Age	4	0.246	-117.046	12.904	< 0.01
		BRI + Age	4	0.246	-117.015	12.935	< 0.01
		K + BRI	4	0.248	-116.773	13.176	< 0.01
		K + GSI	4	0.249	-116.697	13.253	< 0.01
		K + HSI + GSI	5	0.233	-115.436	14.513	< 0.01
MAT (Mature)	Log_{10} THg	**$\delta^{15}N$ + BRI + Age**	**5**	**0.523**	**-172.508**	**0.000**	**0.887**
		$\delta^{15}N$ + Age	**4**	**0.644**	**-166.379**	**6.130**	**0.041**
		$\delta^{15}N$ + BRI + LGR	**5**	**0.608**	**-166.208**	**6.300**	**0.038**
		$\delta^{15}N$ + Age + LWT	5	0.636	-164.302	8.206	0.015
		$\delta^{15}N$ + Age + FL	5	0.643	-163.886	8.622	0.012
		$\delta^{15}N$ + LGR	4	0.699	-162.971	9.537	< 0.01
		$\delta^{15}N$ + K	4	0.932	-150.870	21.638	< 0.01
		$\delta^{15}N$ + BRI + FL	5	0.931	-148.315	24.193	< 0.01
		$\delta^{15}N$ + FL	4	1.030	-146.673	25.836	< 0.01
		$\delta^{15}N$ + BRI	4	1.047	-145.982	26.526	< 0.01
		$\delta^{15}N$	3	1.113	-145.836	26.672	< 0.01
		$\delta^{15}N$ + BRI + LWT	5	1.021	-144.460	28.048	< 0.01
		$\delta^{15}N$ + LWT	4	1.101	-143.865	28.643	< 0.01
		Age + LWT	4	1.115	-143.341	29.167	< 0.01
		BRI + Age + LWT	5	1.083	-141.948	30.560	< 0.01
		Age + FL	4	1.251	-138.485	34.024	< 0.01

	BRI + Age + FL	5	1.220	-136.950	35.558	< 0.01
	LGR	3	1.431	-135.293	37.215	< 0.01
	BRI + LGR	4	1.391	-134.026	38.482	< 0.01
	K + HSI	4	1.615	-127.774	44.734	< 0.01
	K + HSI + GSI	5	1.561	-126.600	45.908	< 0.01
	LWT	3	1.892	-123.562	48.946	< 0.01
	BRI + LWT	4	1.889	-121.182	51.326	< 0.01
	K + Age	4	1.902	-120.896	51.612	< 0.01
	K	3	2.037	-120.469	52.039	< 0.01
	K + GSI	4	2.036	-118.029	54.479	< 0.01
	K + BRI	4	2.037	-118.020	54.488	< 0.01
	FL	3	2.268	-115.949	56.559	< 0.01
	HSI	3	2.305	-115.279	57.229	< 0.01
	BRI + FL	4	2.267	-113.519	58.989	< 0.01
	Age	3	2.569	-110.718	61.790	< 0.01
	BRI + Age	4	2.559	-108.439	64.069	< 0.01
	GSI	3	3.028	-103.813	68.695	< 0.01
	BRI	3	3.075	-103.178	69.330	< 0.01

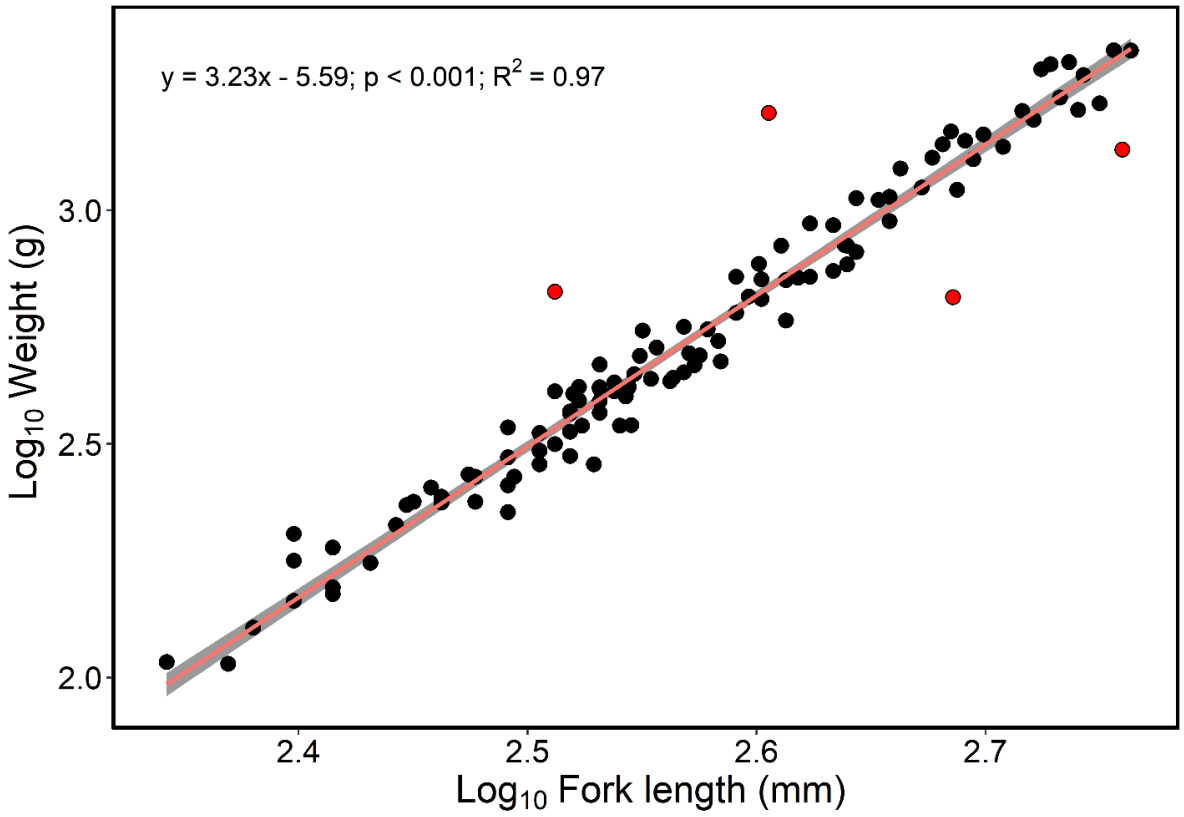

Figure S2.1. Regression of $\log_{10}$ weight (g) as a function of $\log_{10}$ fork length (mm) for anadromous Arctic char caught in inner Frobisher Bay, Nunavut in 2018 and 2019. Linear regression equation, p-value, and adjusted R^2 value are displayed. Linear regression line (orange) and 95% confidence interval (grey) are displayed. Red points were outliers removed from the regression analysis.

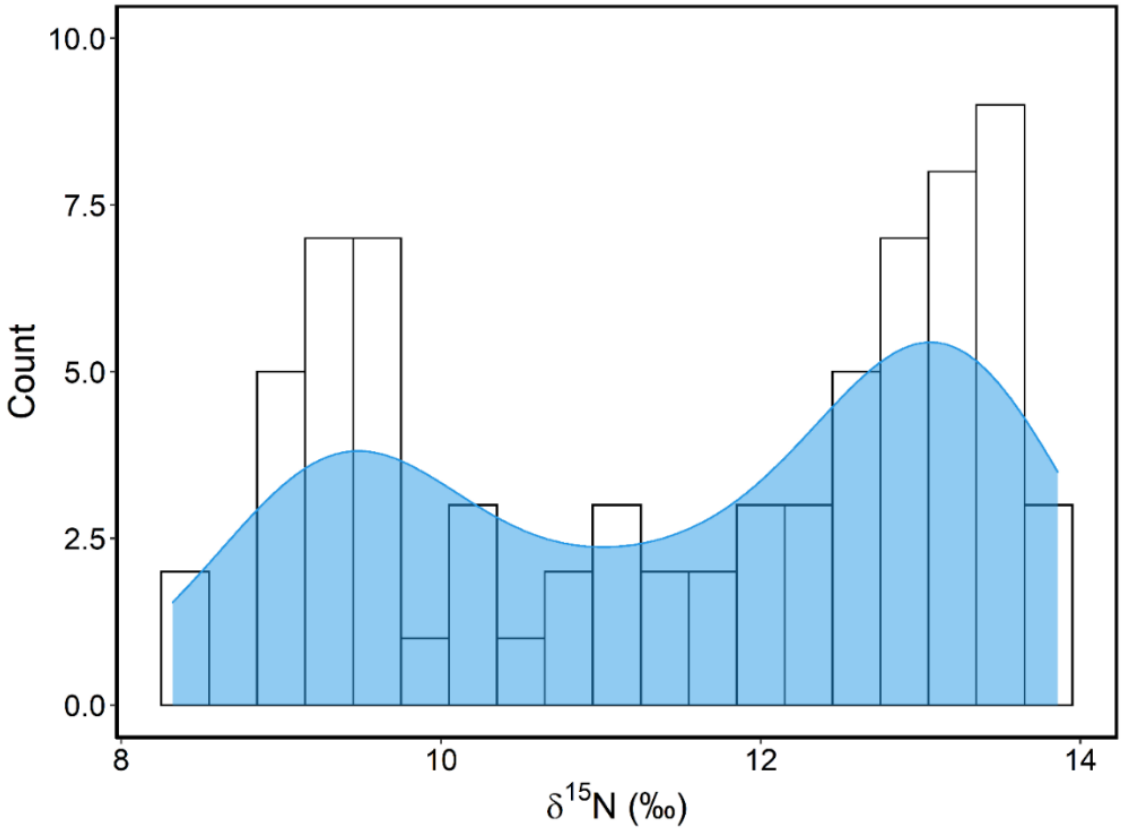

Figure S2.2. Histogram and density distribution of $\delta^{15}N$ values for immature (n = 73) anadromous Arctic char.

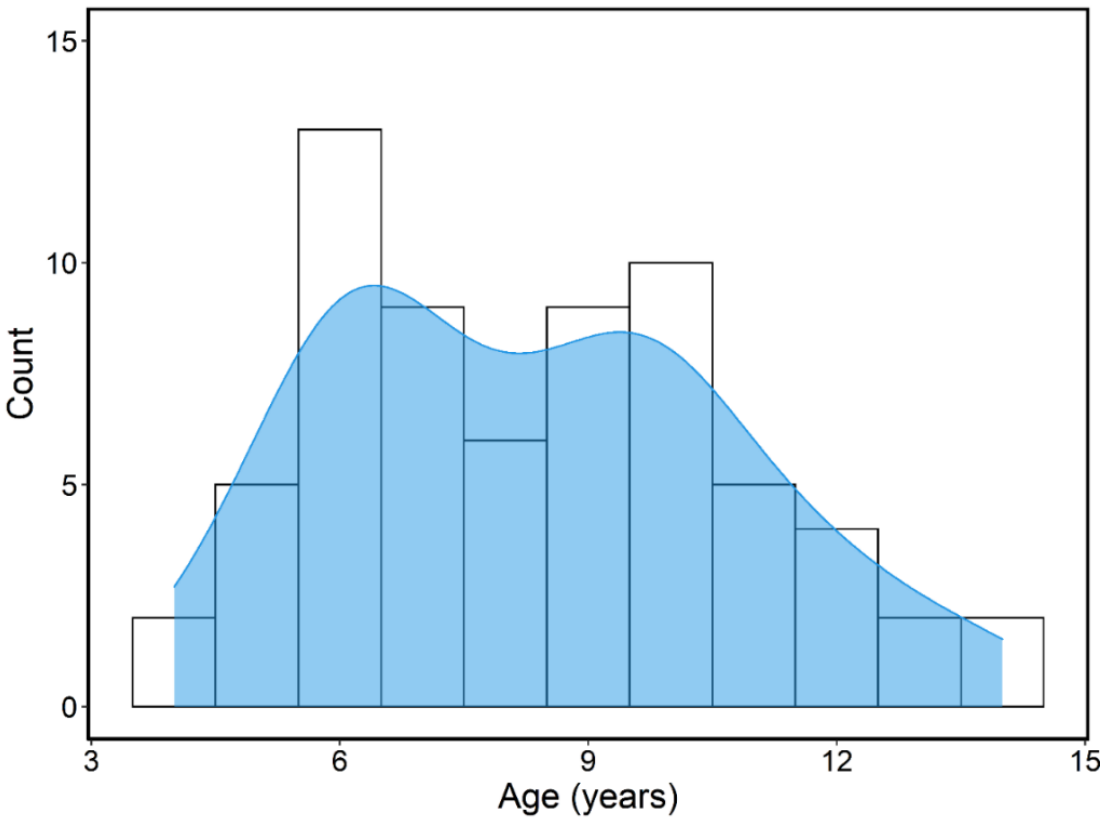

Figure S2.3. Histogram and density distribution of age for immature (n = 67) anadromous Arctic char.

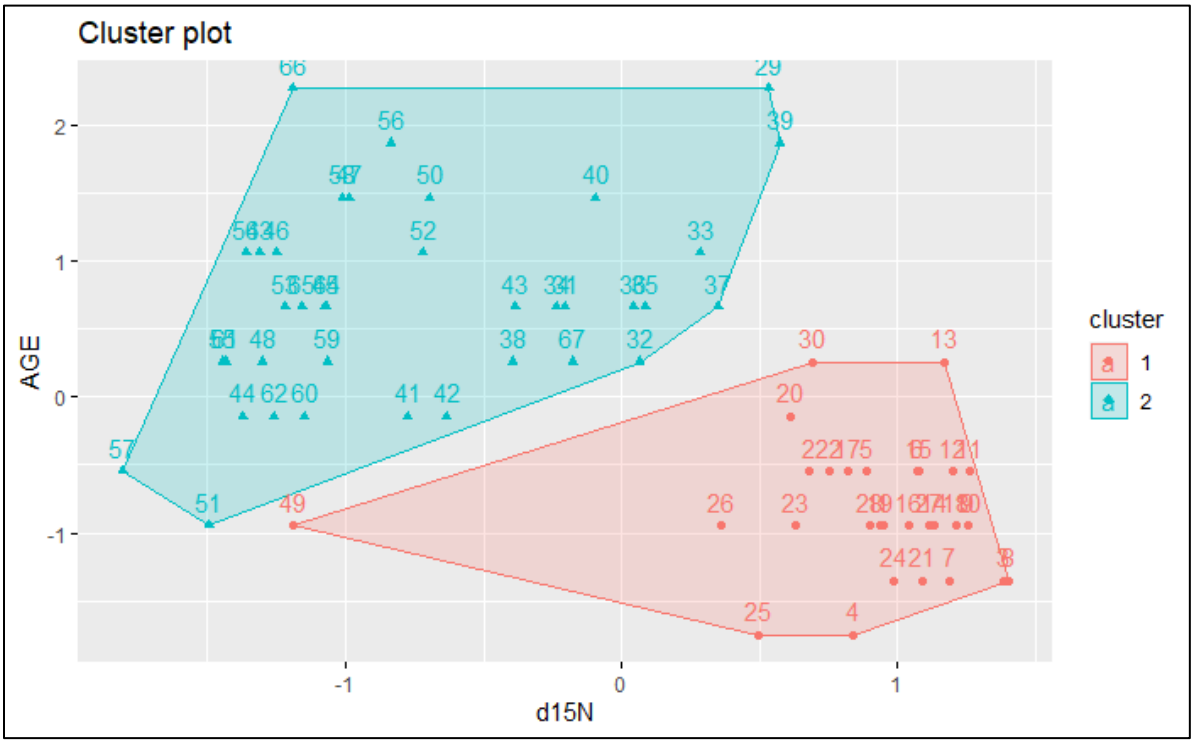

Figure S2.4. Partitioning Around Medoids (PAM) cluster analysis for the immature Arctic char (n = 67) using variables of age (years) and $\delta^{15}N$ (‰). Cluster 1 (red), IM-lo; Cluster 2 (blue), IM-hi.

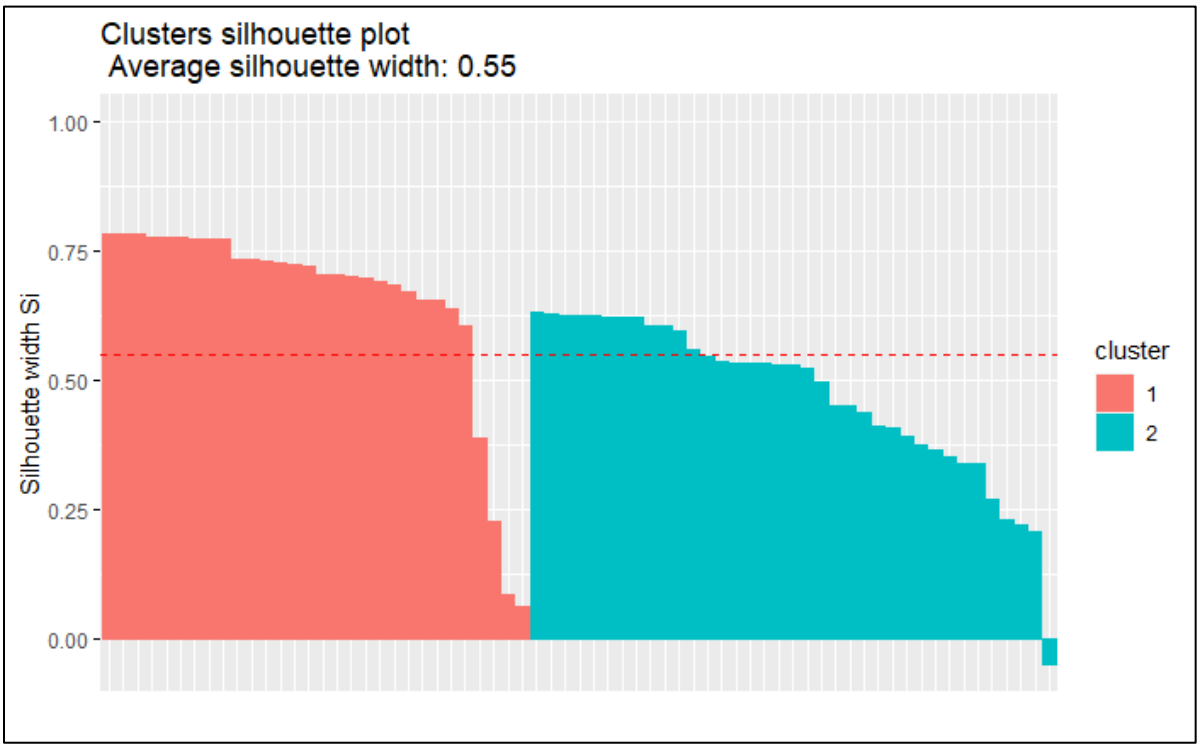

Figure S2.5. Silhouette coefficients for the Partitioning Around Medoids (PAM) cluster analysis for the immature Arctic char (n = 67) using variables of age (years) and $\delta^{15}N$ (‰). Cluster 1 (red), IM-lo; Cluster 2 (blue), IM-hi.

Appendix B – Chapter 3

Table S3.1. Mean and standard error (SE) of $\delta^{15}N$ (‰) values for filter-feeding primary consumer species selected to test for differences in baseline $\delta^{15}N$ (‰) values among sample locations in inner Frobisher Bay, Nunavut. The mean basal $\delta^{15}N$ (‰) values used for baseline correction of all taxa collected from each location are shown. Tukey's HSD results are listed, where significant differences ($p < 0.05$) are indicated by different letters.

Location	Primary consumer spp.	n	Mean $\delta^{15}N$ (‰)	SE $\delta^{15}N$ (‰)	Tukey's HSD Results
Koojesse Inlet	*Mya truncata*	16	6.88	0.06	A
Peterhead Inlet	*Mya truncata*	4	6.61	0.04	A
Faris Island	*Hiatella arctica*	1	8.14	0.22	B
	Musculus niger	1			
Kituriaqannigituq	*Mya truncata*	4	7.61	0.20	B

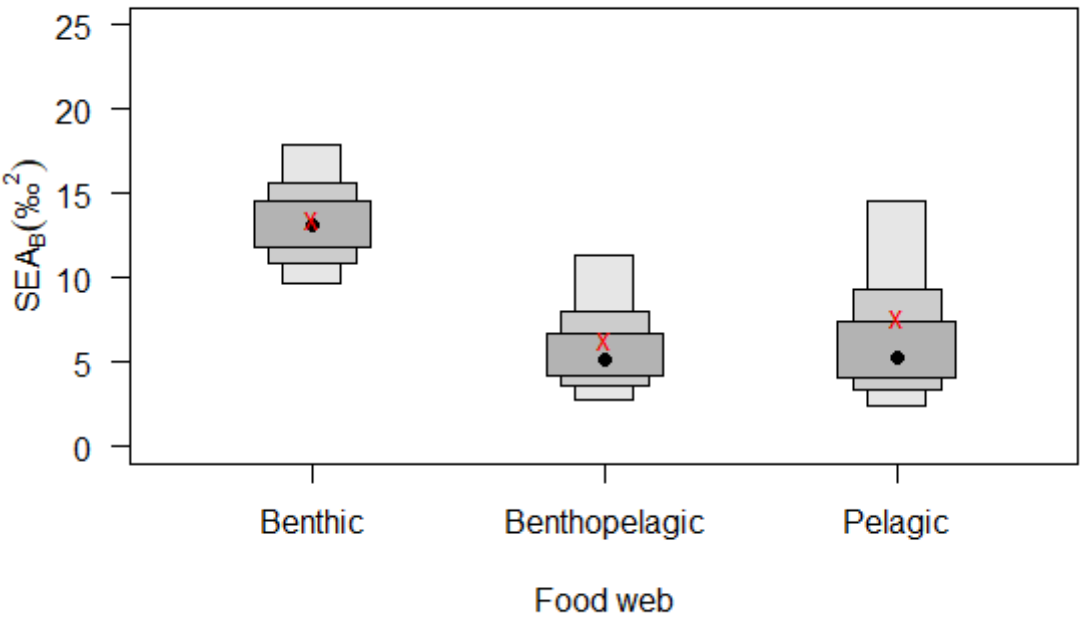

Figure S3.1. Posterior distributions of the Bayesian standard ellipse areas (SEA_B) for each food web. Black circles represent the modal values, boxes represent the 50%, 75%, and 95% credible intervals. The red "X" indicates SEA_C values.

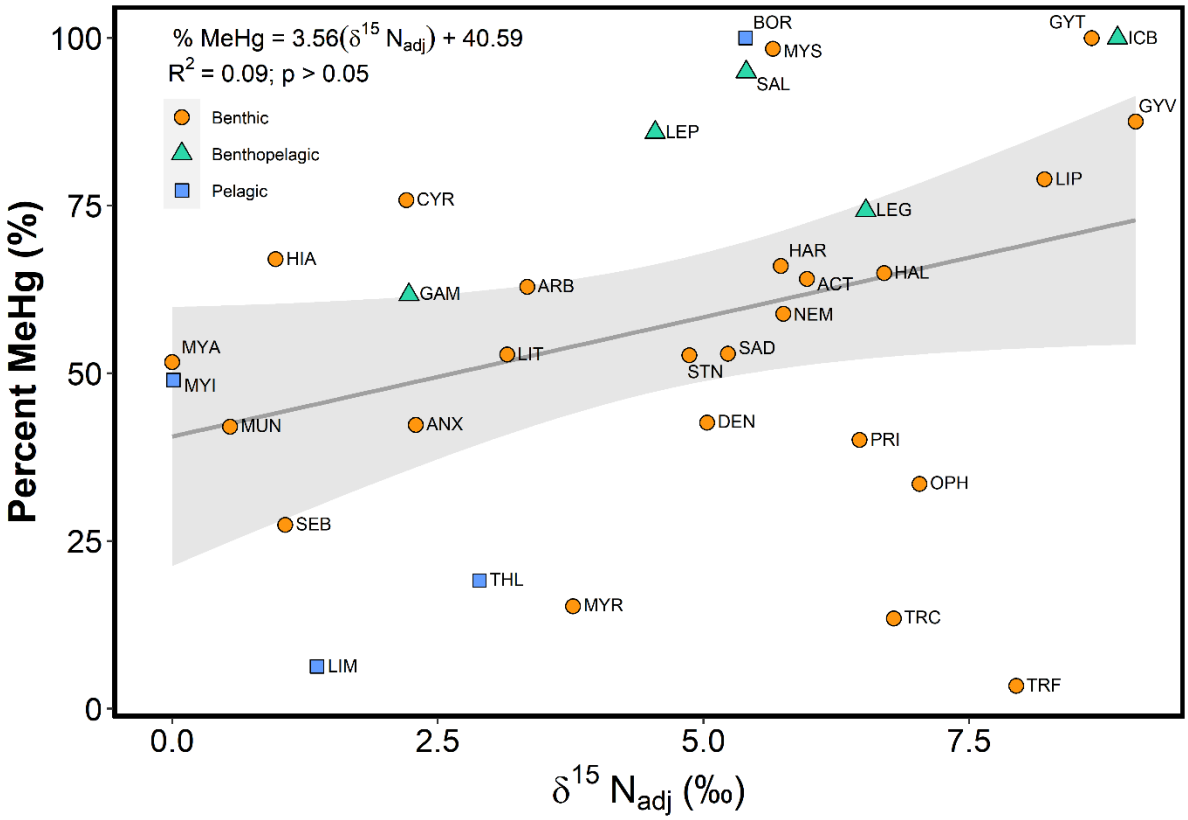

Figure S3.2. Linear regression and 95% confidence interval (grey area) of mean percent methylmercury (% MeHg) and mean $\delta^{15}N_{adj}$ (‰) values for benthic, benthopelagic, and pelagic taxa collected in inner Frobisher Bay, Nunavut, in 2018 and 2019. Linear regression equation and adjusted R^2 values are displayed. Labels refer to codes listed in Table 3.1.

Supplementary Information

SI 3.1. In Figure 3.2A, six organisms are separated from the rest of the organisms based on stable isotope data (depicted in the lower right of the bivariate plot). These organisms are benthic primary producers (i.e., ALG, periphyton; DES, *Desmarestia aculeata*, kelp; FUV, *Fucus vesiculosis*, kelp), intertidal primary consumers (GAS, gastropoda; LIT, *Littorina saxatilis*, gastropoda), and an omnivorous sea cucumber (MYR, *Myriotrochus rinkii*). High $\delta^{13}C$ values associated with relatively low $\delta^{15}N$ values resulted in the observed separation of these items from the other collected organisms presented in the stable isotope bivariate plot (Figure 3.2A). Macroalgae, such as periphyton and kelp, photosynthesize by incorporating CO_2 via carboxylation with the Hath-Slack pathway which results in high $\delta^{13}C$ values in macroalgal tissues (Fry & Sherr, 1984; Rounick & Winterbourn, 1986). Grazing primary consumers, such as gastropods, are low trophic level organisms that are heavily reliant on macroalgal food sources (e.g., Olsson et al., 2007), and therefore their tissue stable isotope values will reflect those of the macroalgae they consume, and thus in the case of our results, led to the distinct separation of these items relative to the other benthic organisms, which were probably reliant on a mix of other basal carbon sources, such as phytodetritus or ice algae, in addition to kelp (e.g., Iken et al., 2005, 2010; Søreide et al., 2013; Tamelander et al., 2006). Given the proximity of the omnivorous sea cucumber (MYR) to the gastropoda (LIT and GAS) in Figure 3.2A, it is possible that it was feeding on similar macroalgal food sources. In terms of Hg concentrations, the primary producers (ALG, DES, and FUV) had the lowest THg concentrations of all biota analyzed (6.99 – 11.11 ng/g dw), and the gastropods (GAS and LIT) and the sea cucumber (MYR) had THg concentrations that were below the median (52.47 ng/g dw) and average (76.27 ng/g dw) THg concentration values reported for the invertebrates. These results indicate that a diet enriched in ^{13}C is associated with relatively low THg concentrations.

Appendix C – Chapter 4

Table S4.1. Mean ± standard error of total mercury (THg) concentrations in ng/g dry weight (dw) and µ/g wet weight (ww), and the percentage of samples for each taxa that were over the Health Canada toxicity threshold of 0.5 ppm ww (Health Canada, 2007), for taxa collected in inner Frobisher Bay, Nunavut, in 2018 and 2019. The number of samples analyzed for THg (n) are listed. B, benthic; BP, benthopelagic; P, pelagic; NA, not analyzed. Concentrations were converted from dry weight to wet weight using a standard conversion factor of 5 (e.g., Cresson et al., 2017).

Taxa	Code	Food web	n	THg (ng/g dw)	THg (µg/g ww)	% samples > 0.5 ppm
Primary producers						
Particulate organic matter	POM	P	NA	NA	NA	NA
Periphyton	ALG	B	8	11.11 ± 1.83	0.00 ± 0.00	0
Desmarestia aculeata	DES	B	2	5.71 ± 0.03	0.00 ± 0.00	0
Fucus vesiculosis	FUV	B	9	6.99 ± 0.77	0.00 ± 0.00	0
Invertebrata						
Annelida						
Polychaeta	POL	B	11	158.41 ± 83.87	0.03 ± 0.02	0
Harmothroe imbricata	HAR	B	3	48.16 ± 6.75	0.01 ± 0.00	0
Travisia carnea	TRC	B	3	39.36 ± 7.84	0.01 ± 0.00	0
Travisia forbesii	TRF	B	1	31.76	0.01	0
Chaetognatha	CHA	P	NA	NA		
Cnidaria						
Actiniaria	ACT	B	4	40.91 ± 7.06	0.01 ± 0.00	0
Halcampa arctica	HAL	B	15	39.74 ± 2.01	0.01 ± 0.00	0
Crustacea						
Amphipoda						
Gammaridea	GAM	BP	12	33.97 ± 2.70	0.01 ± 0.00	0
Anonyx sp.	ANX	B	1	26.87	0.01	0
Themisto libellula	THL	P	2	53.98 ± 19.76	0.01 ± 0.00	0
Calanoida						
Calanus sp.	CAL	P	NA	NA	NA	NA
Caridea						
Argis dentata	ARG	BP	6	238.46 ± 106.47	0.05 ± 0.02	0
Eualus gaimardii	EUG	BP	2	80.32 ± 60.77	0.02 ± 0.01	0
Lebbeus groenlandicus	LEG	BP	9	377.65 ± 59.57	0.08 ± 0.01	0
Lebbeus polaris	LEP	BP	8	87.02 ± 12.39	0.02 ± 0.00	0
Sabinea septemcarinata	SAB	B	3	83.73 ± 32.46	0.02 ± 0.01	0
Sclerocrangon boreas	SCB	B	2	262.36 ± 111.03	0.05 ± 0.02	0
Cirripedia						
Semibalanus balanoides	SEB	B	3	15.75 ± 1.41	0.00 ± 0.00	0
Isopoda						
Arcturus baffini	ARB	B	10	19.44 ± 1.02	0.00 ± 0.00	0
Saduria sabini	SAD	B	3	44.25 ± 3.14	0.01 ± 0.00	0
Mysidacea						
Mysis sp.	MYI	P	1	13.17	0.00	0
Echinodermata						
Echinoidea						
Strongylocentrotus droebachiensis	SOD	B	3	65.00 ± 2.37	0.01 ± 0.00	0
Holothuriodea						
Myriotrochus rinkii	MYR	B	3	20.92 ± 1.43	0.00 ± 0.00	0
Ophiuroidea						

Amphilepidida	AMA	B	5	33.66 ± 2.37	0.01 ± 0.00	0
Ophiacantha bidentata	OPH	B	15	52.47 ± 2.34	0.01 ± 0.00	0
Stegophiura nodosa	STN	B	8	23.77 ± 1.59	0.00 ± 0.00	0
Mollusca						
Bivalvia	BIV	B	3	46.68 ± 6.68	0.01 ± 0.00	0
Astarte sp.	AST	B	6	63.04 ± 3.80	0.01 ± 0.00	0
Cyrtodaria kurriana	CYR	B	4	11.42 ± 3.09	0.00 ± 0.00	0
Ennucula tenuis	ENT	B	1	122.69	0.02	0
Hiatella sp.	HIS	B	2	105.02 ± 32.63	0.02 ± 0.01	0
Hiatella arctica	HIA	B	9	29.02 ± 4.56	0.01 ± 0.00	0
Macoma loveni	MAC	B	1	69.13	0.01	0
Musculus discors	MUD	B	1	81.30	0.02	0
Musculus niger	MUN	B	3	87.72 ± 15.92	0.02 ± 0.00	0
Mya truncata	MYA	B	24	21.03 ± 1.14	0.00 ± 0.00	0
Nuculana pernula	NUC	B	1	67.86	0.01	0
Gastropoda	GAS	B	1	41.22	0.01	0
Buccinidae	BUC	B	2	201.70 ± 89.28	0.04 ± 0.02	0
Colus stimpsoni	COL	B	3	76.72 ± 29.25	0.02 ± 0.01	0
Limacina sp.	LIM	P	1	122.69	0.02	0
Littorina sp.	LIS	B	1	39.33	0.01	0
Littorina saxatilis	LIT	B	2	34.22 ± 0.79	0.01 ± 0.00	0
Scabrotrophon fabricii	SCA	B	1	158.11	0.03	0
Nudibranchia						
Dendronotus sp.	DEN	B	3	72.38 ± 3.86	0.01 ± 0.00	0
Nemertea	NEM	B	1	63.24	0.01	0
Priapulida						
Priapulus caudatus	PRI	B	5	26.62 ± 2.55	0.01 ± 0.00	0
Pisces						
Boreogadus saida	BOR	P	60	60.09 ± 3.48	0.01 ± 0.00	0
Cottidae						
Artediellus atlanticus	ART	B	1	160.22	0.03	0
Gymnocanthus tricuspis	GYT	B	2	990.53 ± 299.79	0.20 ± 0.06	0
Icelus bicornis	ICB	BP	4	571.33 ± 138.03	0.11 ± 0.03	0
Icelus spatula	ICS	BP	8	285.06 ± 60.62	0.06 ± 0.01	0
Myoxocephalus sp.	MYS	B	20	58.49 ± 12.01	0.01 ± 0.00	0
Myoxocephalus scorpioides	MYO	B	1	220.26	0.04	0
Triglops pingelii	TRP	BP	2	53.32 ± 2.14	0.01 ± 0.00	0
Gymnelus viridis	GYV	B	17	219.84 ± 11.89	0.04 ± 0.00	0
Liparis fabricii	LIP	B	2	159.91 ± 2.12	0.03 ± 0.00	0
Salvelinus alpinus	SAL	BP	119	222.26 ± 15.74	0.04 ± 0.00	0